8-10-2018

Quantification of Harmful Algal Blooms in Multiple Water Bodies of Mississippi Using In-Situ, Analytical and Remote Sensing Techniques

Saurav Silwal

Quantification of harmful algal blooms in multiple water bodies of Mississippi using in-situ, analytical and remote sensing techniques

By
Saurav Silwal

A Dissertation
Submitted to the Faculty of
Mississippi State University
in Partial Fulfillment of the Requirements
for the Degree of Doctor of Philosophy
in Earth and Atmospheric Sciences
in the Department of Geosciences

Mississippi State, Mississippi

August 2018

Quantification of harmful algal blooms in multiple water bodies of Mississippi using in-situ, analytical and remote sensing techniques

By
Saurav Silwal

Approved:

_____
Padmanava Dash
(Major Professor)

_____
John C.Rodgers III
(Committee Member)

_____
Qingmin Meng
(Committee Member)

_____
Shrinidhi Ambinakudige
(Committee Member)

_____
Renee M. Clary
(Graduate Coordinator)

_____
Rick Travis
Dean
College of Arts & Sciences

Name: Saurav Silwal

Date of Degree: August 10, 2018

Institution: Mississippi State University

Major Field: Earth and Atmospheric Sciences

Major Professor: Padmanava Dash

Title of Study: Quantification of harmful algal blooms in multiple water bodies of Mississippi using in-situ, analytical and remote sensing techniques

Pages in Study 101

Candidate for Degree of Doctor of Philosophy

Globally, water bodies are increasingly affected by undesirable harmful algal blooms. This dissertation contributes to research methodology pertaining to quantification of the algal blooms in multiple water bodies of Mississippi using *in situ*, analytical, and remote sensing techniques. The main objectives of this study were to evaluate the potential of several techniques for phytoplankton enumeration and to develop remote sensing algorithms for several sensors and evaluate the performance of the sensors for quantifying phytoplankton in several water bodies. Analytical techniques such as “FlowCam”, an imaging flow cytometer; “HPLC”, high performance liquid chromatography with the chemical taxonomy program “ChemTax”; spectrofluorometric analyses; and “ELISA” assay were used to quantify a suite of parameters on algal blooms. Additionally, *in-situ* algal pigment biomass was measured using fluorescence probes. It was found that that each technique has unique potential. While some of the rapid and simpler techniques can be used instead of more involved techniques, sometimes use of several techniques together is beneficial for managing aquatic ecosystems and protecting human health.

Algorithms were developed to quantify chlorophyll *a* using five remote sensing sensors including three currently operational satellite sensors and two popular sensors onboard the Unmanned Aerial Systems (UASs). Empirical band ratio algorithms were developed for each sensor and the best algorithms were chosen. Cluster analysis helped in differentiating the water types and linear regression was used to develop algorithms for each of the water types. The UAS sensor- Micasense was found to be most useful among the UAS sensors and the best overall with highest R^2 value 0.75 with $p<0.05$ and minimum %RMSE of 28.22% and satellite sensor OLCI was found to be most efficient among the three satellite sensors used in the study for chlorophyll *a* estimation with R^2 of 0.75 with $p<0.05$ and %RMSE 13.19%. The algorithms developed for these sensors in this study represent the best algorithms for chlorophyll *a* estimation in these water bodies based on R^2 and %RMSE. The applicability of the algorithms can be extended to other water bodies directly or the approach developed in this study can be adopted for estimating Chl *a* in other water bodies.

DEDICATION

This dissertation is dedicated to my beloved husband Dr. Krishna Mohan Chauhan and my parents Pradeep and Nirmala Silwal

ACKNOWLEDGEMENTS

First and foremost, I would like to thank my advisor, Dr. Padmanava Dash who trusted my abilities and constantly guided me throughout my graduate studies. This dissertation has only been possible with his constant support and guidance. With his positive attitude and his great generosity, he always helped me to get through the challenging times during my Ph.D. and helped find solutions to the problems.

I would also like to thank my committee members Dr. John Rodgers, Dr. Quinmen Meng Dr. Shrinidhi Ambinakudige for their support and encouragement throughout this dissertation research.

I would like to thank my friends and colleagues- Mary Grace Chambers,Kate Grala, Sankar Manalilkada Sasidharan, Shatrughan Singh, Madhur Devkota, Sara Smith, Landon Sanders, and Abdulla Sheriff for their friendship, support, and encouragement.

I would like to extend my thanks to Prof. Clifford Ochs for allowing me to work in his laboratory and Jarrod Sackreiter for training me to use the FlowCam instrument to take images of phytoplankton in the University of Mississippi, Oxford, MS.

I would like to thank Department of Geosciences and Geosystem Research institute for supporting my academic expenses through funding me through teaching and research assistantships. I would also like to thank Dr. William H. Cooke and Dr. Robert J. Moorhead for their support and encouragement. This research was supported by the NOAA Unmanned Aerial Systems Program Office through the Northern Gulf Institute

located at Mississippi State University, a NOAA Cooperative Institute (Grant no. NA11OAR4320199) to Dr. Padmanava Dash, US Department of Treasury through the Mississippi Based RESTORE Act Center of Excellence (MBRACE) located at University of Southern Mississippi and Northern Gulf Institute by NSF Division of Environmental Biology (Grant no. 1126379) to Dr. Clifford A. Ochs, and by the faculty start up grant to Dr. Padmanava Dash. I am thankful to Christopher Zarzar and Gray Turnage for their help during field data collection, and Audra Sawyer, Rayford Parnell, and Patricia Lipson for their help in analyzing samples under FlowCam.

I am grateful to my dearest friends Dr. Douglas Hiser and Dr. Laree M. Hiser who has been a constant support and inspiration throughout this dissertation. Doug and Laree consistently encouraged and supported me to pursue this Ph.D. degree. I cherish those intellectual conversations we have had during our meetings which provided me the positivity I needed to complete this dissertation. I consider myself lucky to have their friendship and support in my life.

Completing a Ph.D. requires a long period of intensive research and redaction, and it would not have been possible to live through this period without the family's support. My mother, Nirmala, my father, Pradeep, my brother, Satish, my sister in law Medina and my little niece Melanie loved and supported me unconditionally during all these years. I am proud of my parents and grateful of the life they have given me. My family supported my higher education with their humble means and they have always stood by me. I am thankful to all of them and specially my sister Sudha Gautam and her husband Dr. Milan Gautam for their continuous support and motivation during this

dissertation research. I also express my sincere thanks to all members of my in -law family who were extremely supportive during my dissertation period.

Finally, I am thankful to my beloved husband Dr. Krishna Mohan Chauhan who always believed in my potential and rooted me for my success. Without his continuous support, encouragement, and patience, it would not have been possible for me to come this far. I consider myself extremely lucky to have his support from the start to end of this dissertation research.

.

TABLE OF CONTENTS

APPENDIX

LIST OF TABLES

LIST OF FIGURES

CHAPTER I

INTRODUCTION

Globally, water bodies are increasingly affected by undesirable harmful algal blooms (HABs) due to increase in nutrient inputs from the natural and anthropogenic discharges, thus creating more amenable environments for algal blooms (Anderson, 2009). HABs are caused by rapid growth of photosynthetic microorganisms in water bodies, which are commonly known as “algae” or phytoplankton. HABSs are detrimental to the aquatic environment for several reasons. Firstly, they can block the sunlight, resulting in shading and affecting the visibility of the aquatic organisms living below the water surface. Secondly, the dissolved oxygen (DO) concentration of the water column depletes because of increased microbial activity as the algae die and sink to the bottom, thus affecting the viability of aquatic life. Third and the most threatening effect of HABs is the capability of certain species to produce toxins which has significant consequences including impacts on public health, commercial fisheries, and recreation, and an increased cost for monitoring and management (D. Anderson, Glibert, and Burkholder 2002). Cyanobacteria, which is commonly known as blue-green algae, is the dominant harmful algal group present in freshwaters and their blooms are aesthetically undesirable. During the bloom state they discolor the water, increase turbidity, form surface scums, and synthesize a large number of low molecular weight compounds, causing taste and odor problems (Paerl et al. 2001). Moreover, cyanobacterial blooms are of concern due to

the ability of cyanobacterial species to produce at least 60 types of toxins (cyanotoxins) which are categorized as, hepatotoxins (causes liver damage), neurotoxins (causes damage to nervous system), cytotoxins (damages cells), dermatotoxins (damages skin) and irritant toxin (Blaha, Babica, and Marsalek 2009). Thus toxic cyanobacteria can cause human and animal health hazards, by introducing risks of illness and mortality (Falconer 1989).

Routine monitoring of algal blooms is important to issue warnings during the outbreak of toxic HABs, which is critical for protecting public health, wild and farmed fish, and aquatic life (Izydorczyk et al. 2005). The conventional monitoring is done by enumerating the number of toxic cells present in water bodies (Alvarez et al. 2014). Such techniques are logistically cumbersome and labor-intensive. Hence, development of alternative methods is essential. There are a few *in situ* and laboratory techniques, which provide rapid detection of harmful algal blooms. Additionally, the optically active nature of pigments in phytoplankton cells make the detection and quantification of algal blooms possible using Remote sensing technology (Jensen 2000). Among the several optically active pigments present in phytoplankton, chlorophyll a is the photosynthetic pigment that is present in all phytoplankton and phycocyanin is the pigment that is present only in cyanobacterial species (Sarada, Pillai, and Ravishankar 1999; Wintermans and De Mots 1965). Chlorophyll a has absorption maxima at 665 and 465 nm in the electromagnetic spectrum and phycocyanin has an absorption maximum at 620 nm (Siegelman and Kycia 1978; Wintermans and De Mots 1965). The total biomass of algal bloom can be estimated in terms of chlorophyll a concentrations and total cyanobacteria can be

estimated in terms of phycocyanin concentrations (Dekker 1993; Schalles and Yacobi 2000; Simis, Peters, and Gons 2005).

Traditionally, phytoplankton communities are monitored by visual inspection using standard microscopy of plankton cell counts (Benfield et al. 2007). This method is tedious and time-consuming, resulting in a long time-lag between sample collection, data analysis, and interpretation. Moreover, a well-trained expert capable of distinguishing subtle morphological features of a wide variety of phytoplankton communities is required to process and handle the samples (Culverhouse et al. 2003). ChemTax, a factor analysis program, offers an alternative to the traditional microscopic technique by providing the relative and absolute abundances of algal groups using concentrations of diagnostic photopigments quantified by high performance liquid chromatography (HPLC)(J. L. Pinckney, Harrington, and Howe 1998). In recent years, FlowCam, which consists of an automated microscope with the ability to compute the community structure by rapidly acquiring large sets of particle image data has been used for visual identification and classification of phytoplankton (Álvarez, López-Urrutia, and Nogueira 2012; Buskey and Hyatt 2006; Garcia et al. 2010; See et al. 2005). FlowCam has the combined capabilities of both flow cytometry and microscopy, and produces the images of all the particles in a water sample along with several statistical parameters by counting, imaging, and analyzing cells rapidly (J.Nicole and Martin L.Jennifer 2010). Meanwhile, spectrofluorometric techniques are used for total phytoplankton biomass estimation by quantifying Chl *a* which is used as a proxy for all the phytoplankton present in the water (Holmes et al. 1965) and phycocyanin (PC) is used as the pigment representing the biomass of cyanobacteria (Dash et al. 2011). Similarly, *in situ* devices also provide

phytoplankton and cyanobacterial biomass by measuring Chl *a* and PC fluorescence(Gregor and Maršálek 2004; See et al. 2005; Zamyadi et al. 2012).

Since conventional HABs monitoring strategies based on sampling at fixed stations cannot provide the information needed for combating the water quality issues, alternative methods (Dash et al. 2015), such as Satellite remote sensing and Unmanned Aerial Systems(UAS), are preferred as they are economical and provide synoptic regional information that is unmatched to the information provided through fixed station sampling (Dash et al. 2011; Watts, Ambrosia, and Hinkley 2012). Although *in situ* sampling is the most accurate way of determining chlorophyll-*a* concentration, yet the use of remote sensing technology has been increasing recently for routine and synoptic chlorophyll-*a* monitoring due to the synoptic coverage (T. Moore et al. 2014).

Many of the satellite sensors are not useful in studying the water quality properties due to the smaller sizes of these water bodies. Low spatial resolution of satellite sensors limits the ability to accurately detect and quantify phytoplankton in water bodies. Unmanned aerial System (UAS) could be the best remote sensing approach in such cases when the UAS is combined with sensors with suitable spectral bands and spatial resolution (Flynn and Chapra 2014). The utility of satellite sensors and UAS sensors in small but ecologically important water bodies are yet not assessed. The overarching goal of this dissertation is to determine the best technique to monitor harmful algal blooms in small but ecologically important water bodies by using an array of available techniques including *in-situ*, analytical, and remote sensing techniques.

The present study is divided into two main chapters, each dealing with specific objectives as documented in these chapters. Briefly, chapter two focuses on

determination of phytoplankton community structure in multiple water bodies (e.g., lakes, estuaries, coastal waters) and comparison of the potential of several *in situ* and laboratory techniques. Chapter three focuses on measurement of phytoplankton abundance using remote sensing technology and comparative analysis of the estimations by three satellite sensors and two popular sensors onboard Unmanned Aerial Systems.

.

CHAPTER II

DETERMINATION OF PHYTOPLANKTON COMMUNITY STRUCTURE IN MULTIPLE WATER BODIES AND COMPARISON OF THE POTENTIAL OF SEVERAL IN SITU AND LABORATORY TECHNIQUES

2.1 Introduction

Globally, water bodies are increasingly affected by undesirable harmful algal blooms (HABs). Algae or phytoplankton are present in water bodies naturally but excessive use of fertilizers in agricultural fields leads to an increase in nutrients through discharge during rainfall and surface runoff, thus causing algal blooms in receiving water bodies (D. M. Anderson 2009). An adverse effect of HABs is that certain species produce phycotoxins. Three types of phycotoxins are widely found in water bodies, including microcystins, brevetoxin, and domoic acid. Microcystins are produced by certain species of cyanobacteria, brevetoxin is produced by the dinoflagellate *Karenia brevis*, and domoic acid is produced by the diatom Pseudo-nitzia spp. (Dash et al. 2015; Garcia et al. 2010; Rinta-Kanto et al. 2005). These toxins negatively impact public health, fisheries and recreation, and increase the need and costs of monitoring and management (D. M. Anderson 2009). Thus, routine monitoring of phytoplankton community structure and species composition is critical for protecting animal and human health, and preventing economic losses by issuing timely advisory of developing bloom conditions or an outbreak of toxic species (See et al. 2005).

To enumerate phytoplankton community structure and species composition rapidly, there are many efficient techniques. However, there is no consensus on the best technique or a specific combination of techniques to determine phytoplankton community structure and species composition operationally. Traditionally, phytoplankton communities are monitored by visual inspection using standard microscopy of plankton cell counts (Benfield et al. 2007). This method is tedious and time-consuming, resulting in a long time-lag between sample collection, data analysis, and interpretation. Moreover, a well-trained expert capable of distinguishing subtle morphological features of a wide variety of phytoplankton communities is required to process and handle the samples (Culverhouse et al. 2003). ChemTax, a factor analysis program, offers an alternative to the traditional microscopic technique by providing the relative and absolute abundances of algal groups using concentrations of diagnostic photopigments quantified by high performance liquid chromatography (HPLC) (J. L. Pinckney, Harrington, and Howe 1998). This program uses steepest descent algorithms to find the best fit for the data based on initial estimates of pigment ratios for the classes to be determined (Mackey et al. 1996). Although ChemTax is a powerful tool for phytoplankton classification, its ability is limited to taxonomical classes, thus genus and species level of identification cannot be achieved by this method.

In recent years, FlowCam, which consists of an automated microscope with the ability to compute the community structure by rapidly acquiring large sets of particle image data has been used for visual identification and classification of phytoplankton (Álvarez, López-Urrutia, and Nogueira 2012; Buskey and Hyatt 2006; Garcia et al. 2010; See et al. 2005). FlowCam has the combined capabilities of both flow cytometry and

microscopy, and produces the images of all the particles in a water sample along with several statistical parameters by counting, imaging, and analyzing cells rapidly (J.Nicole and Martin L.Jennifer 2010). Additionally, previous studies have shown that results obtained from FlowCam showed minimal differences compared to traditional microscopic estimates for a synoptic understanding of phytoplankton species abundance, biomass, and diversity (Alvarez et al. 2014). Meanwhile, spectrofluorometric techniques are used for total phytoplankton biomass estimation by quantifying Chl *a* which is used as a proxy for all the phytoplankton present in the water (Holmes et al. 1965) and phycocyanin (PC) is used as the pigment representing the biomass of cyanobacteria(Dash et al. 2011). Similarly, *in situ* devices also provide phytoplankton and cyanobacterial biomass by measuring Chl *a* and PC fluorescence (Gregor and Maršálek 2004; See et al. 2005; Zamyadi et al. 2012). Previous studies using these *in-situ* devices for phytoplankton concentration measurements produced comparable results as laboratory approaches such as spectrophoto- and fluorometric techniques, HPLC & ChemTax, and microscopic analyses such as FlowCam (Buchaca, Felip, and Catalan 2005; See et al. 2005). Enzyme Linked Immunosorbent Assay (ELISA), a technique used for rapid and reliable determination of algal toxins (Dash et al. 2015; Pierce and Kirkpatrick 2001; Ueno et al. 1996) can provide the toxin concentrations but it cannot differentiate between species because sometimes the same toxin is produced by several species of phytoplankton (e.g. microcystins). Additionally, toxin producing species of phytoplankton produce toxins only at certain stages of their life cycle in response to environmental conditions (Marshall et al. 2000). Hence, it is difficult to discern the ability to produce toxins among algal strains solely based on cellular morphology (Baker

et al. 2002). Furthermore, molecular techniques such as Quantitative Polymerase Chain Reaction (QPCR) can provide rapid quantification of total cells of a specific algal group, genus or species, or the total number of cells producing a specific type of toxin (Galluzzi et al. 2004) but this technique is expensive and time consuming compared to other available techniques when the sample size is large.

For making time sensitive decisions related to harmful algal blooms, there is a need for determining suitable techniques and their potential to acquire accurate results rapidly using economically feasible and technically sound methods. Thus, selection of optimal techniques depending on the purpose can prove most useful and can help save a tremendous amount of time and resources. Hence, the main objective of this study was to determine phytoplankton community structure in multiple water bodies including an estuary, several lakes, and a coastal waterbody by employing a multitude of techniques, and evaluating and comparing the potential of these techniques in Mississippi/Louisiana water bodies.

In this study, we investigated whether some techniques can be used as an alternative to another to obtain critical information on harmful algal bloom. This study highlights the strengths and weaknesses of each of the available techniques and provides recommendations on the preferred techniques in various scenarios in water bodies of Mississippi/Louisiana.

2.2 Materials and Methods

2.2.1 Site description

Surface water samples were collected from four major lakes in Mississippi including Ross Barnett Reservoir (RB), Lake Sardis (LS), Lake Enid (LE), and Lake

Grenada (LG), the Lower Pearl River Estuary (LPRE) and the Eastern Mississippi Sound (EMS) (Fig.2.1). Ross Barnett Reservoir is located adjacent to the City of Jackson, the capital city of Mississippi, and Lakes Sardis, Enid, and Grenada are located in northern Mississippi. The Ross Barnett Reservoir is used as a source of drinking water for the City of Jackson and all four lakes have traditionally been used for recreational activities such as swimming, boating, and sports fishing. These lakes produce large quantities of commercial and recreational fish (Dash et al. 2015). The Pearl River originates in Neshoba County, Mississippi and has a meander length of 714 km before emptying into the Gulf of Mexico. The lower185 km of the river forms the part of the boundary between Mississippi and Louisiana, and is termed the Lower Pearl River. The estuary at the lower most portion of the river, the Lower Pearl River Estuary (LPRE) is considered one of the most critical areas of remaining natural habitat in Louisiana (The Nature Conservancy 2017). The Eastern Mississippi Sound (EMS) is the eastern portion of Mississippi Sound along the coasts of Mississippi and Alabama. The Mississippi Sound is rich in marine biodiversity and widely utilized for commercial fishing, shell-fishing, crabbing, and recreation. Seafood harvests in the Mississippi Sound, particularly shellfish and crabs, have been declining because of pollution, and frequent hurricanes, flooding, and droughts. Since all these water bodies are used either as drinking water sources or for fishing and recreational purposes, the algal blooms in these water bodies pose a serious threat to the human and aquatic ecosystem health. Thus, these water bodies were chosen for this study. Also, the outcome from this study can be applicable to other water bodies in United States and globally.

Field data and water samples were collected from twelve sites in each of the lakes on twelve sampling trips during the summer of 2012 and 2013 (Table 2.1). Each sampling points were approximately 1 km apart from each other and 12 sampling locations per lake made an ideal sample numbers to sample per day that could represent the ecosystem health of the lakes. The sampling was carried out during the summer in the lakes because the motive of our study was to capture high concentration of phytoplankton and algal blooms occur mostly during the summers.

The EMS was sampled once in October 2012 and five times during the summer of 2013, and LPRE was sampled five times, once each in December 2014, March 2015, May 2015, August 2015, and December 2015 (Table 1). EMS was sampled mostly during the summer but one sampling event was carried out during the fall to observe any variability in algal concentration in EMS. The sampling in the Lower Pearl River Estuary was carried out in each season to capture the seasonal variation in algal blooms. In the field, water samples were collected in clean Nalgene bottles. *In situ* remote sensing reflectance measurements were made using a GER 1500 spectro-radiometer (Spectravista Inc., Poughkeepsie, NY, USA), and backscattering and fluorescence measurements made using two Eco-Triplets (Wetlabs Inc., Philomath, OR, USA). Measurements of physical parameters (temperature, pH, salinity, and conductivity) were made using a calibrated multiparameter probe (Hanna Instruments, Woonsocket, RI, USA).

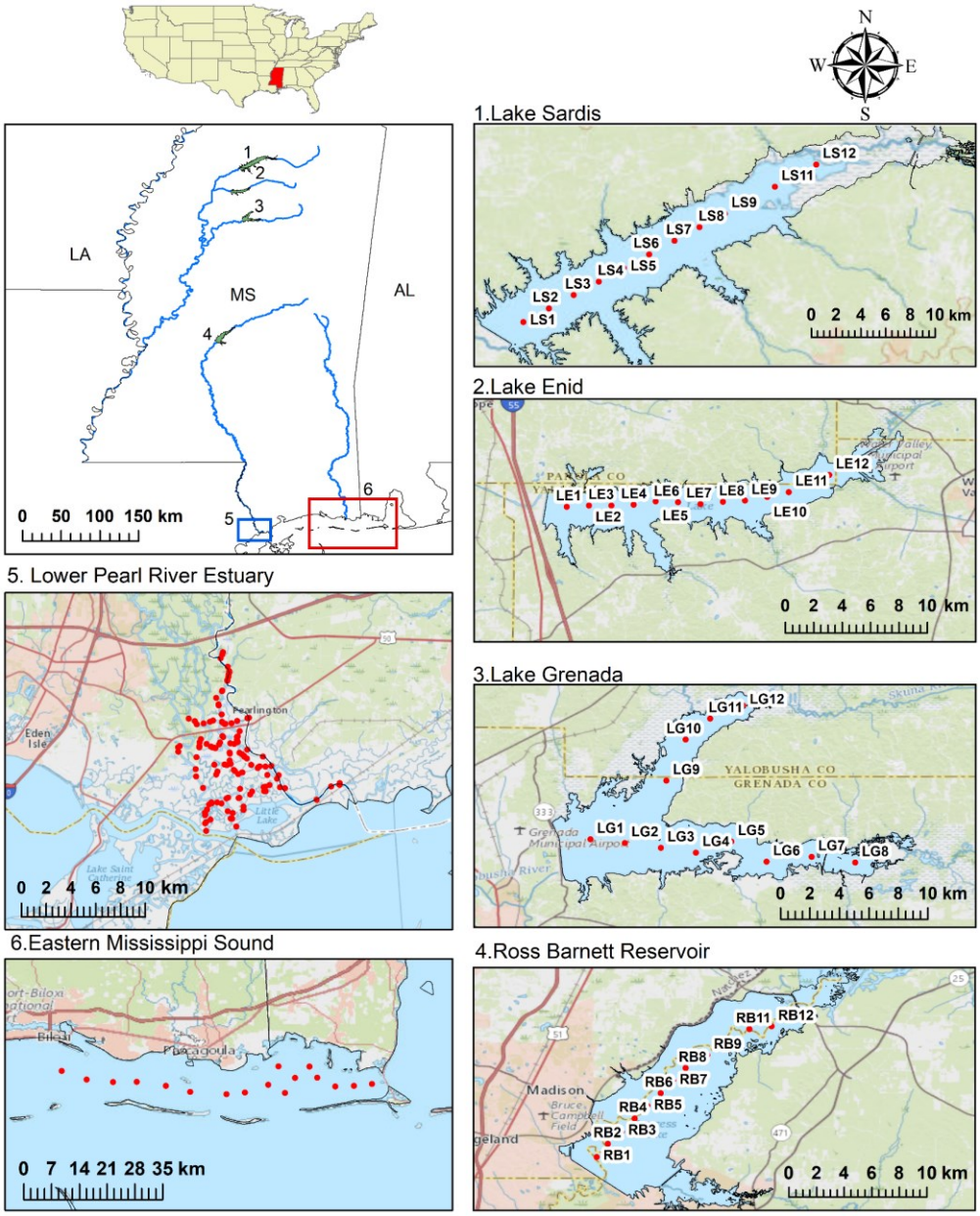

Figure 2.1 Study area map

Table 2.1 Dates of field data and water sample collection in Lower Pearl River Estuary (LPRE), Eastern Mississippi Sound (EMS), Ross Barnett Reservoir (RB), Lake Sardis (LS), Lake Enid (LE), and Lake Grenada (LG)

LPRE	EMS	RB	LS	LE	LG
2014 December16-18	2012 October 18	2012 June 13	2012 June 26	2012 June 20	2012 June 20
2015 March16-19	2013 June 18	2012 June 29	2013 June 18	2013 June 11	2013 June 18
2015 May 18-22	2013 June 23	2013 May 22			
2015 August 10-13	2013 June 30	2013 July 10			
2015 December 14-16	2015 July 10	2014 July 25			
	2015 August 31				
	2015 October 8				

2.2.2 Water sample processing and preservation

Water samples were collected for FlowCam, HPLC, Chl *a*, PC, and phycotoxin analyses. Surface water samples were collected in four clean one liter Nalgene bottles, placed in a cooler with ice, and processed within 5-6 hours of collection. Subsamples were preserved in 4% glutaraldehyde and stored at 4° C until analysis using FlowCam. For HPLC analysis of photopigments including Chl *a*, 100 mL aliquots of surface water were filtered onto 4.7 cm diameter glass fiber filters (Whatman GF/F), immediately frozen, and stored at −80 °C. 50 mL aliquots of surface water were filtered (<50 kPa) for PC and 100 mL aliquots of surface water were filtered (<50 kPa) for Chl *a* and kept frozen (-80°C) until analysis using a Horiba Jovin Yvon FluoroMax-4 Spectrofluorometer (Horiba Scientific, Edision, NJ, USA). For phycotoxins, 20 mL of aliquots of surface samples were stored in 20 ml glass vials and kept frozen at -80 °C until analysis

2.2.3 Semi-automated processing of FlowCam samples for enumeration of phytoplankton and species composition

2.2.3.1 *FlowCam imaging*

One mL aliquots of glutaraldehyde-fixed subsample were run for analysis with 20X magnification to digitize particles between 5 μm and 100 μm in size. The lower limit for magnification corresponds to particles that could not be resolved by the FlowCam procedure we used, and thus they were not considered. In FlowCam, photographs can be captured in either auto-image mode or fluorescence-triggered mode. In auto-image mode, photographs are taken at a constant rate capturing images of each particle passing through the flow cell in front of the camera, while in fluorescence-triggered mode, photographs are taken of particles that emit fluorescent light, such as that emitted by excited phytoplankton photopigments. In this study, the samples were analyzed in fluorescence-triggered mode as we were interested in capturing images of phytoplankton only. Thirty minutes were considered the maximum running time for each subsample with a flow rate of 0.025mL min^{-1} at a capture rate of 20 frames per second. The Visual Spreadsheet software of FlowCam extracts each particle present in the photograph using an image segmentation algorithm, and stores the photographs on the computer. The result is a plankton sample converted into a collection of images, each containing an individual particle. These images are combined in collages that constitute the raw output of the Visual Spreadsheet. In addition to the collage of images, the Visual Spreadsheet also stores ancillary information of each particle that includes over 40 different measurements including area, volume, perimeter, shape, size, and aspect ratio.

2.2.3.2 *Classification of images*

To classify images captured by FlowCam, the semi -automated process of image classification was followed in the Visual Spreadsheet software, where we created a library of each identified species in the sample. Then a training set for each species was generated from visually identified species from the collage of images and were matched with the species stored in library. Once the images of species were sorted based on the training sets, they were manually corrected for any artifacts present in the selected images through visual recognition (Zarauz et al. 2007)

2.2.3.3 *Estimation of Area*

Area Based Diameter (ABD) of each species and taxa, as recorded and calculated by FlowCam. was used to estimate the relative abundance following (Garcia et al. 2010). The reason for using the ABD instead of particle counts was that the area would give more accurate estimates of phytoplankton biomass and would be comparable to the estimates provided by HPLC-ChemTax and *in situ* probes due to the size variation of phytoplankton cells between taxa and species (J.Nicole and Martin L.Jennifer 2010).

To calculate the relative abundance of the phytoplankton groups identified by FlowCam, the species information presented above were further grouped into six taxonomical classes including cyanobacteria, diatoms, dinoflagellates, chlorophytes, chrysophytes, and euglenophytes for comparison with the relative abundance obtained using HPLC and ChemTax. Unresolved particles were grouped as unidentified cells or detritus. Relative abundance was calculated by adjusting cell counts for the surface area for all the species of all taxonomic groups. Area of chlorophytes and euglenophytes were combined for LPRE samples to generate a comparable result of relative abundance as

determined by HPLC-ChemTax because the HPLC-ChemTax estimated the pigment concentration of chlorophytes and euglenophytes combined.

2.2.4 Determination of phytoplankton class abundances using HPLC and ChemTax

For HPLC pigment analysis, the filter papers were shipped overnight on dry ice to the University of South Carolina, Columbia, SC. High performance liquid chromatography (HPLC) was used to separate, identify, and quantify phytoplankton photosynthetic pigments. First, filters were lyophilized (-50˚C, vacuum of 0.50 atm) for 20-24 h, followed by extraction in 90% aqueous acetone (600-750 µl at -20°C for 18-22 h). The internal standard was the synthetic carotenoid pigment β-apo-8'-carotenal (Sigma). Filtered extracts (250 µl) were injected into a Shimadzu HPLC (LC-10AT) equipped with reverse- phase C18 columns (Rainin Microsorb, 0.46 × 1.5 cm, 3 µm packing, Vydac 201TP54, 0.46 × 25 cm, 5 µm packing) in series as the solid phase. Gradients and flow conditions are described in Pinckney et al. (2001). A Shimadzu SPD-M10av photodiode array detector was used to obtain absorption spectra and chromatograms (440 ± 4 nm). Pure standards (DHI, Denmark) were used to confirm peak identities and retention times.

ChemTax (v. 1.95) was used to determine the relative abundances of major phytoplankton groups based on photopigment (Higgins HW, Wright SW 2011; J. Pinckney et al. 2001). The major phytoplankton groups used for ChemTax categories were based on qualitative microscopic examinations of water samples. The initial pigment ratio matrix was derived from (Higgins HW, Wright SW 2011; Schlüter,

Møhlenberg F., Havskum. H 2000) and the convergence procedure outlined by (Latasa Mikel 2007) was used iteratively to correct for inaccuracies in pigment ratio seed values

2.2.5 *In situ* phytoplankton quantification based on Chl *a*, PC, and phycoerythrin.

Ecotriplet FL3B (Wetlabs inc., Philomath, OR), an *in-situ* submersible fluorescence probe with three sensors specific to Chl *a* (ex/em 470/695 nm), PC (ex/em: 630/680 nm) and phycoerythrin (PE) (ex/em: 518/595 nm) was used to measure the pigment concentration of Chl *a*, PC, and PE by lowering the probe into the water so that the sensors are a few centimeters below the water surface.

2.2.6 Spectrofluorometric quantification of PC.

Fifty mL subsamples of surface water were filtered (<50 kPa) onto polycarbonate filters with 4.7 cm diameter and 0.2 μm pore size, and kept frozen at -80 °C freezer until analysis for determination of PC concentrations. PC was extracted in 50 mM phosphate buffer by cell disruption using a probe sonicator (Fisher Scientific™ Model 50 Sonic Dismembrator) and fluorescence intensity was measured using a Horiba Jovin Yvon FluoroMax-4 Spectrofluorometer (Horiba Scientific, Edision, NJ, USA) at 615 nm excitation and 647 nm emission using the standard protocol (Horvátha et al. 2013)

2.2.7 Spectrofluorometric quantification of Chl *a*

To quantify Chl *a* concentration, 100 mL aliquots of surface water were filtered (<50 kPa) onto GF/F filters with 4.7 cm diameter and 0.7 μm pore size, and kept frozen at -80°C until analysis. Chl *a* was extracted using 90% acetone and determined spectrofluorometrically using a Horiba Jovin Yvon FluoroMax-4 Spectrofluorometer

(Horiba Scientific, Edision, NJ, USA) following standard laboratory protocol (Joint global Ocean Flux Study, 1998).

2.2.8 Toxin analysis

The three phycotoxins, microcystins, brevetoxin by dinoflagellates, and domoic acid were analyzed by Enzyme Linked Immunosorbent Assay (ELISA) technique following manufacturer's protocol (Abraxis LLC, PA, USA). Toxins were analyzed manually for samples from lakes and Eastern Mississippi Sound using the toxin analysis kits, but samples from LPRE were analyzed using a Cyanotoxin Automated Assay System (CAAS) (Abraxis LLC, PA, USA). Twenty mL of water sample were collected and frozen at -4˚C until analysis for all three types of toxins in the CAAS. For manual determination of microcystins, 50 ml of subsamples were filtered onto 2.5 cm diameter glass fiber filters (Whatman GF/F), and kept frozen at −80 °C. On the day of the analysis, 5 mL of extraction solvent (methanol: water: acetic acid: 50:49:1) was added to the filter papers, vortexed for 1 minute, sonicated for 2 minutes at 30–40 watts output on ice and centrifuged for 10 minutes at 3000 rpm, and the supernatant was collected for the determination of cellular microcystin concentrations using an ELISA kit (Abraxis LLC, Warminster, PA, USA). Brevetoxin and domoic acid were extracted using deionized water and analyzed using the same protocol as for microcystin.

2.3 Results

2.3.1 Species composition and relative abundance determined by FlowCam

We found 108 different species of phytoplankton in all the study areas combined (Table A1& A2), in which 52 species of phytoplankton were found in EMS (Table A3),

86 species in LPRE (Table A4), 79 species in RB (Table A4), 54 species in LS (Table A5), 58 species in LE (Table A6), and 41 species were found in LG (Table A7).

FlowCAM derived species composition revealed that cyanobacteria were the most diverse class in LPRE, RB, LS, LE, and LG whereas diatoms were the most diverse class in EMS with at least 19 species identified. Among all the study areas, cyanobacteria were found to be most diverse in LPRE (Fig. 2.2 & Fig 2.3). In the lakes (RB, LS, LE, LG), chlorophytes were the second most diverse class after cyanobacteria, except in RB where on two occasions, chlorophytes were the most diverse (Fig.2.4-Fig2.7). Meanwhile, diatoms were the most diverse species in EMS with at least 19 species identified (Fig.2.8 & Fig2.9). Using FlowCam, the toxin-producing diatom genus *Pseudo-nitzschia*, could not be distinguished from cryptic forms of other diatom species. Similarly, dinoflagellates of genus *Prorocentrum* were not further identified into species level, and chlorophytes of genus *Chlamydomonas* could not be further identified to species level. Due to their small cell size, these genera could not be identified to the species level because morphological differences were not distinguishable.

By measurements of relative abundance using FlowCam, cyanobacteria were found to be the most abundant group based on their total surface area at all the study sites in LPRE (Fig.2.10). Similarly, in RB cyanobacteria were dominant on three sampling

dates (Fig.2.11 a, c, and d) and diatoms dominant on one sampling date (Fig. 2.11b), followed by cyanobacteria. Likewise, all remaining lakes (LS, LE and LG) were dominated by cyanobacteria, and the chlorophytes were the second dominant algal group (Fig. 2.12). EMS was also dominated by cyanobacteria during 5 out of 6 sampling dates (Fig.2.13).

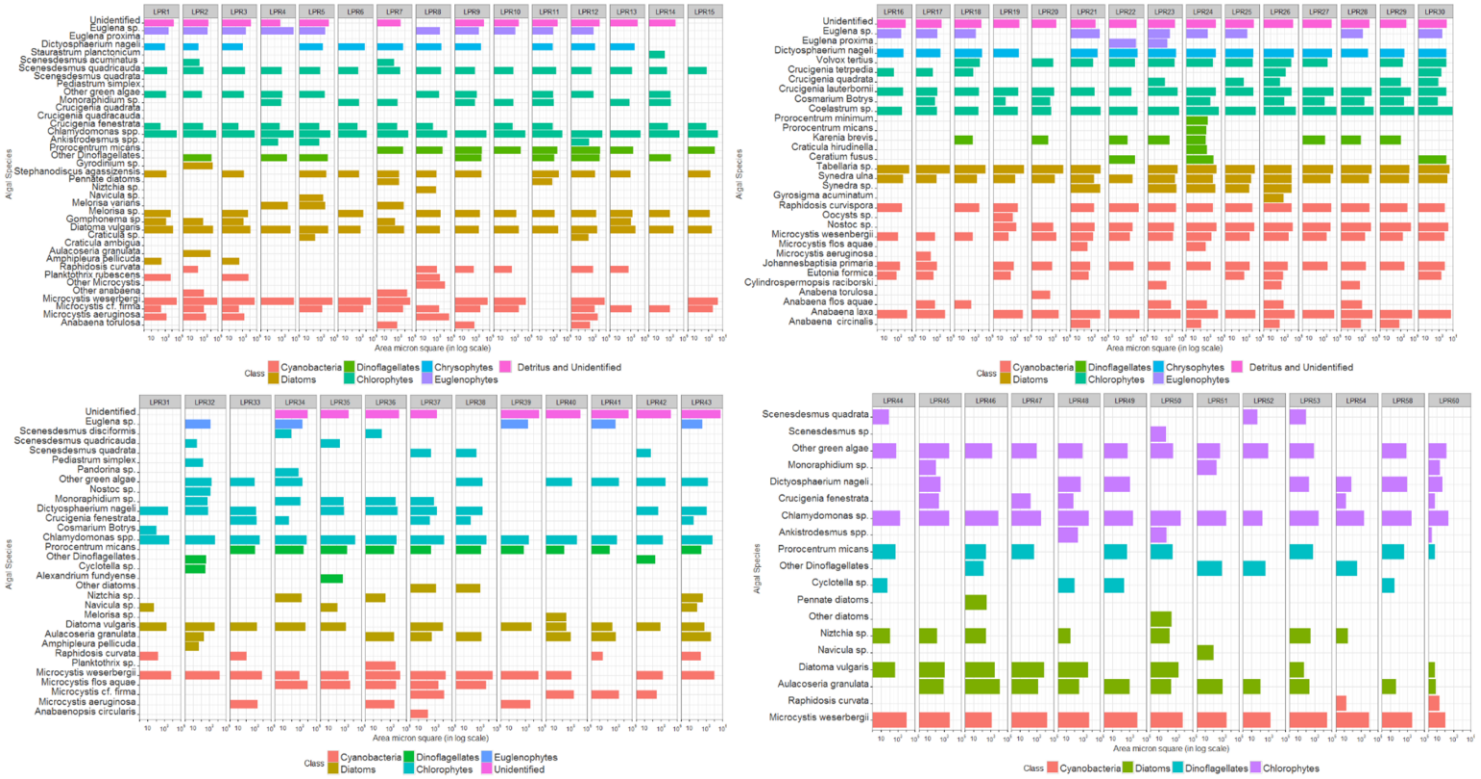

Figure 2.2 Phytoplankton species composition in Lower Pearl River Estuary at sites (LPR1-LPR60).

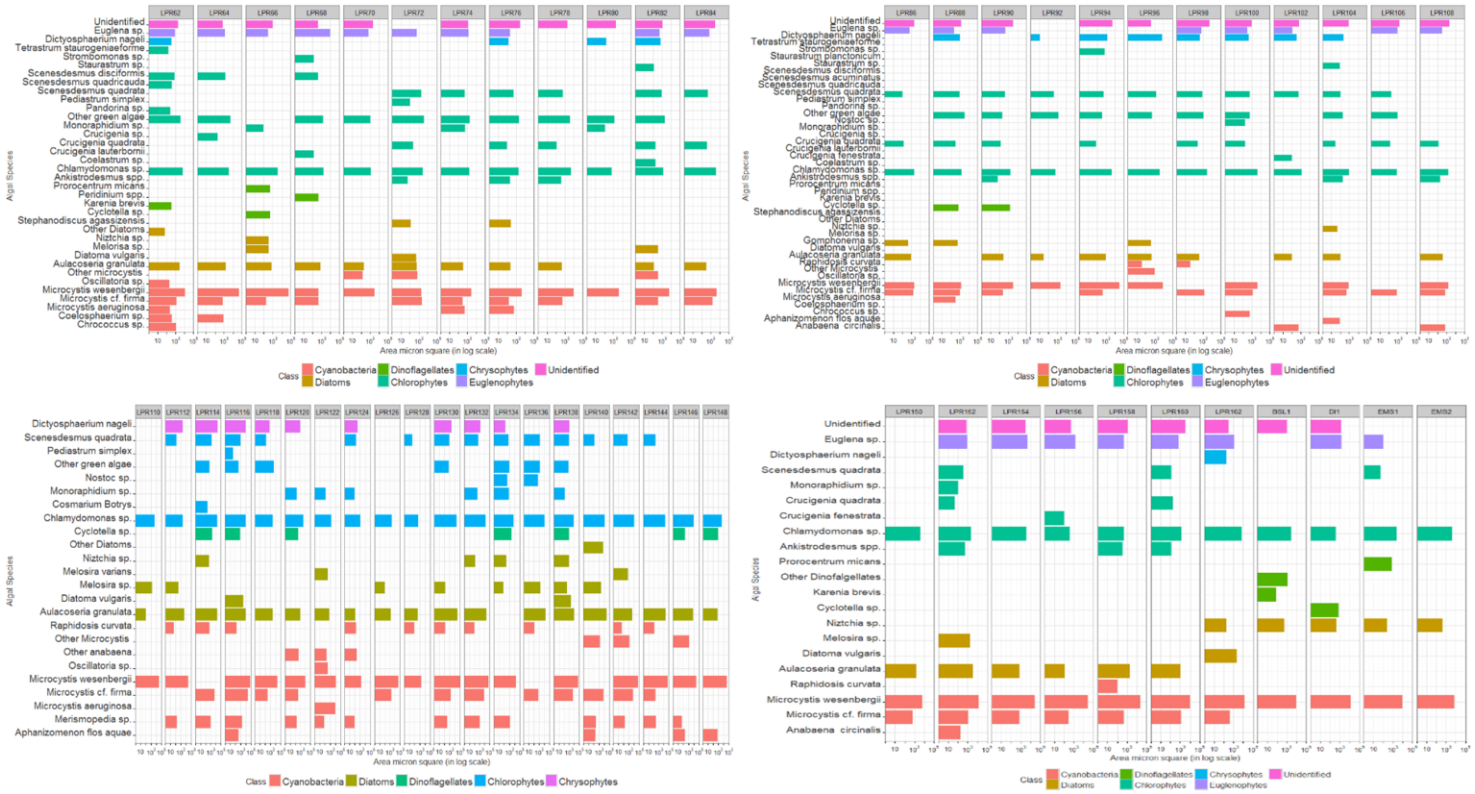

Figure 2.3 Phytoplankton species composition in Lower Pearl River Estuary at selected sites (LPR62-LPR162, BSL1 = near Bay St. Louis, DI1 = near Deer Island, EMS1 = a site in the East Mississippi Sound, and EMS2= another site in the East Mississippi Sound)

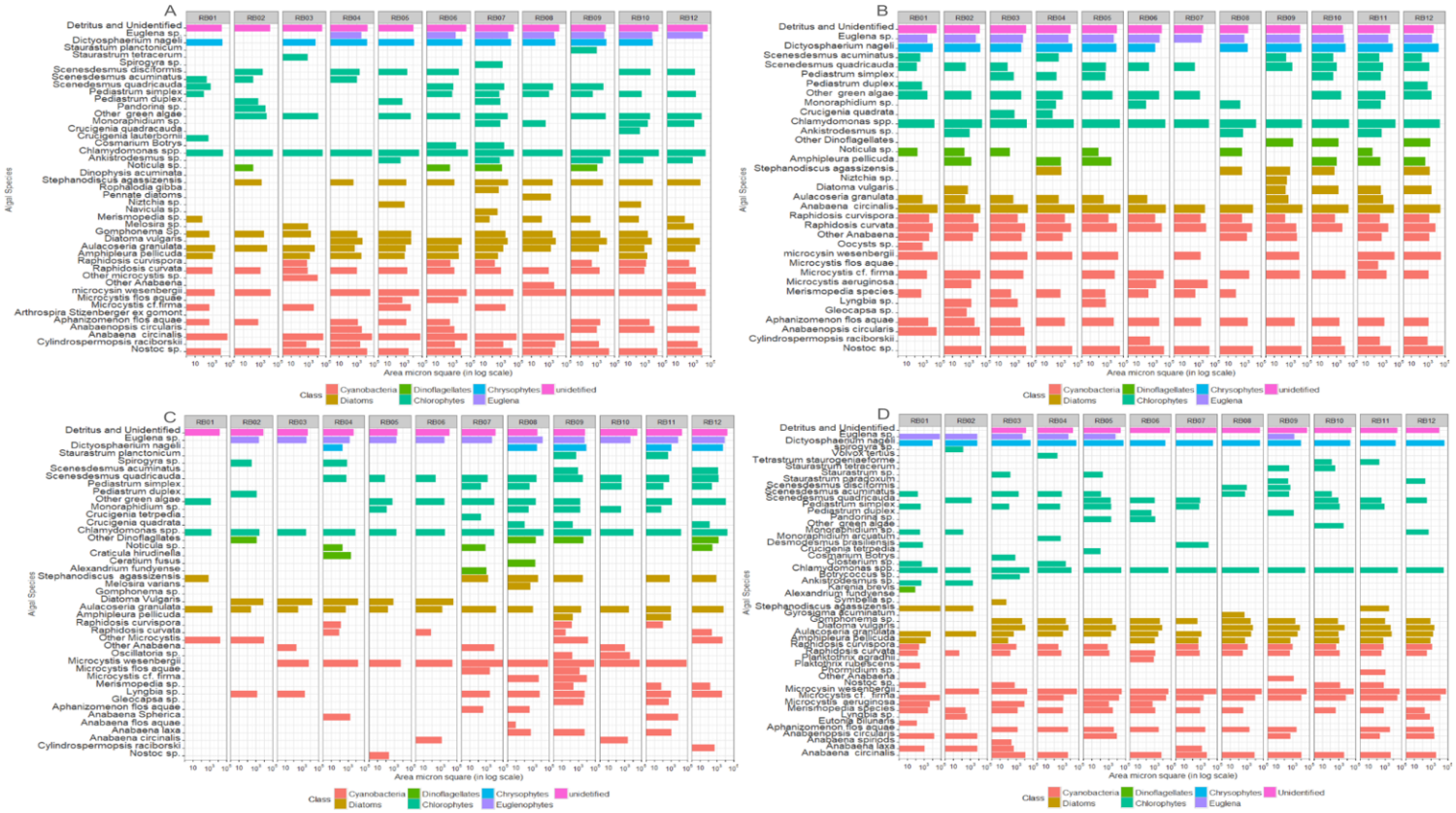

Figure 2.4 Phytoplankton species composition in Ross Barnett Reservoir (RB) on (A) June 13, 2012, (B) June 29, 2012, (C) July 10, 2013, and (D) May 22, 2012)

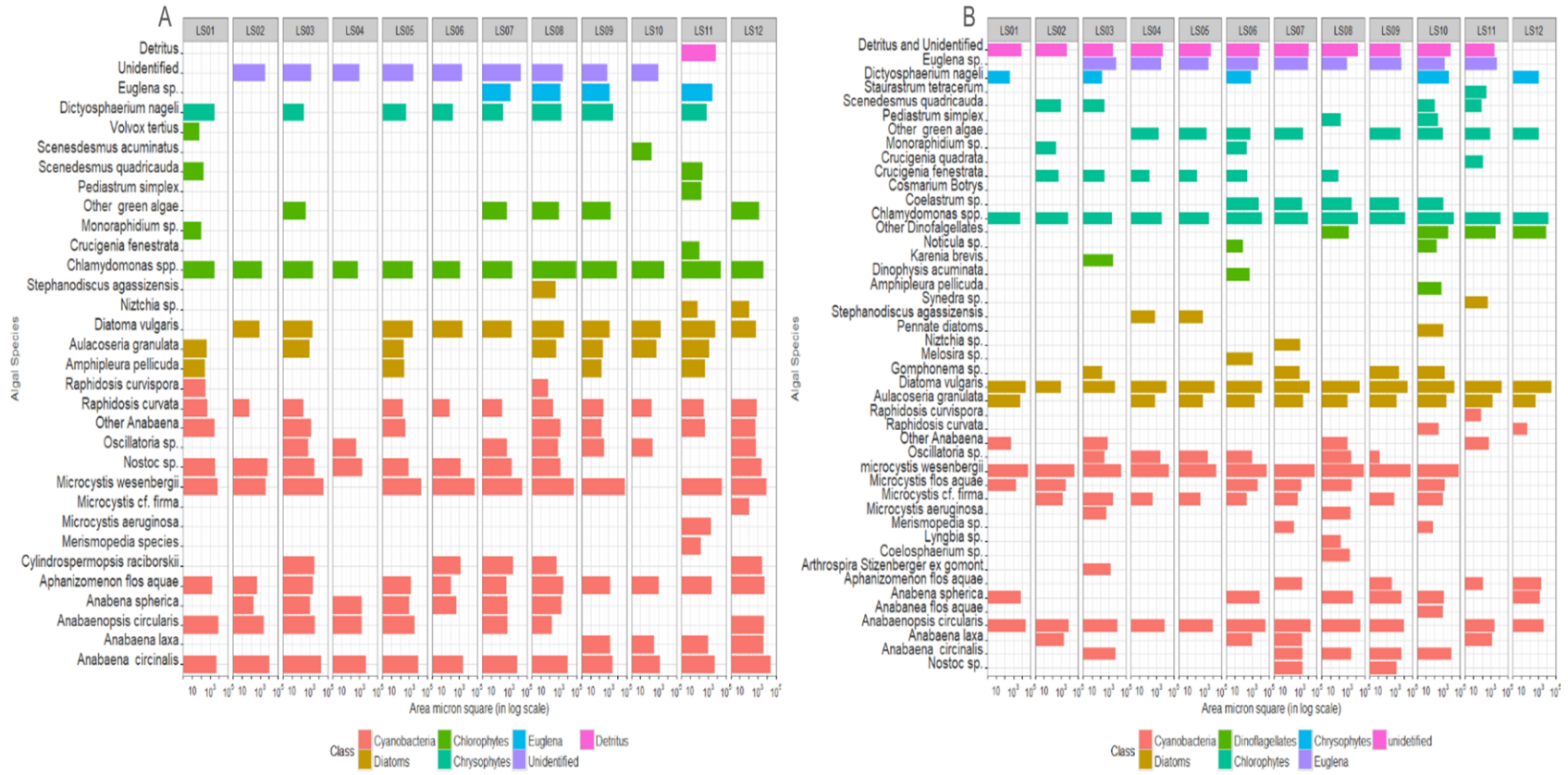

Figure 2.5 Phytoplankton species composition in Lake Sardis (LS) on (A) June 26, 2012, (B) June 18, 2013

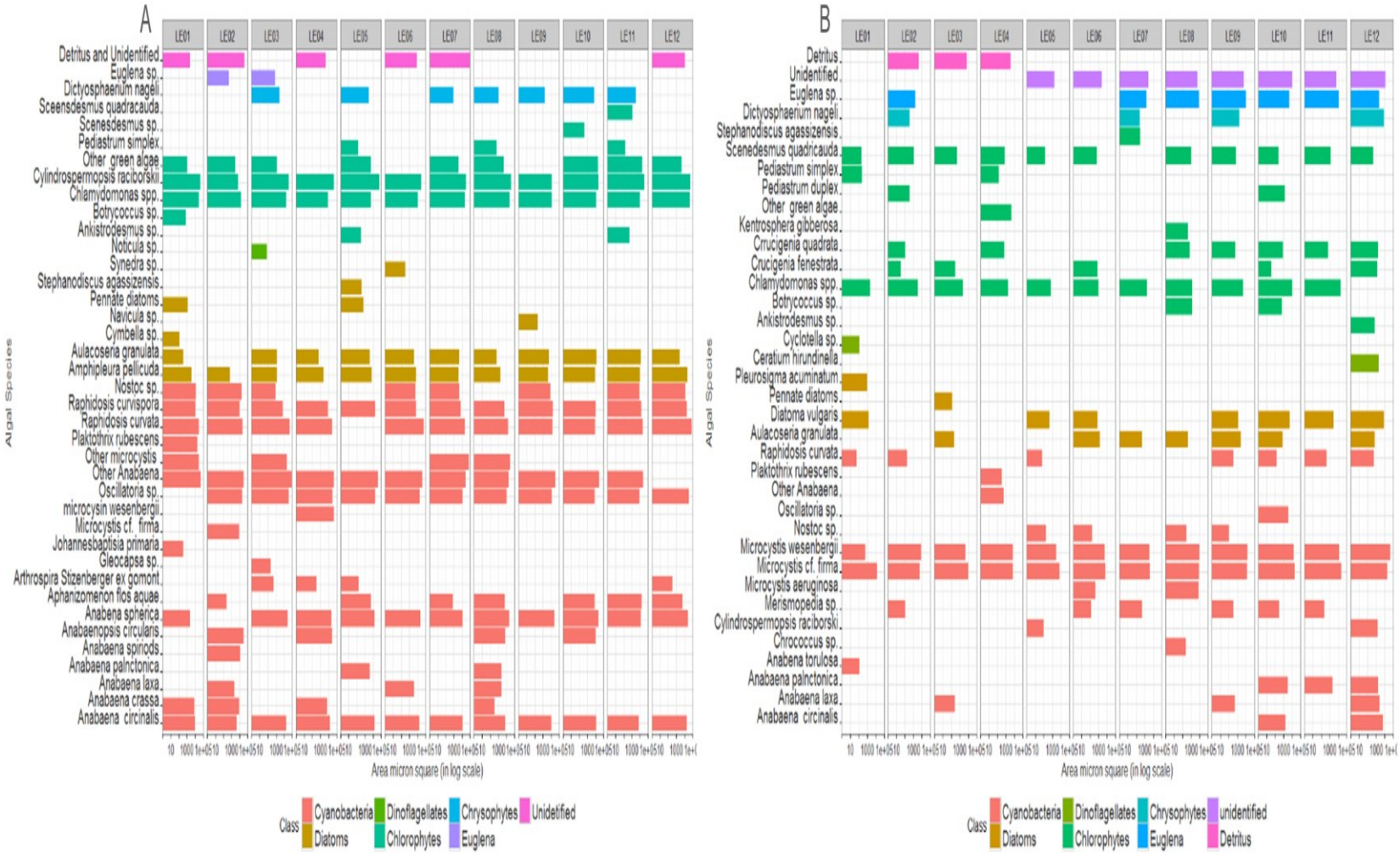

Figure 2.6 Phytoplankton species composition in Lake Enid (LE) on (A) June 20, 2012, (B) June 11, 2013

Figure 2.7 Phytoplankton species composition in Lake Grenada (LG) on (A) June 18, 2012, (B) June 4, 2013

Figure 2.8 Phytoplankton species composition in East Mississippi Sound (EMS) on (A) October 18, 2012, (B) June 2, 2013, (C) June 16, 2013, and (D) June 23, 2013

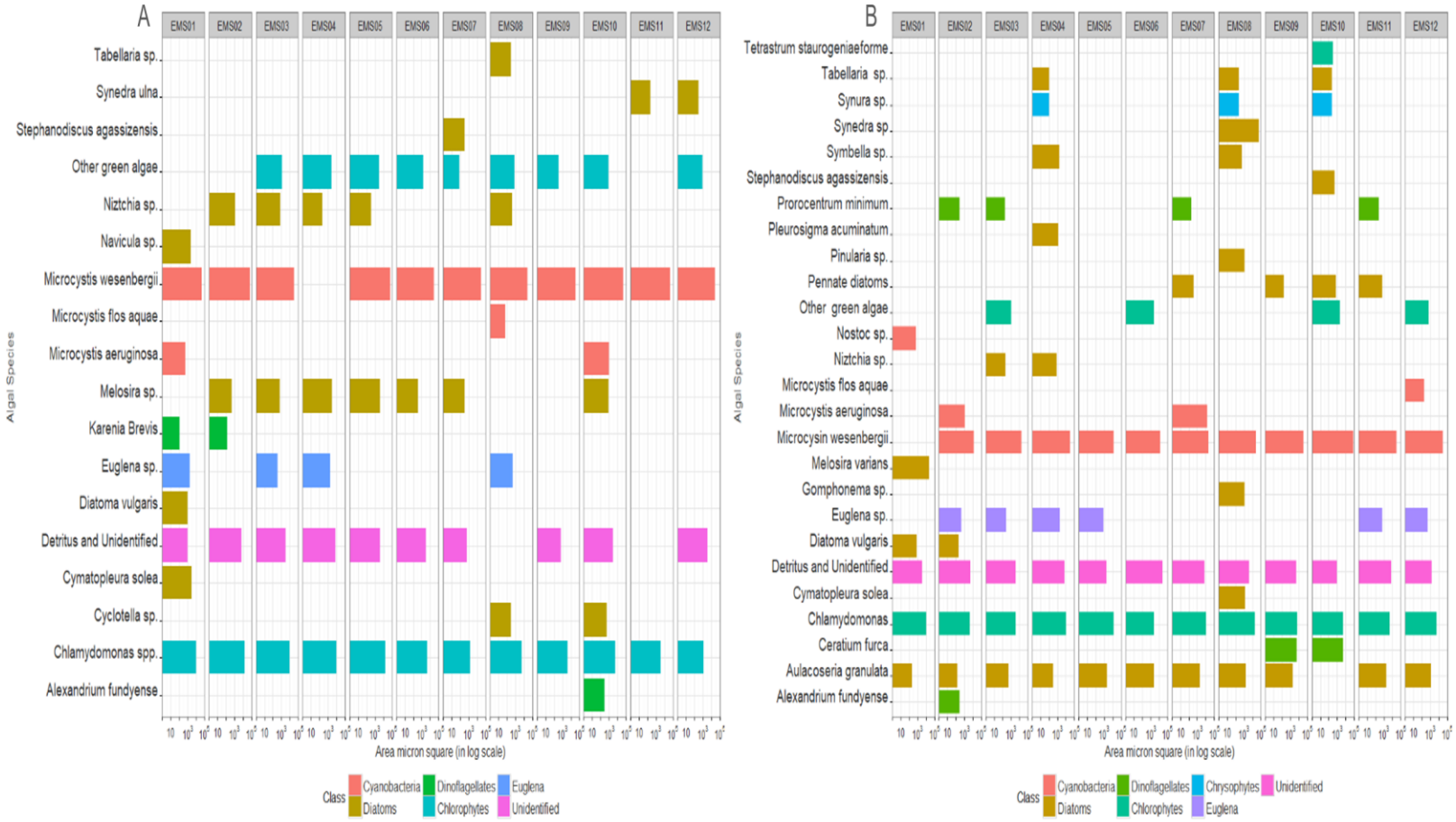

Figure 2.9 Phytoplankton species composition in East Mississippi Sound (EMS) on (A) June 30, 2013 and (B) July 14, 2013

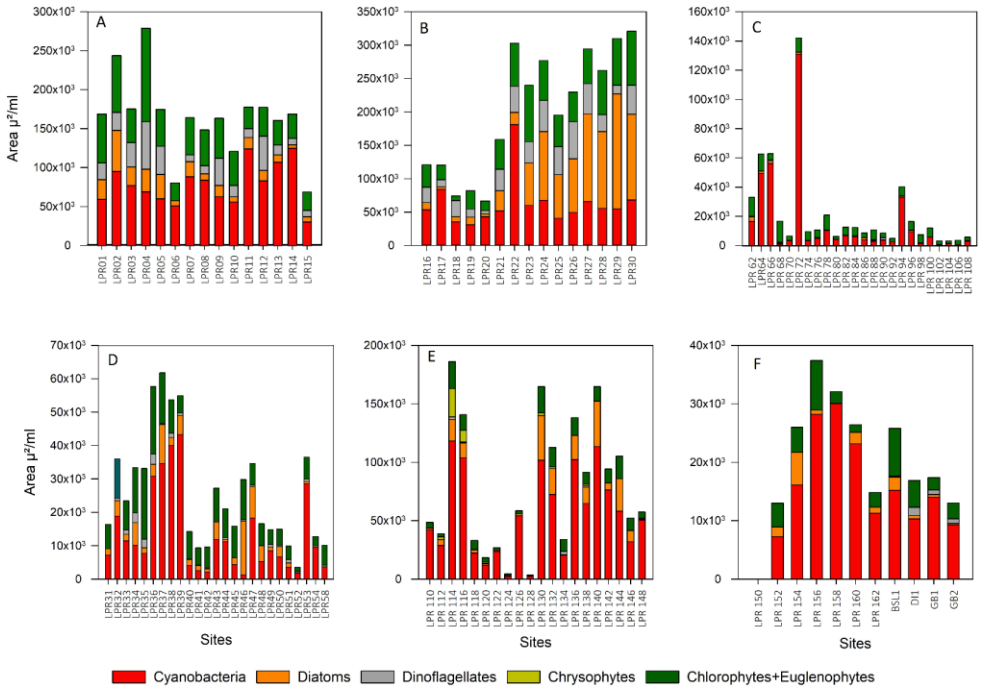

Figure 2.10 Relative abundance of phytoplankton present in Lower Pearl River Estuary (LPRE) determined by FlowCam. Area of species present in each taxon were summed up in order to make the results comparable with ChemTax analysis

A-B) Relative abundance of phytoplankton in samples collected in December 2014, C) Relative abundance of phytoplankton in samples collected on May 2015, D) Relative abundance of phytoplankton in samples collected in March 2015, E) Relative abundance of phytoplankton in samples collected on August 2015, F) Relative abundance of phytoplankton in samples collected on December 2015 from LPRE.

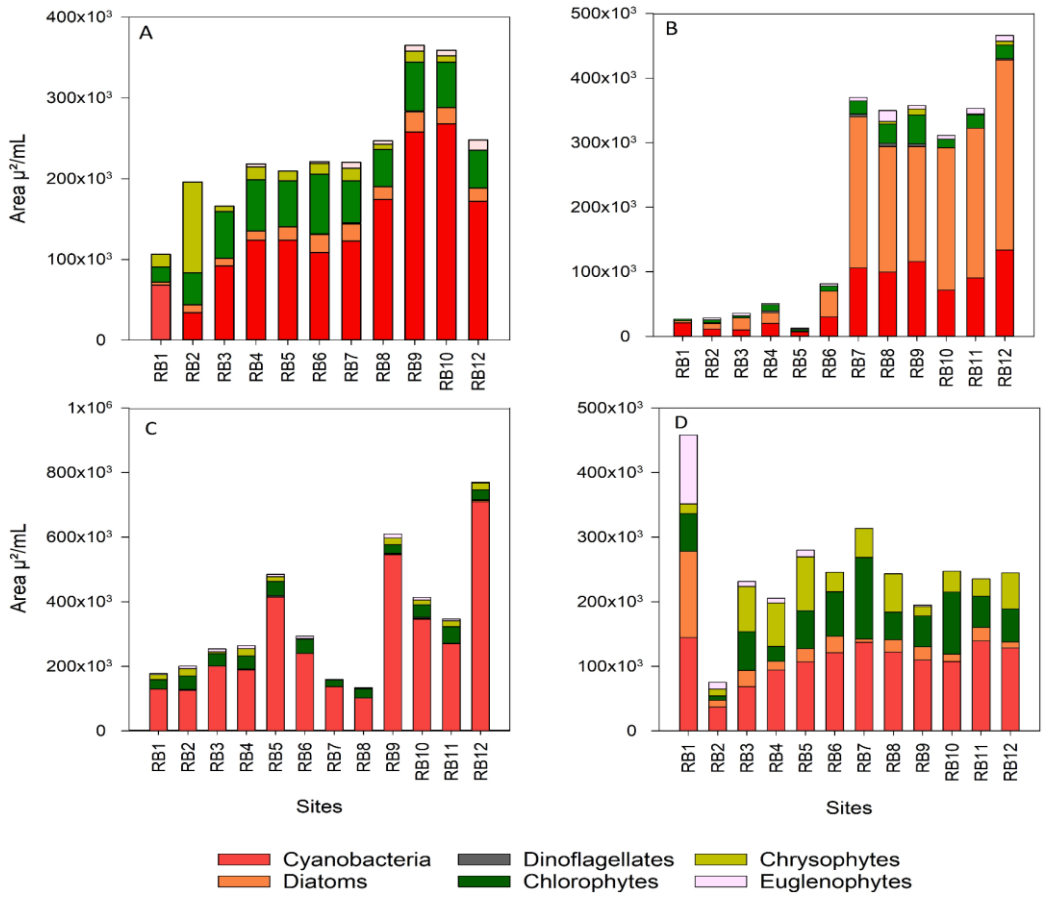

Figure 2.11 Relative abundance of phytoplankton present in Ross Barnett Reservoir (RB) determined by FlowCam.

Area of species present in each taxon were summed up in order to make the results comparable with ChemTax analysis. A) Relative abundance of phytoplankton in samples collected on June 13, 2012, B) Relative abundance of phytoplankton in samples collected on May 22, 2013, C) Relative abundance of phytoplankton in samples collected on June 29, 2012, D) Relative abundance of phytoplankton in samples collected on July 10, 2013

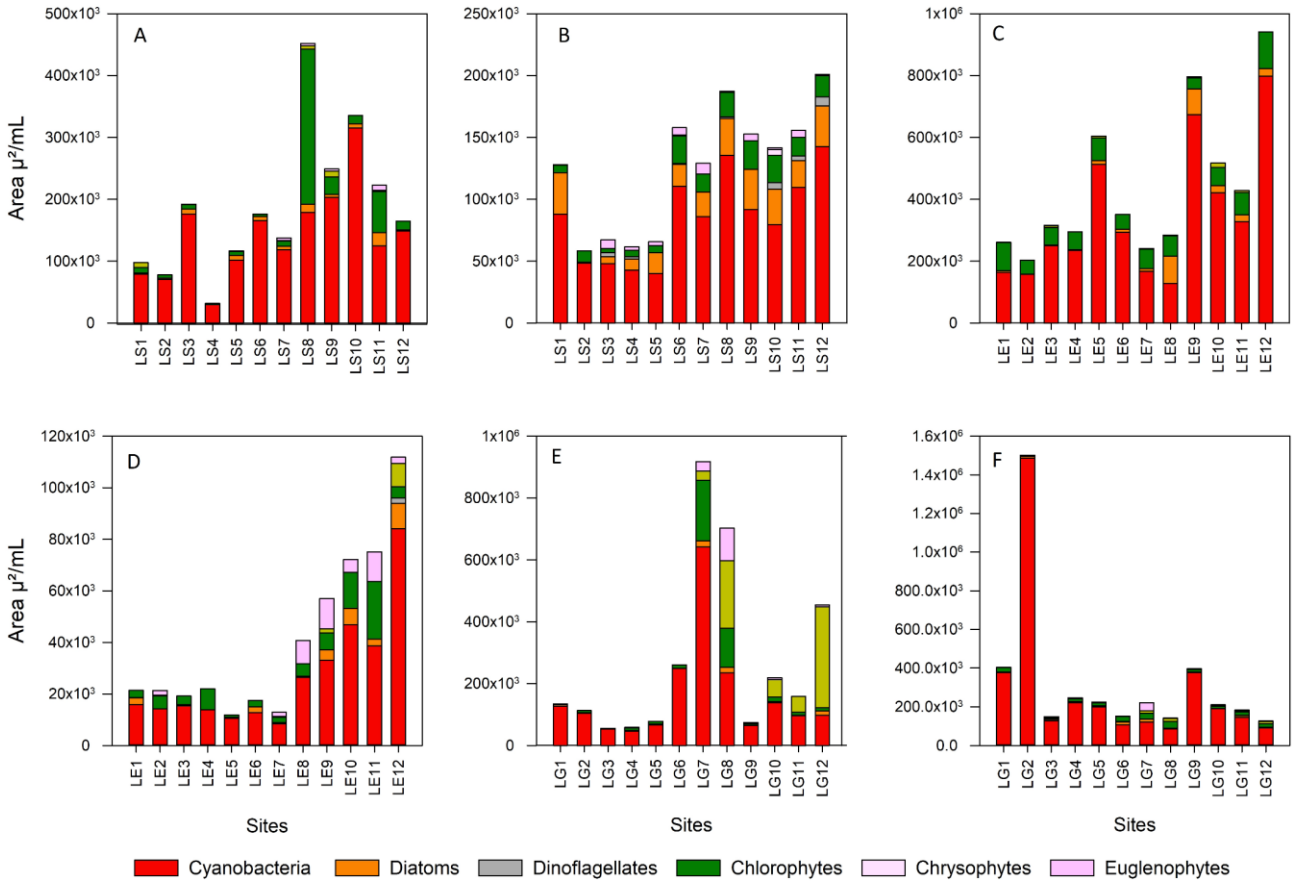

Figure 2.12 Relative abundance of phytoplankton present determined by FlowCam

Place (A, B) in Lake Sardis (LS) on two sampling dates June 26, 2012 and June 18, 2013; (C, D) in Lake Enid (LE) on two sampling dates June 20, 2012 and June 11, 2013; and (E, F) in Lake Grenada (LG) on June 18, 2012 and June 4, 2013

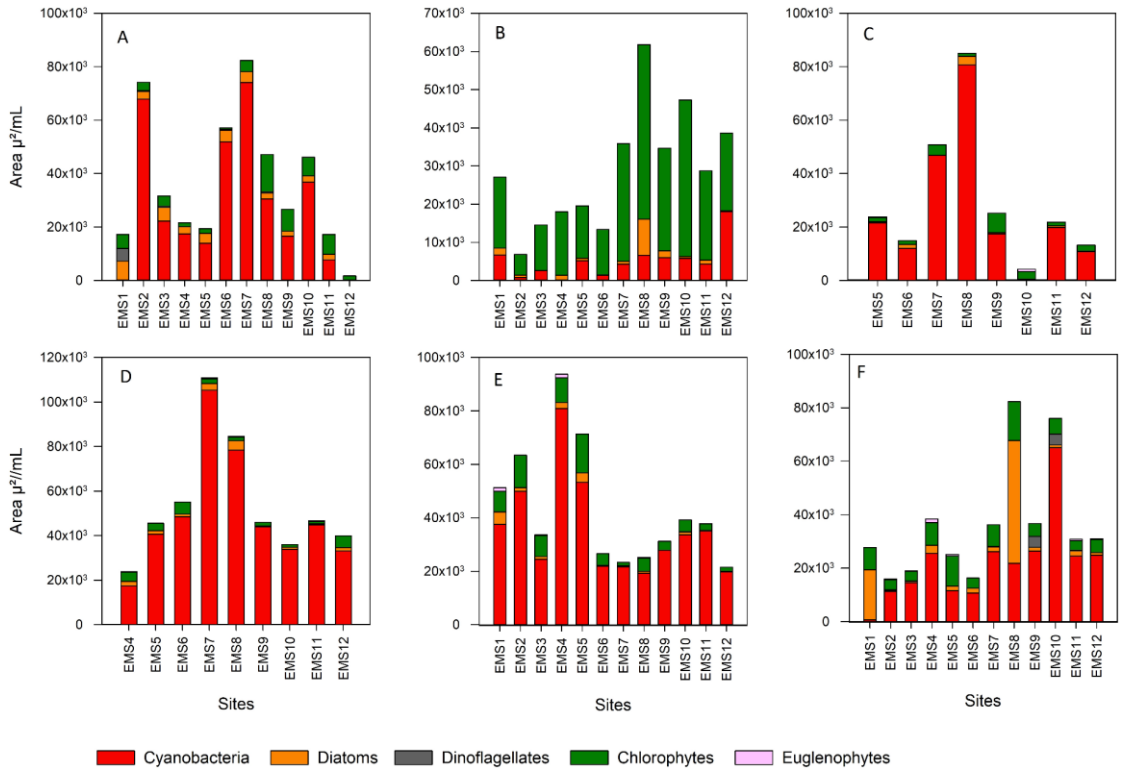

Figure 2.13 Relative abundance of phytoplankton present in East Mississippi Sound (EMS) determined by FlowCam.

Area of species present in each taxon were summed up in order to make the results comparable with ChemTax analysis. A) Relative abundance of phytoplankton in samples collected on October 2012, B) Relative abundance of phytoplankton in samples collected on June 2, 2013, C) Relative abundance of phytoplankton in samples collected on June 16, 2013, D) Relative abundance of phytoplankton in samples collected on June 23, 2013, E) Relative abundance of phytoplankton in samples collected on June 30, 2013, F) Relative abundance of phytoplankton in samples collected on July 14, 2013 from EMS

2.3.2 Relative abundance determined by pigment analysis

Relative abundance of phytoplankton determined by HPLC-ChemTax in LPRE revealed that diatoms were the most abundant group with concentrations ranging from 2 to 7.1 µg Chl *a*/L in December 2014, chlorophytes were found to be most abundant in March, 2015, and chlorophytes and haptophytes were most abundant in May 2015 (Fig. 2.14). The relative abundance of phytoplankton in four Mississippi lakes determined by HPLC-ChemTax have previously been described in Dash et al. 2015(Dash et al. 2015). RB was dominated by euglenophytes on June 13, 2012, May 22, 2013, and July 10, 2013, whereas cyanobacteria was dominant on June 29, 2012. LE was consistently found to be dominated by cyanobacteria whereas LS was dominated by euglenophytes and cyanobacteria, and LG was dominated by chrysophytes and euglenophytes. In all the lakes, cyanobacteria were found to be present in all the sampling sites. The relative abundance of phytoplankton in EMS shows that diatoms were dominant in October 2012 (Fig. 2.15a) but cyanobacteria was dominant during the summer of 2013 (Fig. 2.15b-f). Thus, HPLC-ChemTax method could separate taxa such as haptophytes, cryptophytes and chrysophytes as a separate group that were not clearly distinguishable using FlowCam. Meanwhile, HPLC-ChemTax classified chlorophytes and euglenophytes into a single group so their individual relative abundance could not be quantified, which could be easily separated into two separate groups using FlowCam.

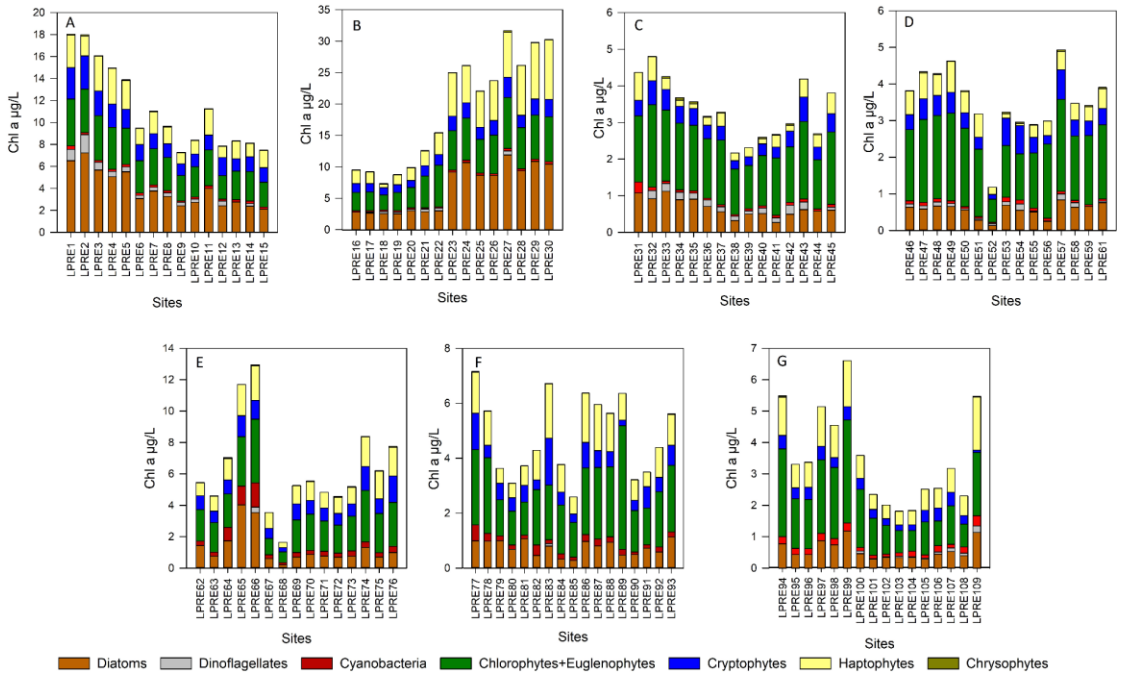

Figure 2.14 Relative abundance of phytoplankton determined by ChemTax in Lower Pearl River Estuary (LPRE) in terms of Chl *a* concentration specific to each taxonomic group

s A,B,C,D,E,F, and G shows the bar graph of relative abundance of phytoplankton in LPRE site 1 through site 109. Sites 1-30 were collected in December 2014, 31-61 were collected in March 2015, and 62-109 were collected in May 2015.

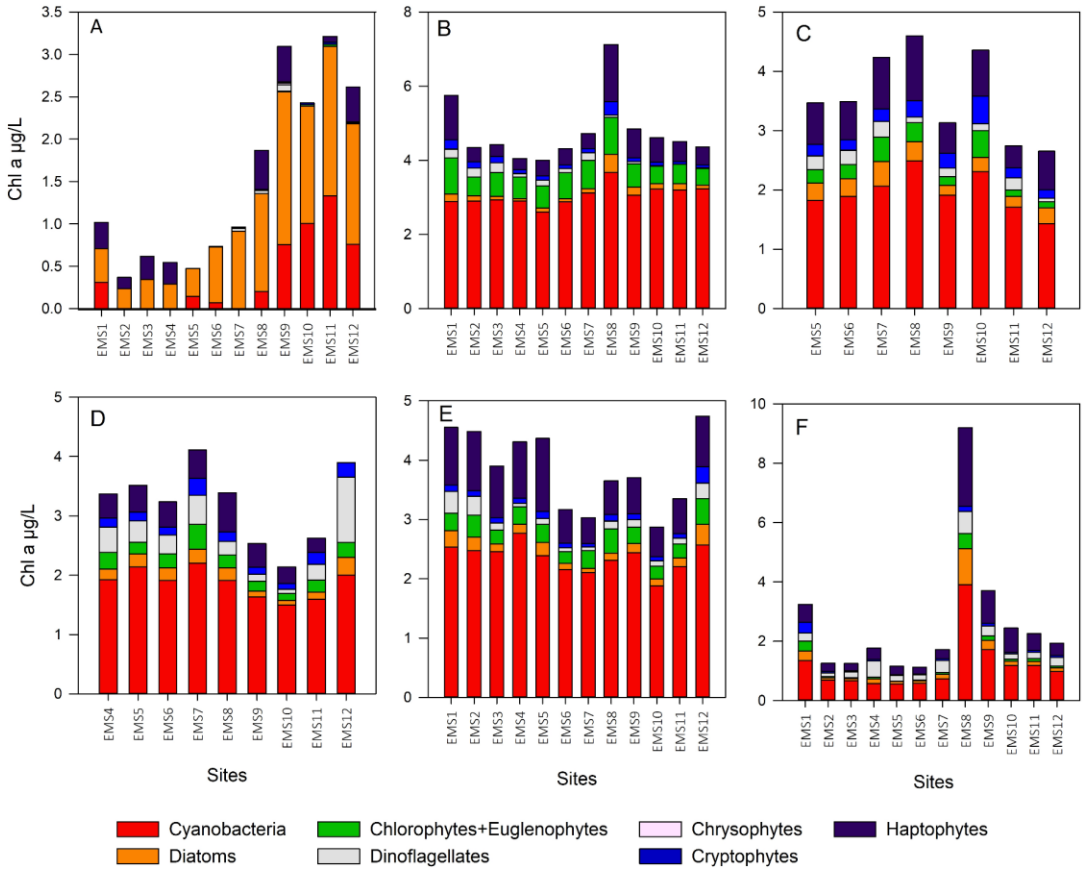

Figure 2.15 Relative abundance of phytoplankton determined by ChemTax in East Mississippi Sound (EMS)

(A) in samples collected on October 18, 2012, (B) in samples collected on June 2, 2013, (C) in samples collected on June 16, 2013, (D) in samples collected on June 23, 2013, (E) in samples collected on June 30, 2013, (F) in samples collected on July 14, 2013

2.3.3 Comparison of relative abundance of phytoplankton determined by FlowCam and ChemTax

The comparison of the results from ChemTax and FlowCam for phytoplankton abundance are shown in Fig. 2.16. In LPRE, we found a good linear relationship ($r=0.9$, $n= 108$, $p<0.01$) between diatoms determined by ChemTax pigment analysis and the relative abundance of diatoms determined using FlowCam (Fig. 2.16a). Also, we found a good correlation between diatom-specific Chl *a* determined by ChemTax and the area of diatoms in two lakes: Lake Grenada ($r=0.79$, $n=12$, $p<0.05$, Fig. 2.16b) and Lake Enid ($r=0.84$; $n=12$, $p<0.05$, Fig. 2.16c). Further, we found a good correlation for chlorophytes ($r=0.72$, $n=12$, $p<0.05$, Fig. 2.16d) in Lake Enid and but a relatively poor correlation for cyanobacteria ($r=0.23$, $n=109$, $p=0.053$, Fig. 2.16e) in LPRE as determined by ChemTax and their area determined using FlowCam. These results suggested that FlowCam and ChemTax can be used as alternative techniques for some groups of phytoplankton, diatoms for example as found in this study, however they do not produce corresponding results for all groups of phytoplankton. Further, use of HPLC-ChemTax approach is limited to taxonomical class, thus no genus and species level of identification can be achieved by using HPLC-ChemTax. If genus or species level information is desired, then FlowCam would be the preferred approach with the caveat that phytoplankton with small cell size cannot be identified to the species level. Thus, both these techniques have some strengths as well as some weaknesses to determine phytoplankton community structure and their abundance.

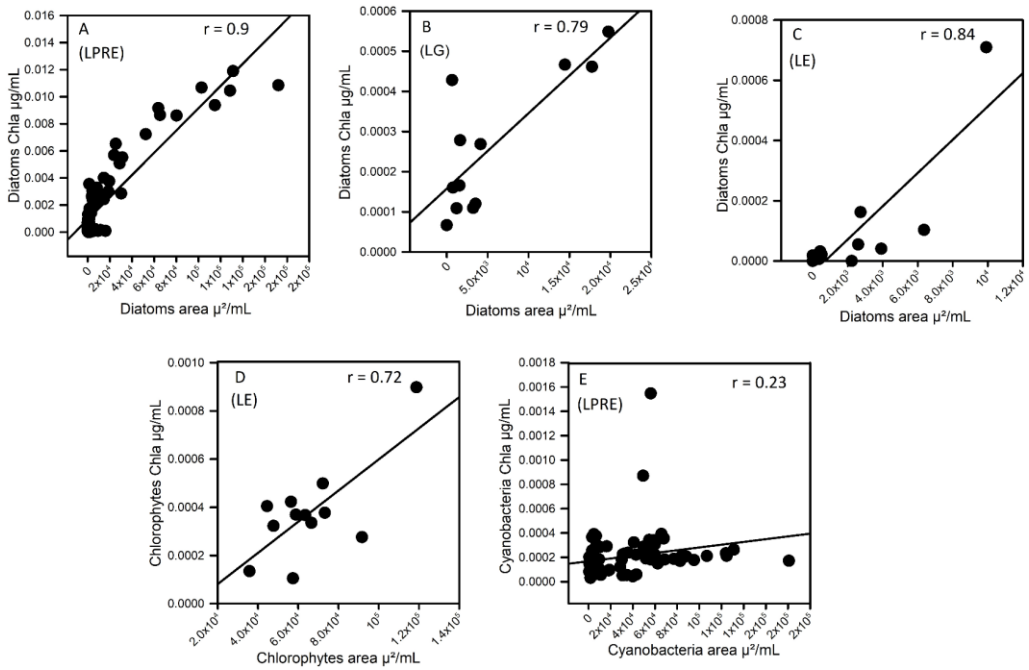

Figure 2.16 Comparison between ChemTax (Y-axis) and FlowCam (X-axis) determined A) diatom abundances in Lower Pearl River Estuary (LPRE) at 109 sites in the samples collected in Dec 2014, and March & May 2015, B) diatom abundances in Lake Grenada (LG) at 12 sites in the samples collected in June 13, 2012, (C) diatom abundances in Lake Enid (LE) at 12 sites in the samples collected on June , 2013; (D) chlorophyte abundances in Lake Enid (LE) in samples collected during June 11, 2012, (E) cyanobacterial abundances in LPRE at 109 sites in samples collected in December 2014, and March & May 2015.

The trend line is shown in each of the plots.

2.3.4 Comparison of Chl *a* and PC concentrations measured by using *in situ* (Eco triplet FL3B probe), HPLC, and spectrofluorometric techniques

HPLC provided much lower estimates for Chl *a* than the probe (Fig. 2.17a) although the correlation was high ($r=0.91$, $n=109$, $p<0.05$) in LPRE. And that in EMS, the probe provided lower estimates than the spectrofluorometer for Chl *a* (Fig 2.18a) although the correlation was high ($r=0.95$ $n=17$, $p<0.05$). In both cases, the correlations are good, but the values do not fall close to the 1:1 line. In contrast, the FL3B probe estimated the PC concentrations close to as estimated by Spectroflorometer in LPRE (Fig. 2.17b) and EMS (Fig. 2.18b). The correlation coefficient was 0.61 for LPRE ($n=152$, $p<0.05$) and 0.8 for EMS ($n=47$, $p<0.05$) and the values of PC are close to the 1:1 line in both the plots (Fig. 2.17b & 2.18b). There was a good correspondence ($r= 0.81$, $p<0.001$, $n=109$) between PC and Chl *a* concentration measured using the FL3B probe (Fig. 2.17c). Also, we found a good correspondence ($r= 0.81$, $p<0.0001$, $n=47$) between PC and Chl *a* concentration measured using the FL3B probe in EMS (Fig. 2.18c). The *in-situ* instrument FL3B provided a rapid measurement of Chl *a* and PC concentrations in water bodies to determine the changes in phytoplankton abundance compared to HPLC and spectrofluorometric techniques.

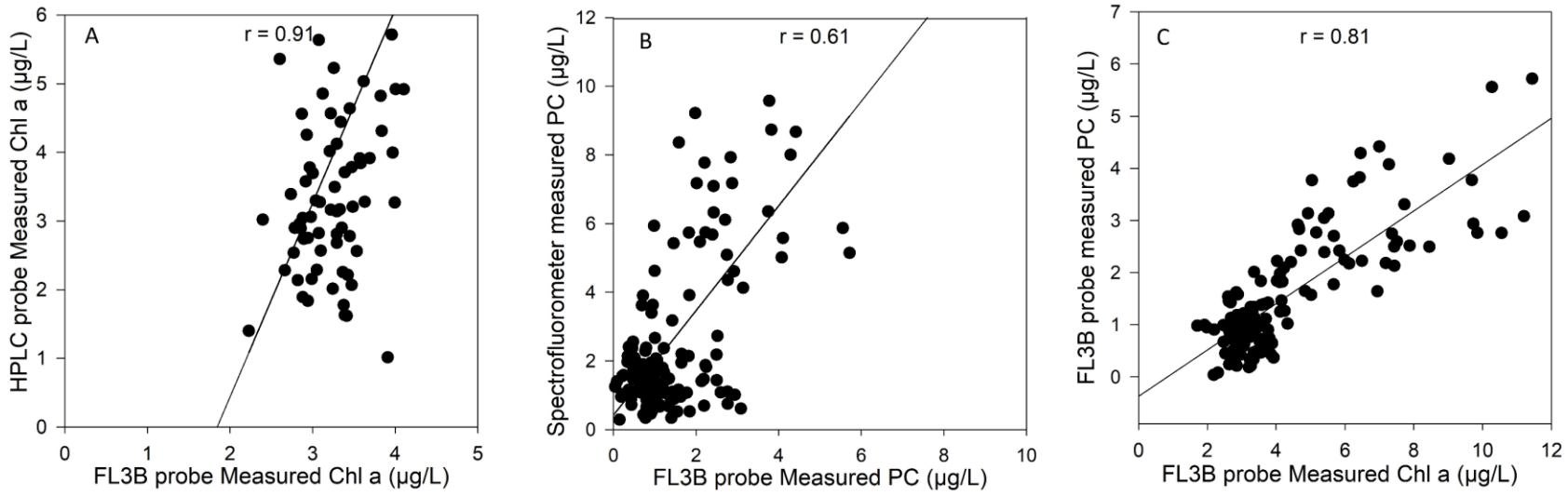

Figure 2.17 Comparison of (A) Chl *a* determined by Eco-triplet FL3B probe and HPLC analysis in Lower Pearl River Estuary (LPRE), (B) PC determined by Eco-triplet FL3B and spectrofluorometer in LPRE, (c) Chl *a* and PC determined by FLEB probe in LPRE. The trend line is shown in each of the plots.

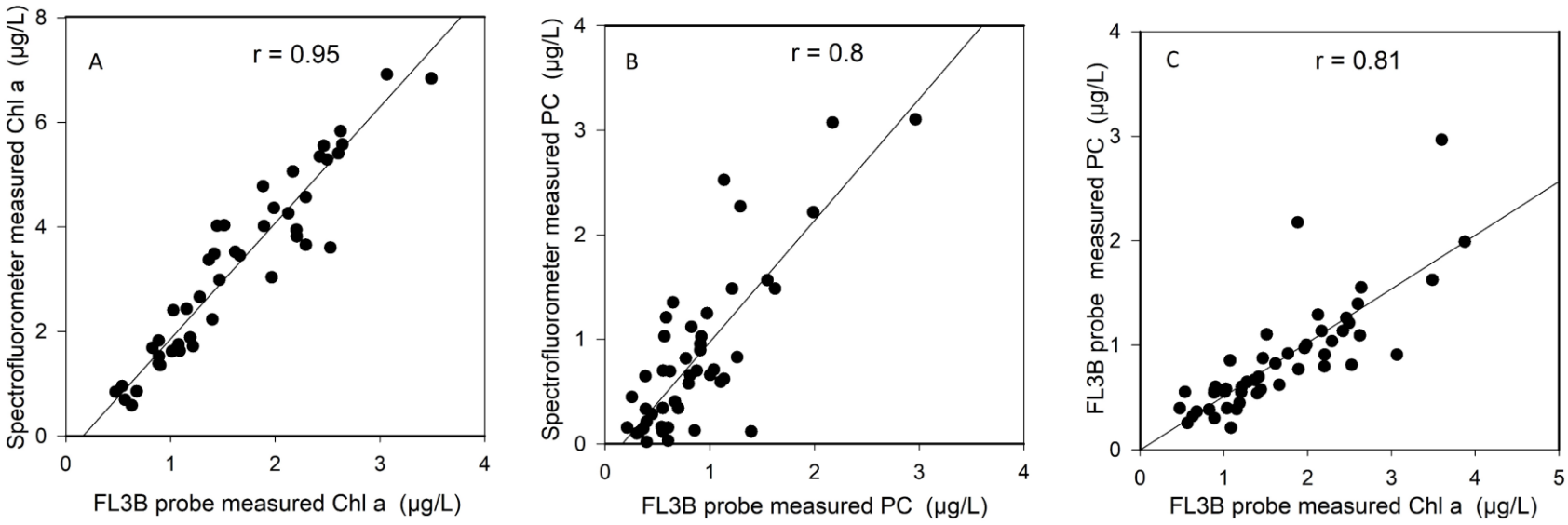

Figure 2.18 Create Comparison of (A) Chl *a* determined by Eco triplet FL3B probe and spectrofluorometer in East Mississippi Sound (EMS), (B) PC determined by Eco triplet FL3B probe and spectrofluorometer in EMS, and (C) Chl *a* and PC determined by FL3B probe in EMS

The trend line is shown in each of the plots.

2.3.5 Algal toxins

Microcystins were present in small concentrations in LPRE ranging from 0- 0.12 µg/L (Fig.2.19a-e). Brevetoxin was detected in LPRE but in very low concentrations (below 0.5 µg/L) in most of the sites in December 2015, and March, May, and August 2015 (Fig. 2.19e), but higher concentrations (between 0.5-1.6 µg/L) at 2 sites in December 2015 when there was a *Karenia brevis* bloom in the coastal waters (Fig. 2.19f). Brevetoxin concentrations were as high as 14.55 µg/L in the samples collected at seven sites in the Mississippi sound (Fig. 2.19f). The phycotoxin concentrations in four Mississippi lakes have been described previously in (Dash et al. 2015). Phycotoxin analysis techniques such as ELISA can confirm whether toxin producing species are present and can also quantify the low level of toxin concentrations. This technique when combined with FlowCam provides valuable insights about which species or group of phytoplankton are responsible for the phycotoxins in the water.

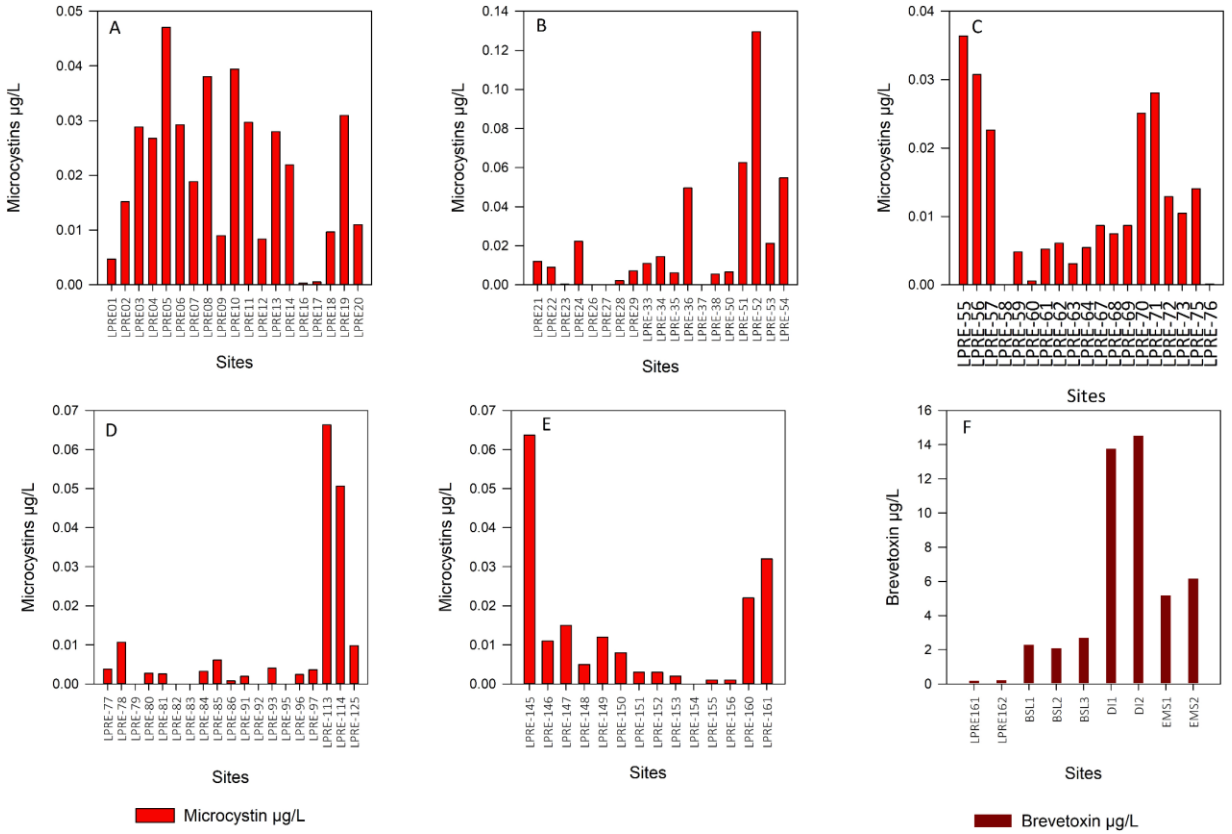

Figure 2.19 ELISA determined (A-E) Microcystins concentration in LPRE and (F) Brevetoxin concentration during a red tide bloom at two sites in LPRE and seven sites in the Mississippi Sound

2.4 Discussion

The community structure of phytoplankton and species composition provides vital information about the health of the ecosystem in water bodies and potential risk to humans and the environment. Due to increased eutrophication in water bodies, rapid and precise monitoring of phytoplankton is very important. An array of techniques is available to investigate the phytoplankton abundance. In this study, we employed *in-situ* instrument (FL3B probe), automated microscopy (FlowCam), spectrofluorometry, and HPLC to obtain valuable information on phytoplankton and compared the obtained results to evaluate the performances as well as utility of each of these techniques. We measured the Chl *a* concentration using *in- situ* FL3B probe, HPLC, and standard spectrofluorometric techniques and compared the results. We determined community structure of phytoplankton using two techniques, a pigment based technique, HPLC-ChemTax, and an automated microscopic technique, FlowCam. The variability in samples and the large number of samples ensured the reliability of the comparisons. A good correspondence between FlowCam and ChemTax was found for determining the relative abundance of diatoms, which corroborated with previous findings (Alvarez et al. 2014; See et al. 2005). The high correlation was because of large cell size of diatoms, which was easily distinguishable in FlowCam thus could be accurately quantified.

Similarly, Chl *a* concentration measured using the *in situ* probe were compared with the Chl *a* measured using HPLC and spectrofluorometric technique. High correlations suggested that *in-situ* fluorescence probe can be used to measure the concentration of Chl *a* as an alternative method to HPLC or standard spectrofluorometric technique, however an underestimation in probe measured Chl *a* is expected.

Additionally, a good correspondence between concentrations measured by *in-situ* probe and spectroflorometric technique suggests that *in-situ* probe can be used for rapid measurement of PC concentration.

Since the standard methods are time-consuming and expensive, a preferred approach would be to obtain a relationship between the two methods using regression by sampling at a few sites and then using the regression equation to calculate the concentration of Chl *a* and PC by converting the *in-situ* measured Chl *a and PC* to HPLC or spectrofluorometrically measured Chl *a* and PC.

FlowCam provides images of the cells allowing not only the calculation of cell abundance but also determination of the species composition and community structure. Species identified by FlowCam can provide solid clues about the presence of toxin producing phytoplankton in the collected samples. However, the presence of phycotoxin producing species of phytoplankton does not always mean a proportionate amount of toxin would be present in the water as they produce toxin only at certain stages of their life cycle in response to environmental conditions. Similarly, the toxin concentration can be high even when the cell counts or Chl *a* is low. For example, we found high brevetoxin concentrations at Chl *a* concentrations below 5 µg/L (Fig. 2 & 11e). Hence, it is not always possible to infer toxicity in the water using the pigment analysis or FlowCam alone. So, use of rapid toxin measurement techniques such as ELISA aids in determining the toxicity level in the water when toxin producing species of phytoplankton is detected using FlowCam or HPLC-ChemTax or measurement of Chl *a* spectrophoto- or fluorometrically or by *in-situ* probes.

The *in-situ* FL3B probe used in our study offers continuous measurement of Chl *a*, PC, and PE concentrations. Furthermore, the *in-situ* probe does not require pretreatment and a large sample volume. The method is simple, nondestructive, selective, sensitive, and rapid thus a greater volume of data can be obtained quickly and in real time. Since, it is not essential to perform taxonomic classification for all samples, it can be done only for locations where changes in phytoplankton biomass (Chl *a* concentrations) or composition (PC and PE concentrations) would be detected by the probe. So, use of such *in-situ* instruments provides information quickly to determine the changes in phytoplankton abundance. In our study, we found a fair correspondence between HPLC measured and *in-situ* FL3B probe measured PC, but the results did not correspond well in the case of Chl *a* possibly due to in vivo measurements of Chl *a* by the probe in LPRE samples where both these techniques were employed. We found good correspondence between results from FlowCam and ChemTax for large-sized phytoplankton, diatoms, but we did not obtain good correspondence between these two techniques for other classes of phytoplankton such as cyanobacteria, dinoflagellates, and chlorophytes. The lack of correspondence between the area of cyanobacterial cells with the pigment based HPLC-ChemTax analysis could be explained by low concentration of pigment zeaxanthin from HPLC, which is used to quantify cyanobacteria in ChemTax or the small cell size of some cyanobacterial cells such as *Microcystis* spp. Physical factors such as water temperature, water clarity, stratification, residence time, or chemical factors such as availability of nitrogen and phosphorus and the salinity regime have been reported to affect cellular zeaxanthin concentrations (Q. Hu 2004). Hu (2004) found that environmental factors particularly light, temperature, nutrient affect photosynthesis and

productivity which result in variation in biomass. Among the above factors, nitrogen limitation may explain the higher value of area estimated by FlowCam because the cellular light harvesting pigment content such as Chl *a* and zeaxanthin decrease under nutrient stress(Latasha Mikel and Elisa 1994). The other plausible reason for this non correspondence could be the presence of many small sized phytoplankton in the sample. Due to their smaller size, they were grouped into the unidentified class in FlowCam analysis but they were accurately classified by ChemTax into their respective classes based on their respective unique pigment. Alvarez et al. (2014) found similar results in case of haptophytes and chlorophytes (Alvarez et al. 2014). We used area based diameter to determine the relative abundance as opposed to the use of cell counts (See et al. 2005) or shape based automatic classifications (Alvarez et al. 2014) used in other studies. Additionally, Alvarez et al. (2014) reported that phytoplankton content must be very high in order to acquire correct estimation of community structure by FlowCam as error can occur while classifying automatically(Alvarez et al. 2014). Hence in such situations, ChemTax is more effective than microscopic analysis using FlowCam.

This study involves comparison and evaluation of several techniques to monitor harmful algal bloom is first attempt in diverse water bodies of Mississippi/Louisiana. These results can be useful for further research in choosing the best techniques to rapidly collect information in an efficient way. The species composition and relative abundance of algal group determined in this study provides preliminary information to continue the research in the Mississippi /Louisiana water bodies.

There were some unavoidable limitations of the study such as fixing the samples using glutaraldehyde which could alter the size of phytoplankton thus giving some

compromised result from FlowCam analysis. Use of glutaraldehyde as a fixative has advantages as it is an effective chemical compared to formaldehyde and does not stain the cells as Lugol's solution, but it could alter the area or shape of phytoplankton to the extent where they cannot be identified in the images. Since, large volume of samples collected per day cannot be run immediately after the collections, the samples needed to be preserved. Another limitation of this study was that the relationship between phytoplankton with the physical parameters such as temperature, solar irradiance, or nutrient were not explored in this study. Investigating those aspects could help better understand the trends of phytoplankton community, species composition, and toxin production.

HPLC-ChemTax provides rapid quantification of algal groups and allows automated analysis as compared to FlowCam where each sample run takes at least 30 minutes to an hour and additional time for classifications. In view of constantly developing technology, we surmise that FlowCam will continue to improve to provide more rapid sample processing and improved software for classifications. Despite these limitations, we have shown that estimates of taxonomic richness derived from FlowCam are reasonably comparable with those obtained by ChemTax.

2.5 Conclusion

This study compared the potential of several laboratory and field techniques used for determining phytoplankton community structure. While in some scenarios one technique is better than others, it was found that use of a few techniques together can extract the crucial information in understanding the phytoplankton community structure and occurrence of phycotoxins in water. For instance, FlowCam could be used for

separating chlorophytes and euglenophytes, or diatoms and dinoflagellates, visually which is not always possible in ChemTax pigment analysis due to shared pigments by both phytoplankton. However, for small cell size phytoplankton, ChemTax produces better results due to difficulties in identifying small cell size phytoplankton using FlowCam. When phycotoxin-producing phytoplankton are considered, if toxin is measured together with FlowCam or HPLC-ChemTax or pigment measurements, it will provide a comprehensive information about the presence of toxins as well as the phytoplankton species responsible for producing the toxins which will be helpful for adopting preventive measures for water managers.

Surface area of phytoplankton can be used to obtain an accurate measure of relative abundance of genus or species within a group of phytoplankton. The three pigment based methods, HPLC-ChemTax, *in situ* fluorescence probe, and fluorescence of extracted Chl *a* and PC, provide complementary information on freshwater and estuarine phytoplankton. The findings of this study conclude that among several techniques available for monitoring phytoplankton structure, FlowCam is the most useful technique for species identification, HPLC-ChemTax for taxonomic classification, *in-situ* probes for gathering information rapidly for initial estimation of phytoplankton biomass, and spectrofluorometric techniques and toxin analysis are needed for precise determination of harmful impacts. These findings provide insights for future studies to make a suitable selection of techniques as per their objectives.

CHAPTER III

COMPARATIVE ANALYSIS OF CHLOROPHYLL A ESTIMATION BY THREE SATELLITE SENSORS AND TWO POPULAR SENSORS ONBOARD UNMANNED AERIAL SYSTEMS

3.1 Introduction

Water quality parameters such as chlorophyll *a* (Chl *a*) concentration, total suspended matter, nutrient concentrations, pathogens, and heavy metals are used as indicators of lake and coastal water environmental health by water resources managers to guide resource management and public safety decisions (Dash et al. 2015). Of these, Chl *a* concentration is arguably the most representative environmental parameter as it is a measure of phytoplankton biomass as well as an indicator of water clarity. Harmful algal blooms represent a major environmental problem worldwide and throughout USA with severe impacts on human health, aquatic ecosystems, and the economy (D. M. Anderson 2009). Although *in situ* sampling is the most accurate way of determining Chl *a* concentration, yet the use of remote sensing technology has been increasing recently for routine Chl *a* monitoring due to the synoptic coverage (T. Moore et al. 2014).

Low spatial resolution of satellite sensors limits the ability to accurately detect and quantify phytoplankton in small water bodies. Unmanned aerial Systems (UASs) offer the best remote sensing approach in such cases with sensors of suitable spectral bands and spatial resolution (Flynn and Chapra 2014). Additionally, algal blooms can be

very dynamic and patchy, changing significantly in a short time. Monitoring such events with even high resolution satellite data is not suitable by itself because such data does not have the temporal resolution needed to monitor the quickly changing blooms (Gholizadeh and Robeson 2016). Thus, these events are well suited for UAS based monitoring (Lekki et al. 2009; Watts, Ambrosia, and Hinkley 2012).

Algorithms used for remote estimation of Chl *a* content are categorized as either empirical or semi-analytical algorithms. The empirical algorithms are based on statistical relationships between either normalized water leaving radiance (*nLw*) or remote sensing reflectance (*Rrs*) ratios at two or more bands and *in situ* Chl *a*, e.g. the SeaWiFS OC4v4 and OC2v4 algorithms (O'Reilly et al. 1998, 2000). The semi-analytical models, on the other hand, are based on theoretical relationships between Rrs and inherent optical properties such as absorption and backscattering coefficients but include some statistical relationships formulated through datasets of relevant in-water parameters and optical properties (Twardowski et al. 2005). In the past, numerous empirical and semi analytical algorithms have been developed for coastal areas and relatively large inland lakes for estimating Chl *a* using remotely sensed data (Gower et al. 2005; Mayo et al. 1995; Ruddick et al. 2001). The inherent optical properties of different water constituents vary with the concentration and specifically with the composition. The specific properties are important for reflectance models used to determine the concentration of water constituents from remote sensing data..(Siegel et al. 2005) IOPs of water bodies can differ due to the variability in trophic conditions, sediment concentration from run off, nutrient and colored dissolved organic matter concentration. As a consequence, a single algorithm developed for a specific water body is not applicable to water bodies with

varying IOPs. ,. (T. Moore et al. 2014)Subsequently, empirical algorithms are standard approaches used to produce global maps of Chl-a concentration from satellite reflectance data (C. Hu, Lee, and Franz 2012). Empirical algorithms have key advantage over semi-analytical algorithms in terms of computational efficiency in comparison to complex structure of semi analytical algorithms. Although the semi-analytical algorithms account for the effect of other optically active constituents in water such as CDOM absorption, backscattering by sediments, and phytoplankton, there is a greater chance of introduction of errors due to sensitivity of semi-analytical algorithms to parameter-tuning. For instance, different types of phytoplankton have different absorption spectra owing to the presence of different pigments (Hoepffner and Sathyendranath 1991); thus universally fixed absorption models in semi analytical algorithms can't represent varying composition of phytoplankton communities. Likewise training data sets for some of the model inputs, such as backscattering coefficients of particles, are not widely available (Dierssen 2010). Meanwhile, a previous study found that empirical methods performed better than semi analytical algorithms in a comparative study (Brewin et al. 2015). Thus, in this study we developed and tested empirical band ratio algorithms for five different sensors in our study areas. The study included two types of water bodies in Mississippi. 1) five lakes in Mississippi and 2) an estuary, the Lower Pearl River Estuary (LPRE). The main aim of this research was to develop remote sensing algorithms to quantify chlorophyll *a* employing five sensors including two popular UAS sensors and three currently operating satellite sensors and evaluate the performance of the sensors in quantifying chlorophyll a in the lakes and the estuary

3.2 Material and Methods

3.2.1 Study areas

Water quality data were collected from five different lakes in Mississippi including Ross Barnett Reservoir (RB), Lake Sardis (LS), Lake Enid (LE), Lake Grenada (LG), and Lake Okatibbee (LO) and Lower Pearl River Estuary (LPRE) (Fig. 3.1). Ross Barnett Reservoir is located adjacent to the City of Jackson, the capital city of Mississippi, and Lakes Sardis, Enid, and Grenada are located in northern Mississippi, and Lake Okatibbee is located in eastern Mississippi. The Ross Barnett Reservoir is used as a source of drinking water for the City of Jackson and all five lakes have traditionally been used for recreational activities such as swimming, boating, and fishing. These lakes produce large quantities of commercial and recreational fish (Dash et al. 2015). The Pearl River originates in Neshoba County, Mississippi and has a meander length of 714 km before emptying into the Gulf of Mexico. The lower185 km of the river forms the part of the boundary between Mississippi and Louisiana, is termed as Lower Pearl River. The estuary at the lower most portion of the river, the Lower Pearl River Estuary (LPRE) is considered as one of the most critical areas of remaining natural habitats in Louisiana-Mississippi coast (The Nature Conservancy 2017).Likewise the four Mississippi Lakes LS, LE , LG and LO are diverse and ecologically important water bodies that are heavily used for fishing and recreational purposes. Additionally, the algorithms developed for these water bodies can be applicable to other water bodies in United States directly or with adjustment of coefficients.

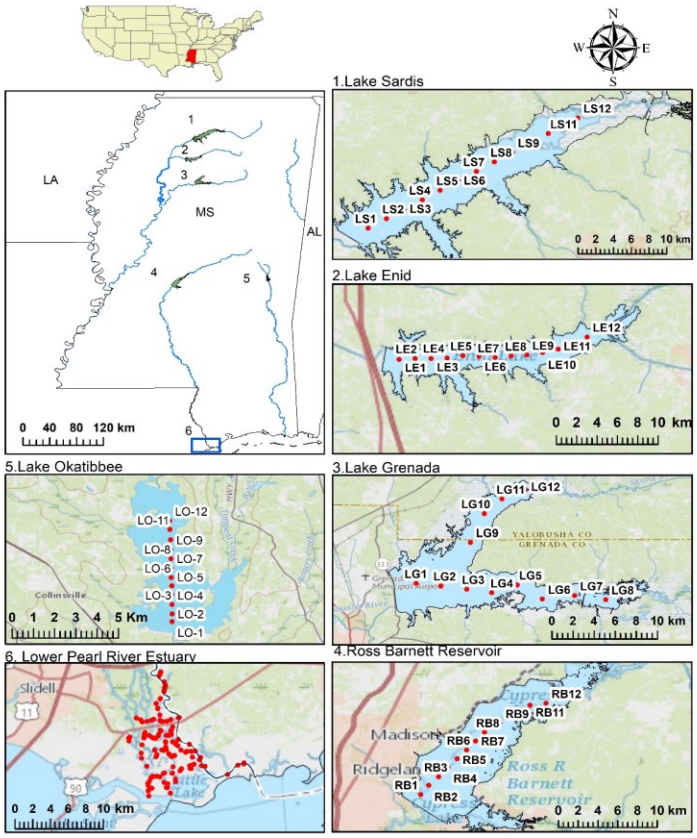

Figure 3.1 Study area Map

3.2.2 Data collection

Five Mississippi lakes including RB, LS, LE, LG, and LO were sampled during 13 field campaigns from 2012 to 2016.Data were collected in during summer in RB, LS, LE, and LG and LO was sampled during winter (February 2015). With 12 sampling points in each lake, a dataset of 156 sampling points were generated (Table 3.1). The dataset from LPRE comprises of 164 stations from 5 sampling events in December 2014 and March, May, August, and December 2015 (Table 3.2). We collected samples for all lakes except LO during summer motive was to capture higher bloom conditions. The

sample collection in LPRE were done in four seasons – Spring, Summer, Fall, and Winter to record the functionality of the entire study area. The field data included water samples collected in clean Nalgene bottles, *in-situ* remote sensing reflectance, *in- situ* phytoplankton pigment concentrations (chlorohyll-*a*, Phycocyanin and phycoerythrin), water quality parameters such as temperature, pH, salinity, and dissolved oxygen. Surface water samples were placed in a cooler with ice after collection, and filtered within 5-6 hours of collection. *In situ* remote sensing reflectance measurements were taken at each sampling points with hyperspectral radiometer GER 1500covering 200 to 1100 nm wavelength. The reflectance data were visually examined individually, and obvious erroneous spectra were not included in the final data set.

Table 3.1 Sample collection sites and dates for Lakes

Sites	RB	RB	RB	RB	RB	RB	LO
Date	6/13/12	6/29/2012	5/22/13	7/10/13	8/28/15	8/27/16	2/6/15
Sample no	12	12	12	12	12	12	12
Sites	LS	LS	LE	LE	LG	LG	
Date	6/18/13	7/6/2014	6/20/12	6/11/13	6/18/12	6/4/13	
							Total N
Sample no	12	12	12	12	12	12	156

Table 3.2 Sample collection sites and dates for LPRE

Sites	LPRE	LPRE	LPRE	LPRE	LPRE	
Date	2014 December	2015 March	2015 May	2015 August	2015 December	Total N
Sample no	30	30	50	38	16	164

3.2.3 Chlorophyll *a* concentration measurement

To quantify Chl *a* concentration, 100 mL aliquots of surface water was filtered (<50 kPa) onto GF/F filters with 4.7 cm diameter and 0.7 μm pore size, and kept frozen at -80°C until analysis. Spectoflorometric and HPLC techniques were used to determine Chl a concentration in each sample. The samples for which HPLC analysis was not carried out, Chl *a* was extracted using 90% acetone and the concentration was determined spectrofluorometrically using a Horiba Jovin Yvon FluoroMax-4 Spectrofluorometer (Horiba Scientific, Edision, NJ, USA) following standard laboratory protocol Joint global Ocean Flux Study 1998). For HPLC pigment analysis, the filter papers were shipped overnight on dry ice to the University of South Carolina, Columbia, SC. High performance liquid chromatography (HPLC) was used to separate, identify, and quantify chlorophyll a concentration following standard protocol (Mackey et al. 1996)The HPLC method and spectroflorometreic methods produced similar results when results from both tehniques were compared

3.2.4 Remote Sensing Reflectance

Remote sensing reflectance (*Rrs)* is defined as the ratio of the upwelling radiance and downwelling irradiance. To derive above water *Rrs* three measurements are generally required: (1) upward radiance (*Lu*), (2) downward sky radiance (*Lsky*), and (3) upward radiance from a standard Spectralon reflectance plaque (*Lplaque*). First, measurements of radiance from a plaque with known spectral directional reflectance (99% Spectralon, Labsphere) were made using a GER 1500 radiometer (Spectravista Inc., Poughkeepsie, NY). Subsequently, three replicate scans of target water surface were made and then sky radiance was measured by pointing the radiometer towards the sky opposite to the sun.

The radiometer data were processed following Hu (2003) for the determination of above water *Rrs* . First, water leaving radiance (*Lw*) was determined by

$$Lw = Lu - (0.02 \times Lsky)$$

Subsequently, *Rrs* was computed by

$$Rrs(0^{-}) = \frac{1.01 \text{ X } Lw}{\text{Lplaque} \times \pi}$$

3.2.5 Conversion of hyperspectral data to sensor specific data

It is difficult to perform a comparative evaluation of satellite sensors using satellite derived *Rrs* due to different ground resolution, inconsistent temporal resolution, and variability in overpass time of sensors. Thus, *in-situ* measured Rrs were converted into each sensor specific *Rr*s by application of the spectral response functions of three currently operating satellite sensors- AQUA MODIS, OLCI SENTINEL- 3, and LANDSAT 8 OLI, and two popular UAS sensors- MicaSense and Color Infra-red (CIR) (Fig.3.2).

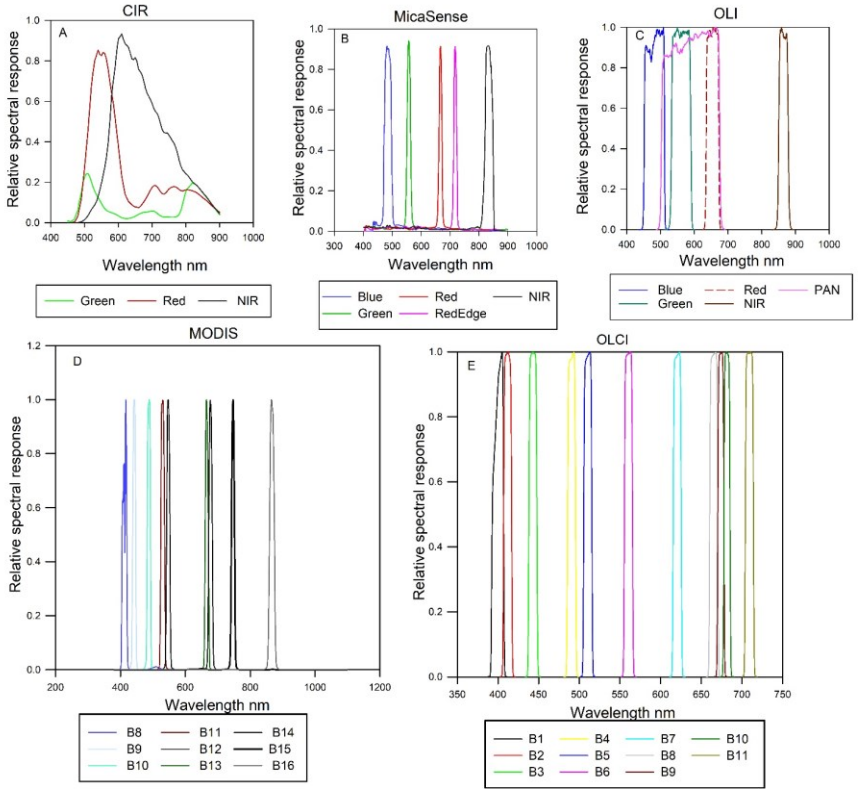

Figure 3.2 Create Spectral response functions (SRF) of sensors A) SRF of three band Unmanned Aerial Systems (UASs) sensor -Colored Infra-red (CIR) B) SRF of five band Unmanned Aerial System (UAS) sensor -MicaSense C) SRF of Operational Land Imager (OLI) onboard LANDSAT-8 satellite D) SRF of Moderate Resolution Imaging

3.2.6 Clustering the radiometric Rrs data

Our attempt to develop one algorithm for lakes and one algorithm for the estuary was not successful. Thus, we adopted the clustering method to separate the sites based on their *Rrs*. The datasets from the five Mississippi lakes were combined which included data from Lakes Sardis, Grenada, Enid, Okatibbee, and Ross Barnett Reservoir for cluster analysis. Samples collected from the Lower Pearl River estuary at various locations and seasons were combined for cluster analysis. Based on cluster analysis of remote sensing reflectance data, we separated the Rrs dataset of Lakes and LPRE into 3 clusters each.

Our choice for cluster analysis was the *k*-means algorithm, which has been used in many classification studies from medical image processing to remote sensing.(T. Moore et al. 2014). Dendrogram and cluster validity function were used to choose the optimum number of clusters. The *k*-means clustering algorithm was applied to the *in-situ Rrs* data using R (v. 3.3.2) software. The *k*-means clustering algorithm produces clustering of the data into a specified number of clusters, herein denoted by k. The basic function of this algorithm is to choose clusters that minimizes the difference between the data points and the prototype cluster centers or cluster means. Cluster centers are iteratively adjusted until optimization criteria are met to achieve the minimum sum of the differences and minimum change in the residuals. The clustering routine then returns the mean reflectance vectors for the *k* classes, and a matrix containing the memberships of each point to each class. The cluster analysis separated and differentiated subsets based on both the shape and the magnitude of *Rrs* and resulted in three optimal clusters for the Lakes and three clusters for LPRE (Fig. 3.3). The clusters for best performing sensors in this study are shown in plots (Fig 3.4& Fig 3.5) The number of clusters was deemed best based on a suite of cluster validity functions. When three clusters are specified, the relation of data points to each other and cluster centers (mean vectors) in terms of compactness and separation aspects were collectively in a better configuration compared to other cluster choices. The differences between clusters can be more readily observed when their reflectance means plotted together for three sensors (Fig.3.6, Table A.8-Table A.13). Collectively, these *Rrs* means formed the optical water types (OWTs). They are representations of averaged conditions governed by the optical properties of the water column and ultimately depend on the absorption and scattering properties of the in-water

constituents (e.g., phytoplankton and non-phytoplankton particles). In general, *Rrs* spectra separated the OWTs based on their unique characteristics. In the lakes, OWTs one and two have low overall spectral magnitude, and show relatively flat features above 600 nm compared to OWT three. These OWTs all show peaks around 700 nm, but are different from each other in magnitude. OWT three shows a prominent peak at 700 nm compared OWTs one and two. This peak is characteristic of strong particle backscattering and has been associated with high algal particle concentration (Gilerson et al. 2007; Gower et al. 2005; Zimba and Gitelson 2006). All the OWTs show a reflectance peak to some degree at or near 555 nm, which is most pronounced in OWT three of lakes and OWTs one and two of LPRE. The peak at 555 nm can be attributed to enhanced particle scattering from living (e.g., phytoplankton) and non-living (e.g., sediments) sources (Ahn, Bricaud, & Morel, 1992; Kutser, 2004). Other secondary peaks are seen at or near 650 nm in these OWTs. While it is not possible to associate these features to unique constituents without more complete optical information,

phytoplankton are playing a significant role in the shape of the reflectance spectrum.(T. Moore et al. 2014).

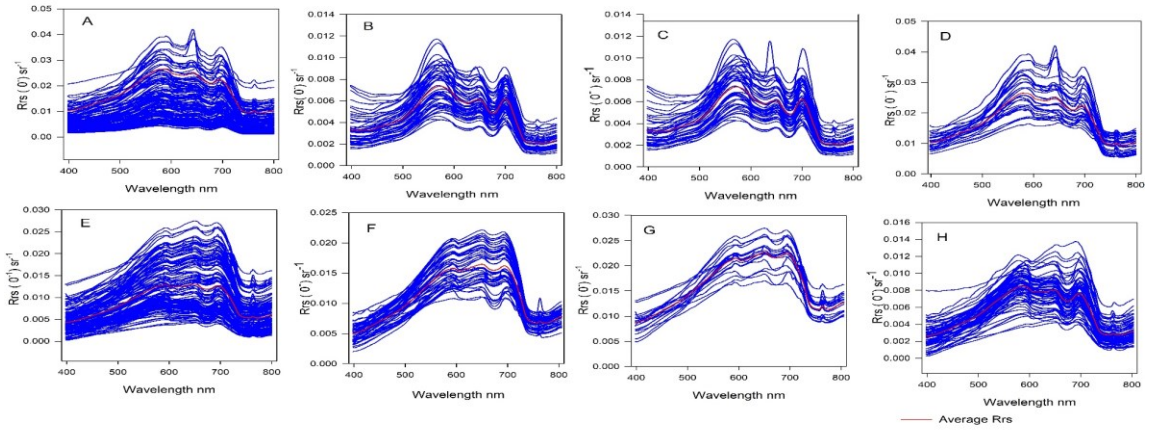

.

Figure 3.3 Clusters of remote sensing reflectance (*Rrs*) spectra of the lakes and LPRE

A) Total *Rrs* spectra of lakes before clustering, B) *Rrs* spectra of cluster 1 of lakes, C) *Rrs* spectra of cluster 2 of lakes, D) *Rrs* spectra of cluster 3 of lakes, E) Total *Rrs* spectra of LPRE before clustering, F) *Rrs* spectra of cluster 1 of LPRE, G) *Rrs* spectra of cluster 2 of LPRE, H) *Rrs* spectra of cluster 3 of LPRE.

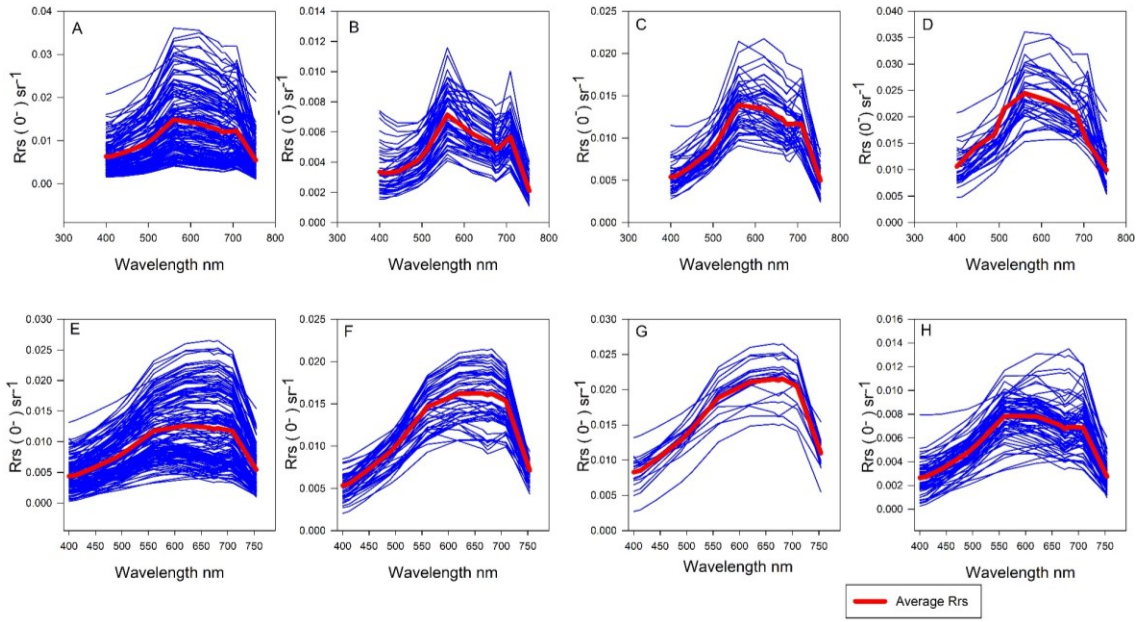

Figure 3.4 Clusters for OLCI sensor in lakes and LPRE

A) Total *Rrs* spectra of lakes, B) Cluster 1 *Rrs* spectra of lakes, C) Cluster 2 *Rrs* spectra of lakes, D) Cluster 3 *Rrs* spectra of lakes, E) Total *Rrs* spectra of LPRE, F) Cluster 1 *Rrs* spectra of LPRE, G) Cluster 2 *Rrs* spectra of LPRE, and H) Cluster 3 *Rrs* spectra of LPRE

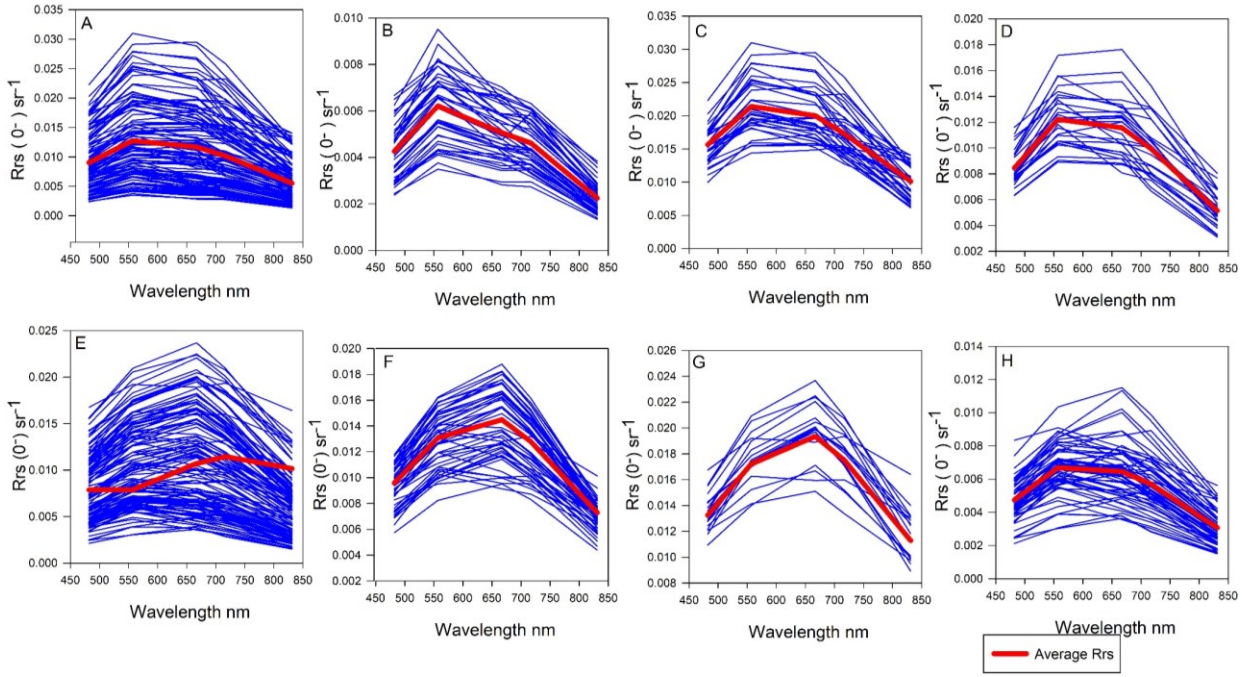

Figure 3.5 usters for Micasense sensor in lakes and LPRE,

A) Total *Rrs* spectra of lakes, B) Cluster 1 *Rrs* spectra of lakes, C) Cluster 2 *Rrs* spectra of lakes, D) Cluster 3 *Rrs* spectra of lakes, E) Total *Rrs* spectra of LPRE, F) Cluster 1 *Rrs* spectra of LPRE, G) Cluster 2 *Rrs* spectra of LPRE, and H) Cluster 3 *Rrs* spectra of LPRE

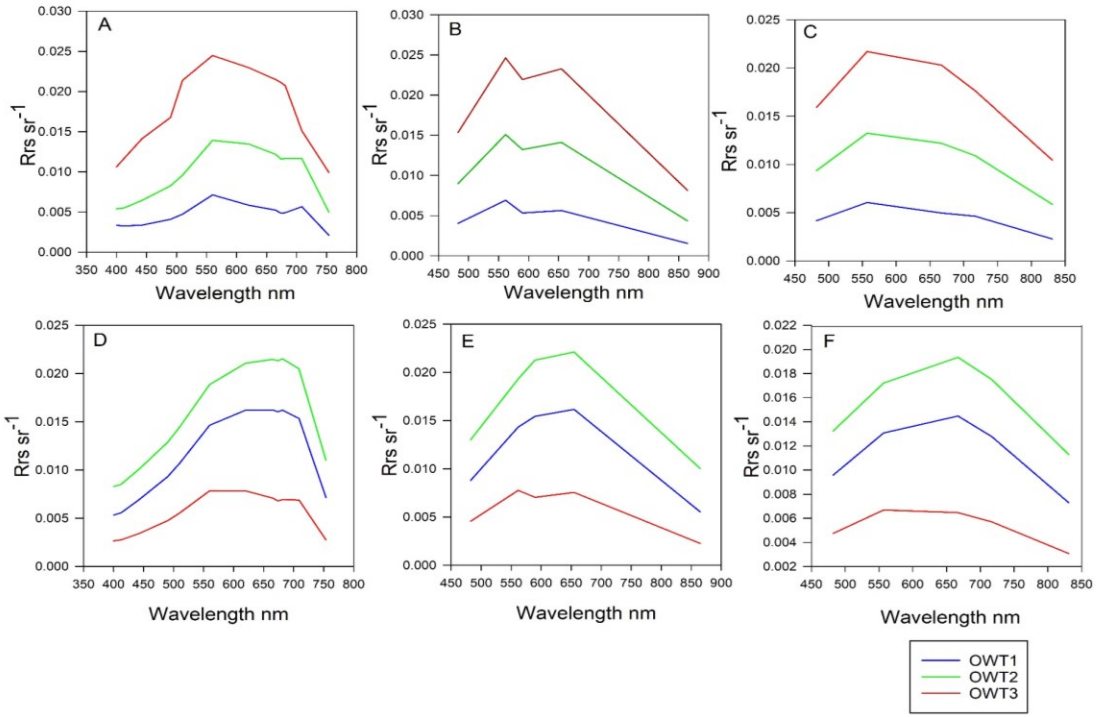

Figure 3.6 Mean *Rrs* spectra of satellite and UAS sensors for the optical water types (OWTs) in the lakes and LPRE

A) OLCI spectra of the lakes, B) OLI spectra of the lakes, C) Micasense spectra of the lakes, D) OLCI spectra of LPRE, E) OLI spectra of LPRE, and F) Micasense spectra of LPRE

3.2.7 Optimal Band Ratio Selection

The use of Rrs band ratio instead of singular Rrs bands is popular in remote sensing algorithm development. The reflectance of a singular band can be influenced by more than one component, whereas the use of band ratios gives enhanced spectral signatures of different water constituents. It is also less sensitive to the atmospheric correction errors when applied to satellite data (Gilerson et al. 2010). To select the most suitable band ratio, we accessed all the combinations of band ratios for each sensor and simple linear regression was computed against the measured Chl a concentration. We also tested the popular band ratios as proposed by previous studies with available bands in the used sensors. However, the best band ratio algorithm was chosen based on highest R^2 obtained from the regression between band ratio and measured Chl a concentration.

3.2.8 Algorithm development

Randomly chosen 3/4 th of data were used in band ratio algorithm development and $1/4^{th}$ of data were used in model validation. Same data points were used in algorithm development and validation for all five sensors to make the results comparable.

3.2.9 Model validation

All the algorithms were applied to the one fourth of randomly chosen validation dataset to investigate the applicability of the newly developed algorithms and accuracy was evaluated using root mean square error (RMSE) and mean absolute error (MAE). In order to remove the effect of magnitude of observations, RMSE and MAE were normalized using the range of observations and expressed in percentages. Expressions for relative RMSE and relative MAE are given as

$$\text{Relative RMSE \%} = \frac{\text{RMSE}}{\text{Measured maximum} - \text{Measured minimum}} \times 100$$

$$\text{Relative MAE\%} = \frac{1}{n} \frac{\sum_{i=1}^{n} |\text{Estimated} - \text{Measured}|}{(\text{Measured Maximum} - \text{Measured Minimum})} \text{X}100$$

3.3 Results

3.3.1 Measured Chl a concentration

The range of Chl a in lakes is between 1.8-57.1 µg/L and LPRE is found to be 1.3-22.1 µg/L (Fig.3.7).

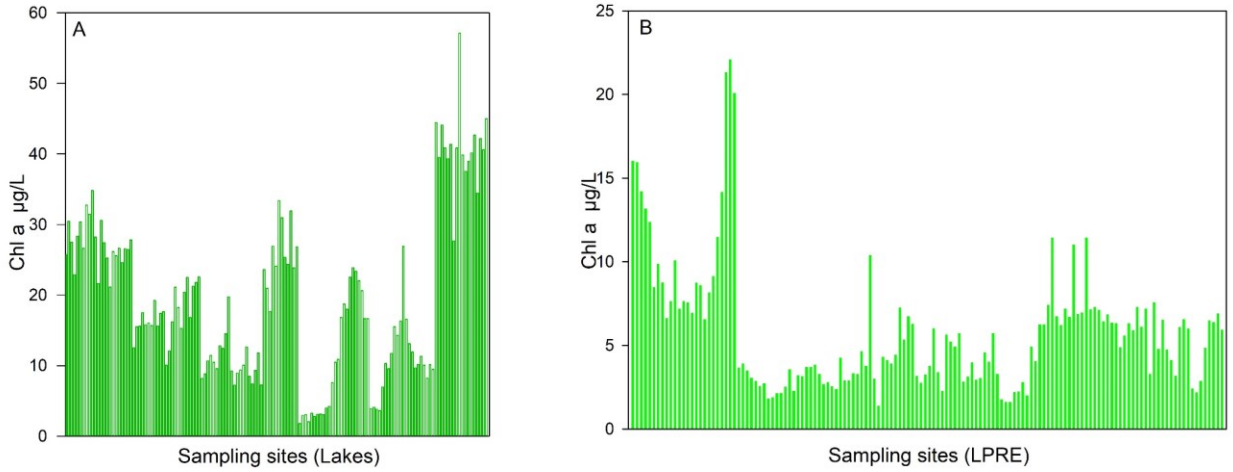

Figure 3.7 Measured chlorophyll a in A) Lakes and B) LPRE

3.3.2 Chlorophyll-*a* algorithms developed for the satellite sensors

3.3.2.1 Lakes

Among the three satellite sensors used, we found the best algorithm from OLCI Sentinel 3 and Landsat 8 OLI to quantify Chl a in our study areas (Fig.3.8). For OWT1 and OWT2 of lakes, Landsat band ratio PAN/NIR performed better in predicting the Chl a with minimum errors in terms of RMSE of 5.6 µg/L and %MAE of 20.48 with an R^2 of

0.49 for OWT1 and RMSE of 9.24 µg/L and %MAE of 38.80 with an R^2 of 0.28 for OWT2. However, for OWT3, algorithm developed by OLCI, i.e band ratio Green/NIR (Band6/Band11) performed best among all the sensors with an RMSE of 1.69, %MAE of 10.09, and an R^2 of 0.73. The results for three OWTs in terms of RMSE, MAE and R^2 are shown in tables A.14, A.15 and A.16 respectively. Although some of the algorithm has low R^2 value, that is the maximum we found among all the sensors used (Tables A.14, A.15, A.16). Tables 3, 4, and 5 below show the concentration of Chl a ranged between 2.9-15.7 µg/L for OWT1, 1.8-40 µg/L for OWT2, and 10.02-57.1µg/ L for OWT3 in the lakes.

.

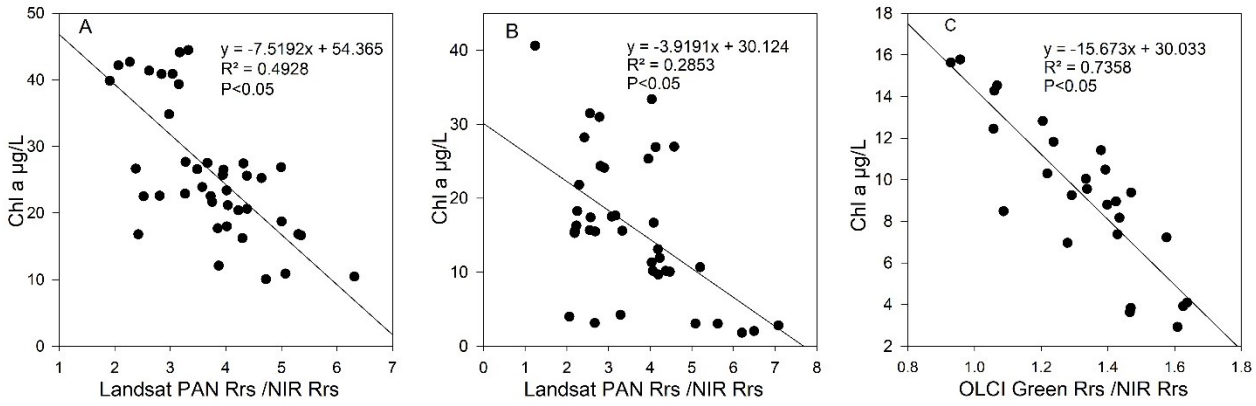

Figure 3.8 Algorithms developed for three optical water types (OWTs) of lakes, A) OWT1, B) OWT2, and C) OWT3

3.3.2.2 Lower Pearl River Estuary

For LPRE, OLCI band ratio algorithm performed better in all three optical water types (Tables A.17, A.18, and A.19). Among the three water types determined from cluster analysis, the band ratio algorithm Green/Red (Band6/Band 10) performed best for

OWT3 with an RMSE of 2.09 and % MAE of 26.23 with an R^2 of 0.32 (Fig.3.9). In OWT1 and OWT2 Green//Red band ratio performed best among all three satellite sensors with an RMSE of 4.09 µg/L and % MAE of 57.83, and an RMSE of 1.36 and % MAE of 45.9 respectively.

The measured versus modeled Chl a for lakes and LPRE for the aforementioned satellite sensors are shown below (Fig.3.10, Tables A.14-A.19)

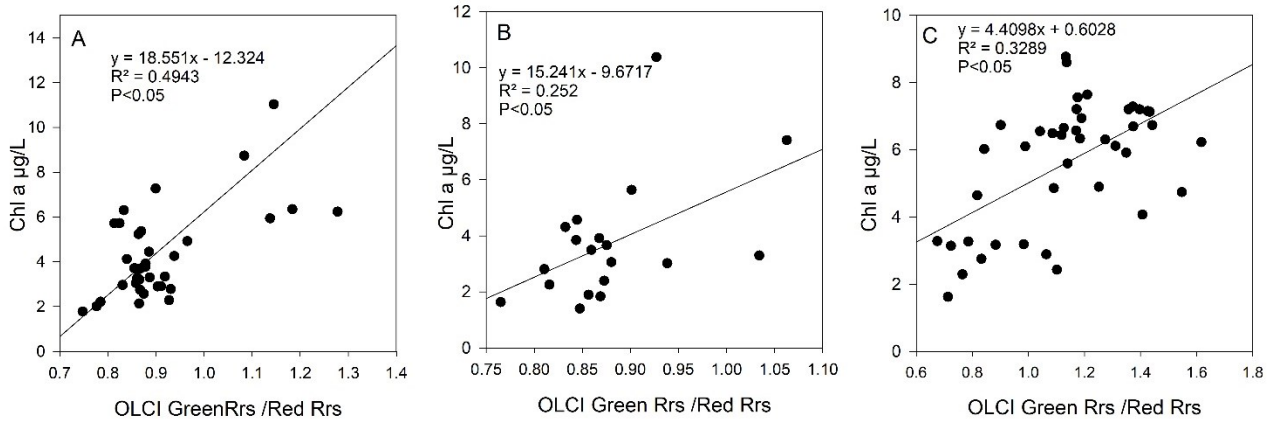

Figure 3.9 Algorithms developed for three optical water types (OWTs) of LPRE, A) OWT1, B) OWT2, and C) OWT3

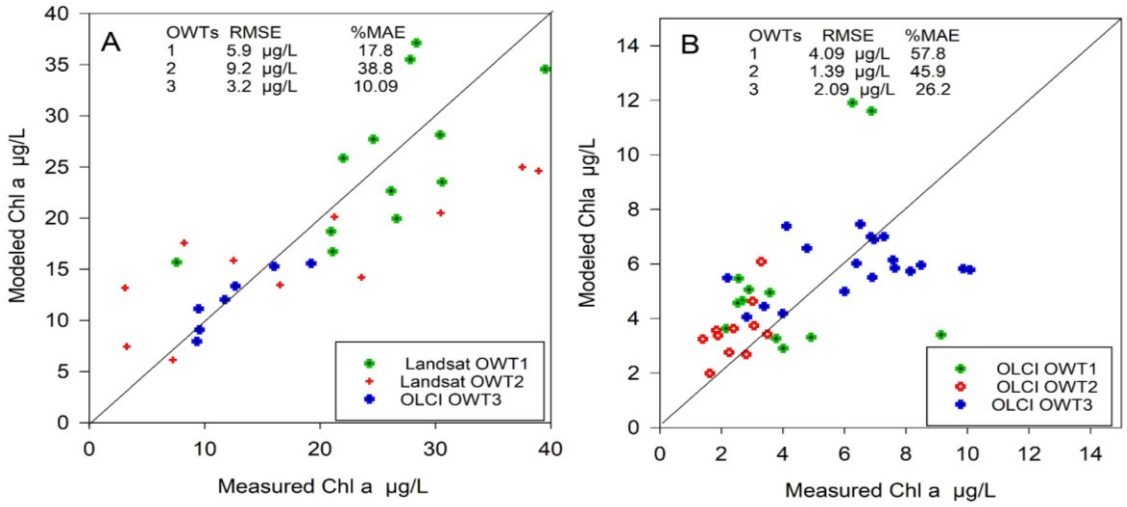

Figure 3.10 Create Algorithm validation for optical water types 1, 2, and 3 of lakes using satellite sensors A) Lakes, and B) LPRE

3.3.3 Chlorophyll a algorithms developed for the UAS sensors

3.3.3.1 Lakes

Algorithms developed for the five-band sensor, MicaSense, performed better than the 3 band CIR sensor for quantifying Chl *a* in all three optical water types in Lakes (Tables A.20, A.21, A.22) Among the three water types, band ratio algorithm (Blue/Rededge) developed for OWT3 performed better among the three OWT based on RMSE (3.01 µg/L), % MAE (20%), and R^2 (0.73). In OWT1 and OWT2 Blue/NIR and Green/Rededge band ratio performed better among all sensors with an RMSE of 5.08 µg/L and % MAE of 12.85, and an RMSE of 11.10 µg/L and % MAE of 46.5%, respectively. The algorithms developed for each OTWs are shown below (Fig. 3.11)

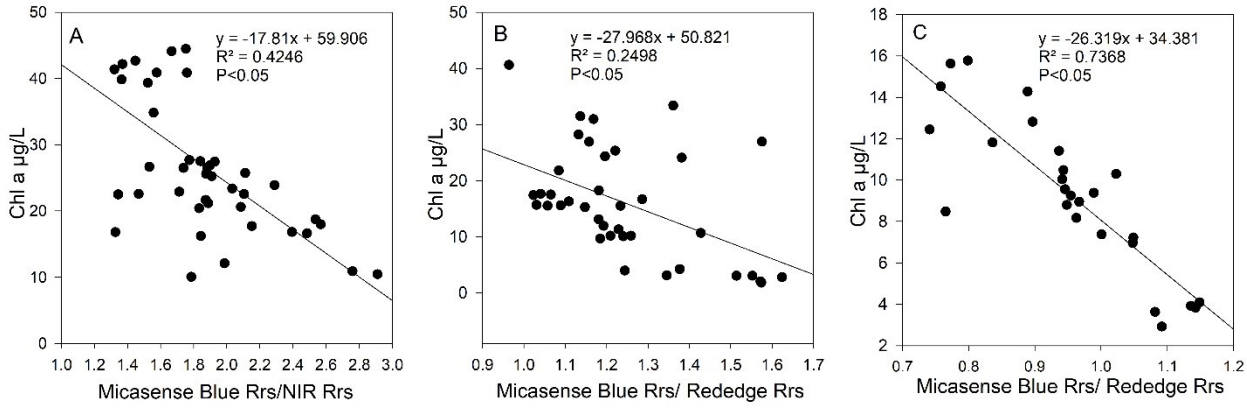

Figure 3.11 Algorithms developed for the optical water types (OWTs) 1, 2, and 3 of lakes using UAS sensors, A) OWT1, and B) OWT2, and C) OWT3

3.3.3.2 Lower Pearl River Estuary

The band ratio algorithm (Green/Red) developed for the MicaSense sensor performed better than CIR in all the three OWTs of LPRE. The algorithms developed for each OTWs are shown in the below (Fig.3.12). Among three OWTs, the algorithm developed for OWT3 performed better among the three water types with an RMSE of 2.038 µg/L and %MAE of 25.64%. The algorithms developed for OWT1 and OWT2 had an RMSE of 4.08 µg/L and %MAE of 57.1%, and an RMSE of 2.1 µg/L and %MAE of 39.96%, respectively. Tables A.23, A.24, and A.25 show the result for the UAS sensors and their performances in each OWTs of LPRE.

The measured vs modeled Chl *a* for lakes and LPRE for the aforenoted sensors are shown in below (Fig.3.13)

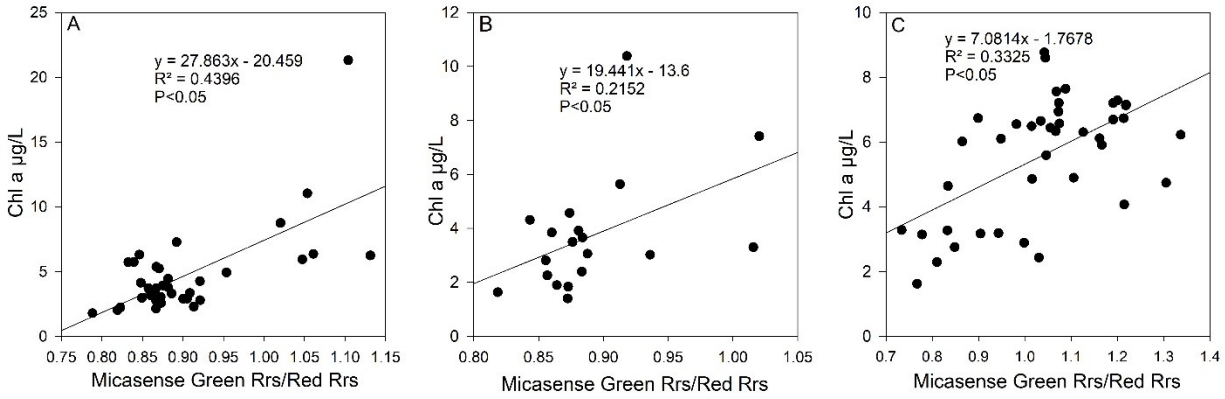

Figure 3.12 Algorithms developed for three optical water types (OWTs) for using UAS sensors in LPRE A) OWT1, B) OWT2, and C) OWT3

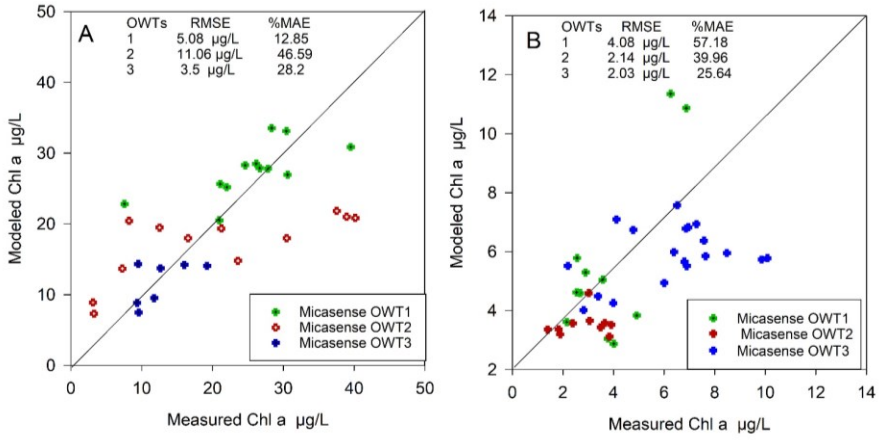

Figure 3.13 Algorithm validation optical water types OWT1, OWT2 and OWT3 of Lakes using UAS sensors A) Lakes, and B) LPRE

3.4 Discussion

3.4.1 Satellite sensors derived algorithms in Lakes

This study shows that over the full range of *in situ* Chl a, among the three satellite sensors used, OLCI sensor estimated Chl a reasonably well with mean absolute errors below 30% (for OWT1 and OWT3) shown in tables A.14, A.15 and A.16, which is consistent with previous studies using similar satellite sensors (C. Hu, Feng, and Lee

2013; Kahru et al. 2014). In general, the algorithms developed for Chl a using remote sensing are considered within acceptable goal if the algorithm meet accuracy goals of 5% and 35% for the retrieved surface remote sensing reflectance and chlorophyll-a concentrations in the surface ocean (Hooker et al., 1992). Since, the optical properties of water in inland waters such as lakes and estuaries are more complex than oceans due to higher influence of land and surface run offs, the results for lakes, the accuracy obtained from our algorithms are consistent with previous work.

Algorithms using Green and NIR band of OLCI performed well among all other band ratios. Although best performing algorithms for all three OWTs had Green/NIR band ratios, the band center for Green was different for OWT2 from OWT1 and OWT3 and error was also much higher. The difference in spectral shape due to optically active constituents likely played a role in change of band center for OWT2. It is shown in Fig 4A that the Rrs in the green region is highest near 560 nm for OWT1 and OWT 3, whereas the Rrs peak for OWT2 is close to 510 nm. The Landsat band ratio algorithm performed better among all the satellite sensors used for OWT2. However, error was higher than those on OWT1 and OWT3 with an RMSE of 9.2 µg/L and %MAE of 38.8%. The high range of Chl a concentration in OTW2 is the likely reason for the resulting high error which was also the case in a previous study (T. Moore et al. 2014).In OWT2, the Chl a in lower concentration or higher concentration can have greater influence in the algorithm coefficient which produce errors in validation .The range of Chl a concentration for algorithm development was 1.8 to 40 µg/L ,with majority of Chl a concertation in higher concentration, which were greater than 10 µg/L with weak R^2

(0.28) at 0.05 level of significance. The Chl a concentration in validation data set were in lower concentration (1.3-3.4 µg/L) which resulted into higher errors.

Thus, our assessment of clustered Chl a algorithm in Mississippi Lakes showed that OLCI band ratio algorithm performed best with minimum RMSE (1.6 µg/L), % RMSE (13.1%), and % MAE (10.09%) when Chl a was at range of 2.9-15 µg/L and average Rrs at Green and Red bands as shown in table 4 A.

3.4.2 Satellite derived algorithms in LPRE

The algorithms developed for the OLCI sensor to quantify Chl a in LPRE performed the best among the algorithms for all the three satellites sensors in terms of R^2 of the algorithm and errors; RMSE, % RMSE and % MAE. OLCI algorithm developed from Green/ Red band performed well in all three OWTs but best performing algorithm was developed for OWT3 with low RMSE and low %MAE (Table 8). The range of Chl a was lower than that of OWT1 and OWT2. For OWT3, algorithms developed from MODIS and Landsat also performed well with slightly higher RMSE and % MAE. The bands used in algorithm development have distinct peaks at those two regions which can be seen in Fig. 3.6 D. The Rrs was low near 560 nm (Band6) and high at 681 m (Band 10). Band 6 is the visible part of the spectrum hence it was absorbed the most by Chl a, in contrast to band 10, which is close to Rededge region where reflectance from Chl a is highest that allows the band ratio algorithm to extract the valuable information about Chl a concentration

3.4.3 UAS Algorithms derived for the lakes

The algorithms developed for the five-band sensor, MicaSense, performed well on all three OWTs of lakes with mean absolute error below 30% for OWT1 and OWT3. These errors were less than the errors obtained for the algorithms developed for the satellite sensors. The bands for the ratios were different for three OWTs (Table 9, Table10 &Table 11), which corresponds well with the spectral shape of each water types (Fig.3.6 E). Hence the bands Blue, Green, NIR and Red of the MicaSense are useful in Chl *a* estimation.

3.4.4 UAS Algorithms derived for LPRE

The algorithms developed for the MicaSense sensor performed well on all three OWTs of LPRE. The results were similar to the algorithms developed for the satellite sensor OLCI in terms of RMSE and mean absolute error. The band ratios were Green/ Red for all the OWTs in case of both satellite and UAS sensors. Green/Red band ratio performed best among all other band ratios in contrast to the algorithms developed for the lakes that included three different band ratios for the three OTWs in the lakes. Dissimilarity in water constituent such as sediments, CDOM and phytoplankton concentration in lakes and estuary could be the possible reasons for such contrast.

3.5 Conclusion

Monitoring Chl a concentration is essential to prevent the effects of harmful algal blooms which severely impacts human health, aquatic ecosystems, and the economy. Given the dynamic nature of algal blooms which can be highly unpredictable, monitoring such events can be challenging with satellite sensors since the sensors have low spatial

resolution with respect to the size of water bodies, revisit time, and cloud coverages. Application of remote sensing techniques using Unmanned Aerial Systems (UASs) offer best remote sensing approaches to accurately detect and quantify phytoplankton concentration in smaller water bodies. An assessment of suitable sensors to determine the best algorithm for quantifying Chl a concentration can help continuous monitoring of HABs and take preventive measures to protect human health and environment in the most effective manner. Inland and coastal waters are highly susceptible to effects from land such as runoff of sediments, nutrients and organic matter and re-suspension of sediments from shallow bottoms. In addition, the concentrations of particles including phytoplankton can be much variable in different water types. As a result, algorithms developed for a particular water type are less effective and not applicable to optically different water types (Melin et al. 2011; T. S. Moore, Campbell, and Dowell 2009). Our assessment of a clustered chlorophyll-*a* product approach showed lower RMSE and MAE than for either of the single algorithms over the entire range of the *in situ* data set. From our analysis, each algorithm generally performed best at certain ranges of Chl *a* and certain intensity of Rrs at each band centers of sensors. From our results, we found that a single algorithm is not applicable for all water types as defined by the optical characteristics governed by concentration of phytoplankton, suspended sediments, CDOM etc. that was also demonstrated by previous studies(T. Moore et al. 2014; T. S. Moore, Campbell, and Dowell 2009) Overall, the UAS sensor MicaSense developed algorithm performed the best for all the sensors used in this study and the satellite sensor OLCI performed better than Landsat OLI and MDIS sensors in chlorophyll-*a* estimation. Hence, the algorithms developed for those sensors in this study represent the best

algorithms at present for chlorophyll-*a* estimation in these water bodies. These findings support the view that empirical algorithms tuned and developed for specific ranges of conditions perform better than an algorithm tuned to a larger variety of conditions, and a multiple sensor algorithm approach is superior to single sensor developed algorithms when considering the entire dynamic range of environmental conditions.

For empirical algorithm, the seasonality of data collection does not influence in algorithm performance greatly because the empirical algorithm does not take in account for any other variables. In our study, the empirical algorithm provided the linear relation between the Chl a concertation and band ratio Rrs. The data collected in lakes were mostly in summer seasons but it could capture the variability and the range of Chl a from low concentration to higher concentration through the sampling dates. Likewise, we found a well distributed Chl a concertation range in LPRE sampled in four different seasons. For instance, the average Chl a concentration for sample collected during December 2014 was 11.3 µg/L with range of 6.5-22.1 µg/L and again when the samples were collected in 2015 December, the average Chl a was 4.9 µg/L with range of 2.1 to 6.9 µg/L.

We are limited by data in this study. So, currently we do not know whether all possible optical classes of estuaries and lakes are represented in three OWTs. To gain more insight on this aspect, more data needs to be collected at throughout the year to represent overall conditions in these water bodies. A larger dataset could also improve the algorithm performance with improved R^2 and reduced errors.

CHAPTER IV

CONCLUSIONS

This study was carried out in multiple water bodies including lakes, estuary and coastal regions. In this study several laboratory and *in-situ* techniques were used for determining phytoplankton community structure present in each water bodies and five sensors were used to quantify chlorophyll -*a* which represents total phytoplankton biomass. While in some scenarios one technique is better than others, it was found that use of a few techniques together can extract the crucial information in understanding the phytoplankton community structure and occurrence of phycotoxins in water. For instance, FlowCam could be used for separating chlorophytes and euglenophytes, or diatoms and dinoflagellates visually which is not always possible in ChemTax pigment analysis due to shared pigments by both phytoplankton. However, for small cell size phytoplankton, ChemTax produces better results due to difficulties in identifying small cell size phytoplankton using FlowCam. When phycotoxin-producing phytoplankton are considered, if toxin is measured together with FlowCam or HPLC-ChemTax or pigment measurements, it will provide a comprehensive information about the presence of toxins as well as the phytoplankton species responsible for producing the toxins which will be helpful for adopting preventive measures for water managers. Surface area of phytoplankton can be used to obtain an accurate measure of relative abundance of genus or species within a group of phytoplankton. The three pigment based methods, HPLC-

ChemTax, *in situ* fluorescence probe, and fluorescence of extracted Chl *a* and PC, provide complementary information on freshwater and estuarine phytoplankton. The findings of this study conclude that among several techniques available for monitoring phytoplankton structure, FlowCam is the most useful technique for species identification, HPLC-ChemTax for taxonomic classification, *in-situ* probes for gathering information rapidly for initial estimation of phytoplankton biomass, and spectrofluorometric techniques and toxin analysis are needed for precise determination of harmful impacts. Traditionally, phytoplankton identification and enumeration are done manually using a microscope (Benfield et al., 2007) which is tedious, time consuming, costly and needs highly skilled expertise. From our study, we found that several species of phytoplankton can be identified rapidly by using FlowCam. Similarly, we attempted to determine algal class based on area of phytoplankton and obtained comparable result with standard pigment analysis method (HPLC). Our finding also corroborated the previous studies (Alvarez et al. 2014; See et al. 2005). Likewise, from the comparative analysis of *in-situ* verses analytical techniques to quantify Chlorophyll a, we confirmed the reliability of *in-situ* probes to rapidly quantify the phytoplankton biomass in our study areas. See et al., 2005 in their study also found out the similar results when they compared Chl a obtained from HPLC with Chl a measured by in-situ probe. From our toxin analysis, we could detect the algal toxins as low as 0.1 µg/L using ELISA. Our results suggested that even though there were no significant correlation between phytoplankton pigment concentration, toxins can be present. Hence, in water bodies where frequent human and animal interactions occur for drinking water, recreation , fishing and swimming, ELISA can be very useful for early detection of toxic algal outbreaks. Thus, these findings

provide insights for future studies to make a suitable selection of techniques as per their objectives.

Conventional analytical and *in-situ* techniques of phytoplankton quantification and toxin analysis are expensive and time consuming and they do not provide the synoptic coverage. Hence for early detection and warning the bloom conditions, remote sensing quantification of chlorophyll-*a* serves as the best technique which is economic as well as time efficient. So, use appropriate sensors in UASs can be an efficient technique to provide valuable information to water managers and agencies to issue early warning during the outbreak of harmful algal blooms. Among five sensors used in our study, we found that MicaSense sensor was most efficient in quantifying Chl a with minimum errors hence, we suggest using the algorithm developed by this sensor for future quantification of Chl a in these and similar water bodies. We tested the applicability of multiple sensors, three currently operational satellite sensors – MODIS, OLI, OLCI and two popular UAS sensors CIR and MicaSense for quantifying Chl a in five major Mississippi Lakes and an estuary LPRE for the first time. We found the best algorithms for these water bodies using those sensors. Among three satellite sensors, OLCI and OLI produced better performing algorithm in terms of RMSE and %MAE for quantifying Chl a. For OLCI , the algorithm with maximum R^2 of 0.73 was obtained with % RMSE of 13.1% in lakes , similar results were obtained by (Watanabe et al. 2017) when using MSI sensors which is the similar sensor in Sentinel -2 satellite platform developed band ratio algorithm for Chl a estimation. Likewise, for OLI sensors, the algorithm with maximum R^2 of 0.73 was obtained with % RMSE of 13.1% in lakes, and clustering improved the

algorithm which was also mentioned by (Watanabe et al. 2017) since their algorithm had lower R^2 value (0.02)when a single algorithm was developed for entire water body.

In summary, this study emphasized the application of in-*situ*, laboratory and remote sensing techniques to access the phytoplankton community structure to determine the overall health of aquatic ecosystem. Early detection and identification of phytoplankton including toxin producing harmful algal blooms are critical to protect the health of human, animals and ecosystem and prevent economic loss. Thus, this study helped us better understand the application of various techniques and their potentials in quantifying harmful algal blooms.

4.1 Significance of this study

This dissertation research focused on identifying and enumerating phytoplankton species composition and relative abundance as well as quantifying pigment concentration of phytoplankton using in-situ, precise laboratory and remote sensing techniques. Knowledge of species composition and relative abundance of phytoplankton is necessary to predict and prevent possible hazards caused by harmful algal blooms. Based on the scenarios one technique serve better than another and use of appropriate technique can be efficient and economically feasible to prevent hazards related to harmful algal blooms. With increased nutrient run off from agricultural lands, the problem of HAB's is inevitable hence continuous monitoring of HAB's is essential for health of human and environment. Present study provided an insight on utility of techniques to quantify harmful algal blooms in relatively smaller but ecologically important water bodies of

Mississippi. The results from the study can be used to quantify harmful algal blooms in these and similar water bodies for continuous monitoring.

REFERENCES

Alvarez, Eva et al. 2014. "Routine Determination of Plankton Community Composition and Size Structure: A Comparison between FlowCAM and Light Microscopy." *Journal of Plankton Research* 36(1): 170–84.

Álvarez, Eva, Ángel López-Urrutia, and Enrique Nogueira. 2012. "Improvement of Plankton Biovolume Estimates Derived from Image-Based Automatic Sampling Devices: Application to FlowCAM." *Journal of Plankton Research* 34(6): 454–69.

Anderson, Donald, Patricia Glibert, and Joann Burkholder. 2002. "Harmful Algal Blooms and Eutrophication: Nutrient Sources, Compositions, and Consequences." *Estuaries* 25(4): 704–26.

Anderson, Donald M. 2009. "Approaches to Monitoring, Control and Management of Harmful Algal Blooms (HABs)." *Ocean and Coastal Management* 52(7): 342–47. http://dx.doi.org/10.1016/j.ocecoaman.2009.04.006.

Baker, Judith A, Barrie Entsch, Brett A Neilan, and David B Mckay. 2002. "Monitoring Changing Toxigenicity of a Cyanobacterial Bloom by Molecular Methods." 68(12): 6070–76.

Benfield, Mark et al. 2007. "RAPID: Research on Automated Plankton Identification." *Oceanography* 20(2): 172–87.

Blaha, Ludek, Pavel Babica, and Blahoslav Marsalek. 2009. "Toxins Produced in Cyanobacterial Water Blooms - Toxicity and Risks." *Interdisciplinary toxicology* 2(2): 36–41. http://www.pubmedcentral.nih.gov/articlerender.fcgi?artid=2984099&tool=pmcentrez&rendertype=abstract.

Brewin, Robert J.W. et al. 2015. "The Ocean Colour Climate Change Initiative: III. A Round-Robin Comparison on in-Water Bio-Optical Algorithms." *Remote Sensing of Environment* 162: 271–94. http://dx.doi.org/10.1016/j.rse.2013.09.016.

Buchaca, Teresa, Marisol Felip, and Jordi Catalan. 2005. "A Comparison of HPLC Pigment Analyses and Biovolume Estimates of Phytoplankton Groups in an Oligotrophic Lake." 27(1).

Buskey, Edward J., and Cammie J. Hyatt. 2006. "Use of the FlowCAM for Semi-Automated Recognition and Enumeration of Red Tide Cells (Karenia Brevis) in Natural Plankton Samples." *Harmful Algae* 5(6): 685–92.

Culverhouse, Phil F. et al. 2003. "Do Experts Make Mistakes? A Comparison of Human and Machine Identification of Dinoflagellates." *Marine Ecology Progress Series* 247(February): 17–25.

Dash, Padmanava et al. 2011. "Estimation of Cyanobacterial Pigments in a Freshwater Lake Using OCM Satellite Data." *Remote Sensing of Environment* 115(12): 3409–23. http://dx.doi.org/10.1016/j.rse.2011.08.004.

Dash,Padmanava et al. 2015. "Water Quality of Four Major Lakes in Mississippi, USA: Impacts on Human and Aquatic Ecosystem Health." *Water (Switzerland)* 7(9): 4999–5030.

Dekker, A. G. 1993. Management *Detection of Optical Water Quality Parameters for Eutrophic Waters by High Resolution Remote Sensing*.

Dierssen, H. M. 2010. "Perspectives on Empirical Approaches for Ocean Color Remote Sensing of Chlorophyll in a Changing Climate." *Proceedings of the National Academy of Sciences* 107(40): 17073–78. http://www.pnas.org/cgi/doi/10.1073/pnas.0913800107.

Falconer, Ian R. 1989. "Effects on Human Health of Some Toxic Cyanobacteria (Blue-Green Algae) in Reservoirs, Lakes, and Rivers." *Toxicity Assessment* 4(2): 175–84. http://doi.wiley.com/10.1002/tox.2540040206 (September 12, 2016).

Flynn, Kyle F., and Steven C. Chapra. 2014. "Remote Sensing of Submerged Aquatic Vegetation in a Shallow Non-Turbid River Using an Unmanned Aerial Vehicle." *Remote Sensing* 6(12): 12815–36.

Galluzzi, Luca et al. 2004. "Development of a Real-Time PCR Assay for Rapid Detection and Quantification of Alexandrium Minutum (a Dinoflagellate)." *Applied and environmental microbiology* 70(2): 1199–1206.

Garcia, Ana C. et al. 2010. "Evaluating the Potential Risk of Microcystins to Blue Crab (Callinectes Sapidus) Fisheries and Human Health in a Eutrophic Estuary." *Harmful Algae* 9(2): 134–43.

Gholizadeh, Hamed, and Scott M. Robeson. 2016. "Revisiting Empirical Ocean-Colour Algorithms for Remote Estimation of Chlorophyll-a Content on a Global Scale." *International Journal of Remote Sensing* 37(11): 2682–2705. http://dx.doi.org/10.1080/01431161.2016.1183834.

Gilerson, Alexander A et al. 2007. “Fluorescence Component in the Reflectance Spectra from Coastal Waters. Dependence on Water Composition.” *Optical Scoiety of America* 15: 24.

Gilerson, Alexander A. et al. 2010. “Algorithms for Remote Estimation of Chlorophyll-a in Coastal and Inland Waters Using Red and near Infrared Bands.” *Optics Express* 18(23): 109–24.

Gower, J, S King, G Borstad, and L Brown. 2005. “Detection of Intense Plankton Blooms Using the 709 Nm Band of the MERIS Imaging Spectrometer.” *International Journal of Remote Sensing* 26: 2005–12.

Gregor, J., and B. Maršálek. 2004. “Freshwater Phytoplankton Quantification by Chlorophyll a: A Comparative Study of in Vitro, in Vivo and in Situ Methods.” *Water Research* 38(3): 517–22.

Higgins HW, Wright SW, Schlüter L. 2011. “Quantitative Interpretation of Chemotaxonomic Pigment Data.” *Phytoplankton pigments.Cambridge University Press, NY*: 257–313.

Hoepffner, Nicolas, and Shubha Sathyendranath. 1991. “Effect of Pigment Composition on Absorption Properties of Phytoplankton.” *Marine Ecology Progress Series* 73: 11–23.

Holmes, Holmes Robert W John D.H, Hansen Holm, Carl J Lorenzen, and John D.H Strickland. 1965. “Fluorometric Determination of Chlorophyll.” *ICES Journal of marine sciences* 30: 3–15.

Horvátha, Hajnalka, Attila W. Kovácsa, Caitlin Riddickb, and Présinga Mátyás. 2013. “Extraction Methods for Phycocyanin Determination in Freshwater Filamentous Cyanobacteria and Their Application in a Shallow Lake.” *European Journal of Phycology* 48(3): 278–86.

Hu, Chuanmin, Lian Feng, and Zhongping Lee. 2013. “Uncertainties of SeaWiFS and MODIS Remote Sensing Reflectance: Implications from Clear Water Measurements.” *Remote Sensing of Environment* 133: 168–82. http://dx.doi.org/10.1016/j.rse.2013.02.012.

Hu, Chuanmin, Zhongping Lee, and Bryan Franz. 2012. “Chlorophyll a Algorithms for Oligotrophic Oceans: A Novel Approach Based on Three-Band Reflectance Difference.” *Journal of Geophysical Research: Oceans* 117(1): 1–25.

Hu, Quian. 2004. “Environmental Effects on Cell Composition.” *Handbook of Microalgal culture:Biotechnology and Applied Phycology* 1: 83–93.

Izydorczyk, Katarzyna et al. 2005. "Measurement of Phycocyanin Fluorescence as an Online Early Warning System for Cyanobacteria in Reservoir Intake Water." *Environmental Toxicology* 20(4): 425–30.

J.Nicole, Poulton, and Martin L.Jennifer. 2010. "Imaging Flow Cytometry for Quantitative Phytoplankton Analysis — FlowCAM." In *Microscopic and Molecular Methods for Quantitative Phytoplankton Analysis*, ed. Cusack Caroline and Bresnan Eileen Karlson Bengt. UNESCO, 47–54. http://www.jodc.go.jp/info/ioc_doc/Manual/187824e.pdf#page=16.

Jensen, J R. 2000. 1 Prentice Hall, Upper Saddle River, NJ *Remote Sensing of the Environment: An Earth Resource Perspective*.

Joint global Ocean Flux Study. 1998. "Standard Protocol for Measurement of Chlorophyll a." In *(Standard Protocol for Measurement of Chlorophyll.*, http://ocean.stanford.edu/cal/ (http://ocean.stanford.edu/cal/)

Joint global Ocean Flux Study. 1998. "Standard Protocol for Measurement of Chlorophyll a." In *(Standard Protocol for Measurement of Chlorophyll.*, http://ocean.stanford.edu/cal/ (http://ocean.stanford.edu/cal/.

Falconer, Ian R. 1989. "Effects on Human Health of Some Toxic Cyanobacteria (Blue-Green Algae) in Reservoirs, Lakes, and Rivers." *Toxicity Assessment* 4(2): 175–84. http://doi.wiley.com/10.1002/tox.2540040206 (September 12, 2016).

Flynn, Kyle F., and Steven C. Chapra. 2014. "Remote Sensing of Submerged Aquatic Vegetation in a Shallow Non-Turbid River Using an Unmanned Aerial Vehicle." *Remote Sensing* 6(12): 12815–36.

Galluzzi, Luca et al. 2004. "Development of a Real-Time PCR Assay for Rapid Detection and Quantification of Alexandrium Minutum (a Dinoflagellate)." *Applied and environmental microbiology* 70(2): 1199–1206.

Garcia, Ana C. et al. 2010. "Evaluating the Potential Risk of Microcystins to Blue Crab (Callinectes Sapidus) Fisheries and Human Health in a Eutrophic Estuary." *Harmful Algae* 9(2): 134–43.

Gholizadeh, Hamed, and Scott M. Robeson. 2016. "Revisiting Empirical Ocean-Colour Algorithms for Remote Estimation of Chlorophyll-a Content on a Global Scale." *International Journal of Remote Sensing* 37(11): 2682–2705. http://dx.doi.org/10.1080/01431161.2016.1183834.

Gilerson, Alexander A et al. 2007. "Fluorescence Component in the Reflectance Spectra from Coastal Waters. Dependence on Water Composition." *Optical Scoiety of America* 15: 24.

Gilerson, Alexander A. et al. 2010. “Algorithms for Remote Estimation of Chlorophyll-a in Coastal and Inland Waters Using Red and near Infrared Bands.” *Optics Express* 18(23): 109–24.

Gower, J, S King, G Borstad, and L Brown. 2005. “Detection of Intense Plankton Blooms Using the 709 Nm Band of the MERIS Imaging Spectrometer.” *International Journal of Remote Sensing* 26: 2005–12.

Gregor, J., and B. Maršálek. 2004. “Freshwater Phytoplankton Quantification by Chlorophyll a: A Comparative Study of in Vitro, in Vivo and in Situ Methods.” *Water Research* 38(3): 517–22.

Higgins HW, Wright SW, Schlüter L. 2011. “Quantitative Interpretation of Chemotaxonomic Pigment Data.” *Phytoplankton pigments.Cambridge University Press, NY*: 257–313.

Hoepffner, Nicolas, and Shubha Sathyendranath. 1991. “Effect of Pigment Composition on Absorption Properties of Phytoplankton.” *Marine Ecology Progress Series* 73: 11–23.

Holmes, Holmes Robert W John D.H, Hansen Holm, Carl J Lorenzen, and John D.H Strickland. 1965. “Fluorometric Determination of Chlorophyll.” *ICES Journal of marine sciences* 30: 3–15.

Hooker, S. B., Esaias, W. E., Feldman, G. C., Gregg, W. W., & McClain, C. R. (1992). An overview of SeaWiFS and ocean color. NASA Tech. Memo., Vol. 104566, Greenbelt, MD: National Aeronautics and Space Administration, Goddard Space Flight Center.

Horvátha, Hajnalka, Attila W. Kovácsa, Caitlin Riddickb, and Présinga Mátyás. 2013. “Extraction Methods for Phycocyanin Determination in Freshwater Filamentous Cyanobacteria and Their Application in a Shallow Lake.” *European Journal of Phycology* 48(3): 278–86.

Hu, Chuanmin, Lian Feng, and Zhongping Lee. 2013. “Uncertainties of SeaWiFS and MODIS Remote Sensing Reflectance: Implications from Clear Water Measurements.” *Remote Sensing of Environment* 133: 168–82. http://dx.doi.org/10.1016/j.rse.2013.02.012.

Hu, Chuanmin, Zhongping Lee, and Bryan Franz. 2012. “Chlorophyll a Algorithms for Oligotrophic Oceans: A Novel Approach Based on Three-Band Reflectance Difference.” *Journal of Geophysical Research: Oceans* 117(1): 1–25.

Hu, Quian. 2004. “Environmental Effects on Cell Composition.” *Handbook of Microalgal culture:Biotechnology and Applied Phycology* 1: 83–93.

Izydorczyk, Katarzyna et al. 2005. "Measurement of Phycocyanin Fluorescence as an Online Early Warning System for Cyanobacteria in Reservoir Intake Water." *Environmental Toxicology* 20(4): 425–30.

J.Nicole, Poulton, and Martin L.Jennifer. 2010. "Imaging Flow Cytometry for Quantitative Phytoplankton Analysis — FlowCAM." In *Microscopic and Molecular Methods for Quantitative Phytoplankton Analysis*, ed. Cusack Caroline and Bresnan Eileen Karlson Bengt. UNESCO, 47–54. http://www.jodc.go.jp/info/ioc_doc/Manual/187824e.pdf#page=16.

Jensen, J R. 2000. 1 Prentice Hall, Upper Saddle River, NJ *Remote Sensing of the Environment: An Earth Resource Perspective*.

Kahru, Mati et al. 2014. "Evaluation of Satellite Retrievals of Ocean Chlorophyll-a in the California Current." *Remote Sensing* 6(9): 8524–40.

Lekki, John, Robert Anderson, Quang-viet Nguyen, and James Demers. 2009. "The Early Detection and Monitoring of Harmful Algal Blooms." (April): 1–14.

Mackey, M. D., D. J. Mackey, H. W. Higgins, and S. W. Wright. 1996. "CHEMTAX - A Program for Estimating Class Abundances from Chemical Markers: Application to HPLC Measurements of Phytoplankton." *Marine Ecology Progress Series* 144(1–3): 265–83.

Marshall, Harold G. et al. 2000. "Comparative Culture and Toxicity Studies between the Toxic Dinoflagellate Pfiesteria Piscicida and a Morphologically Similar Cryptoperidiniopsoid Dinoflagellate." *Journal of Experimental Marine Biology and Ecology* 255(1): 51–74.

Mayo, M., A. Gitelson, Y. Z. Yacobi, and Z. Ben-Avraham. 1995. "Chlorophyll Distribution in Lake Kinneret Determined from Landsat Thematic Mapper Data." *International Journal of Remote Sensing* 16(1): 175–82.

Melin, F et al. 2011. "Multi-Sensor Satellite Time Series of Optical Properties and Chlorophyll-a Concentration in the Adriatic Sea. Progress in Oceanography." *Progress in Oceanography* 91(3): 229–44.

Mikel, Latasa. 2007. "Improving Estimations of Phytoplankton Class Abundances Using CHEMTAX." *Mar Ecol Prog Ser* 329: 13–21.

Mikel, Latasha, and Berdalate Elisa. 1994. "Effects of Nitrogen or Phosphorus Starvation on Pigment Composotion of Heterocapsa Sp." *Journal of Phycology* 16: 83–94.

Moore, Timothy, Mark.D Dowell, Shane Bradt, and Antonio Ruiz Verdu. 2014. "An Optical Water Type Framework for Selecting and Blending Retrievals from Bio-Optical Algorithms in Lakes and Coastal Waters." 143: 97–111.

Moore, Timothy S., Janet W. Campbell, and Mark D. Dowell. 2009. "A Class-Based Approach to Characterizing and Mapping the Uncertainty of the MODIS Ocean Chlorophyll Product." *Remote Sensing of Environment* 113(11): 2424–30. http://dx.doi.org/10.1016/j.rse.2009.07.016.

O'Reilly, John et al. 2000. "Ocean Color Chlorophyll a Algorithms for SeaWiFS, OC2 and OC4: Version 4." In *SeaWiFS Post Aunch Calibration and Validation Analyses, Part 3*, , 8–22.

O'Reilly, John . et al. 1998. "Ocean Color Chlorophyll Algorighms for SeaWiFS." *Journal of Geophysical Research* 103(C11): 24937–53.

Paerl, Hans W., Rolland S. Fulton, Pia H. Moisander, and Julianne Dyble. 2001. "Harmful Freshwater Algal Blooms, With an Emphasis on Cyanobacteria." *The Scientific World JOURNAL* 1: 76–113. http://www.hindawi.com/journals/tswj/2001/139109/abs/.

Pierce, RH, and GJ Kirkpatrick. 2001. "Innovative Techniques for Harmful Algal Toxin Analysis." *Environmental toxicology and ...* 20(1): 107–14. http://onlinelibrary.wiley.com/doi/10.1002/etc.5620200110/full.

Pinckney, J L, M B Harrington, and K E Howe. 1998. "Annual Cycles of Phytoplankton Community-Structure\rand Bloom Dynamics in the Neuse River Estuary, North Carolina." *Marine Biology* 131: 371–81.

Pinckney, James, Tammi Richardson, David Millie, and Hans \ Paerl. 2001. "Application of Photopigment Biomarkers for Quantifying Microalgal Community Composition and in Situ Growth Rates." *Organic Geochemistry* 32(4): 585–95.

Rinta-Kanto, J. M. et al. 2005. "Quantification of Toxic Microcystis Spp. during the 2003 and 2004 Blooms in Western Lake Erie Using Quantitative Real-Time PCR." *Environmental Science and Technology* 39(11): 4198–4205.

Ruddick, Kevin George, Herman J Gons, Machteld Rijkeboer, and Gavin Tilstone. 2001. "Optical Remote Sensing of Chlorophyll a in Case 2 Waters by Use of an Adaptive Two-Band Algorithm with Optimal Error Properties." *Applied Optics* 40(21): 3575–85.

Sarada, R., Manoj G. Pillai, and G. A. Ravishankar. 1999. "Phycocyanin from Spirulina Sp: Influence of Processing of Biomass on Phycocyanin Yield, Analysis of Efficacy of Extraction Methods and Stability Studies on Phycocyanin." *Process Biochemistry* 34(8): 795–801.

Schalles, John F, and Yosef Z Yacobi. 2000. "Remote Detection and Seasonal Patterns of Phycocyanin, Carotenoid and Chlorophyll Pigments in Eutrophic Waters." *Ergebnisse Der Limnologie* 55: 153–68.

Schlüter, Møhlenberg F., Havskum. H, Larsen. S. 2000. "The Use of Phytoplankton Pigments for Identifying and Quantifying Phytoplankton Groups in Coastal Areas: Testing the Influence of Light and Nutrients on Pigment/chlorophyll a Ratios." *Marine Ecology Progress Series* 192: 49–63.

See, Jason H. et al. 2005. "Combining New Technologies for Determination of Phytoplankton Community Structure in the Northern Gulf of Mexico." *Journal of Phycology* 41(2): 305–10.

Siegel, Herbert, M. Gerth, T. Ohde, and T. Heene. 2005. "Ocean Colour Remote Sensing Relevant Water Constituents and Optical Properties of the Baltic Sea." *International Journal of Remote Sensing* 26(2): 315–30.

Siegelman, HW, and JH Kycia. 1978. "Algal Billiproteins." In *Handbook of Phycologial Methods: Physiological and Biocemical Methods*, eds. Johan A. Hellebust and J.S. Craigie. New York: Cambridge University Press, 71–79.

Simis, Stefan G. H., Steef W. M. Peters, and Herman J. Gons. 2005. "Remote Sensing of the Cyanobacterial Pigment Phycocyanin in Turbid Inland Water." *Limnology and Oceanography* 50(1): 237–45.

The Nature Conservancy. 2017. "Mississippi Lower Pearl River Partnership." https://www.nature.org/ourinitiatives/regions/northamerica/unitedstates/mississippi/placesweprotect/lower-pearl-river-partnership.xml (September 10, 2017).

Twardowski, Michael S., Marlon R. Lewis, Andrew H. Barnard, and J. Ronald V. Zaneveld. 2005. "In-Water Instrumentation and Platforms for Ocean Color Remote Sensing." In *Remote Sensing for Coastal Aquatic Environments*, , 69–100.

Ueno, Y. et al. 1996. "Detection of Microcystins, a Blue- Green Algal Hepatoxin, in Drinking Water Sampled in Haimen and Fusui, Endemic Areas of Primary Liver Cancer in China, by Highly Sensitive Immunoassay." *Carcinogenesis* 17(18): 1317–21.

Watts, Adam C., Vincent G. Ambrosia, and Everett A. Hinkley. 2012. "Unmanned Aircraft Systems in Remote Sensing and Scientific Research: Classification and Considerations of Use." *Remote Sensing* 4(6): 1671–92.

Wintermans, J.F.G.M., and A. De Mots. 1965. "Spectrophotometric Characteristics of Chlorophylls a and B and Their Phenophytins in Ethanol." *Biochimica et Biophysica Acta (BBA) - Biophysics including Photosynthesis* 109(2): 448–53. http://linkinghub.elsevier.com/retrieve/pii/0926658565901706 (September 13, 2016).

Zamyadi, Arash et al. 2012. “Cyanobacterial Detection Using in Vivo Fluorescence Probes: Managing Interferences for Improved Decision-Making.” *Journal - American Water Works Association* 104(8).

Zarauz, L., X. Irigoien, A. Urtizberea, and M. Gonzalez. 2007. “Mapping Plankton Distribution in the Bay of Biscay during Three Consecutive Spring Surveys.” *Marine Ecology Progress Series* 345(September): 27–39.

Zimba, Paul V., and Anatoly Gitelson. 2006. “Remote Estimation of Chlorophyll Concentration in Hyper-Eutrophic Aquatic Systems: Model Tuning and Accuracy Optimization.” *Aquaculture* 256(1–4): 272–86.

APPENDIX A

TABLE

Table A.1 List of identified class and taxa found in the study areas

Class	Taxa	Class	Taxa	Class	Taxa
Cyanobacteria	*Anabaena circinalis*	Cyanobacteria	*Merismopedia sp.*	Diatoms	*Stephanodiscus agassizensis*
Cyanobacteria	*Anabaena crassa*	Cyanobacteria	*Microcystis aeruginosa*	Diatoms	*Symbella sp.*
Cyanobacteria	*Anabaena laxa*	Cyanobacteria	*Microcystis cf. firma*	Diatoms	*Amphipleura pellicuda*
Cyanobacteria	*Anabaena palnctonica*	Cyanobacteria	*Microcystis flos aquae*	Diatoms	*Aulacoseria granulata*
Cyanobacteria	*Anabaena spiriods*	Cyanobacteria	*microcystis wesenbergii*	Diatoms	*Craticula ambigua*
Cyanobacteria	*Anabaenopsis circularis*	Cyanobacteria	*Nostoc sp.*	Diatoms	*Cyclotella sp.*
Cyanobacteria	*Anabena spherica*	Cyanobacteria	*Oocysts sp.*	Diatoms	*cylindrotheca closterium*
Cyanobacteria	*Anabena torulosa*	Cyanobacteria	*Oscillatoria sp.*	Diatoms	*Cymatopleura solea*
Cyanobacteria	*Aphanizomenon flos aquae*	Cyanobacteria	Other Anabaena	Diatoms	*Cymbella sp.*
Cyanobacteria	*Arthrospira Stizenberger ex gomont*	Cyanobacteria	Other microcystis	Diatoms	*Diatoma vulgaris*
Cyanobacteria	*Chrococcus sp.*	Cyanobacteria	*Phormidium sp.*	Diatoms	*Gomphonema sp.*
Cyanobacteria	*Cocconies pediculus*	Cyanobacteria	*Plaktothrix rubescens*	Diatoms	*Navicula sp.*
Cyanobacteria	*Coelosphaerium sp.*	Cyanobacteria	*Planktothrix agradhii*	Diatoms	*Niztchia sp.*

Table A.1 (continued)

Class	**Taxa**	**Class**	**Taxa**	**Class**	**Taxa**
Chlorophytes	*Staurastrum tetracerum*	Chlorophytes	*Tetrastrum staurogeniaeforme*	Chlorophytes	*Scenedesmus quadricauda*
Chlorophytes	*Staurastum planctonicum*	Chlorophytes	*Botrycoccus sp*	Chlorophytes	*Scenesdesmus acuminatus*
Diatoms	*Synedra sp.*	Chlorophytes	*Cosmarium Botrys*	Chlorophytes	*Scenesdesmus disciformis*
Diatoms	*Synedra ulna*	Chlorophytes	*Crucigenia lauterbornii*	Chlorophytes	*Spirogyra*
Diatoms	*Tabellaria flocculosa*	Chlorophytes	*Crucigenia quadracauda*	Chlorophytes	*Staurastrum paradoxum*
Diatoms	*Tabellaria sp.*	Chlorophytes	*Crucigenia quadrata*	Chlorophytes	*Staurastrum sp*
Dinoflagellates	*Alexandrium fundyense*	Chlorophytes	*Crucigenia tetrpedia*	Chlorophytes	*Closterium sp*
Dinoflagellates	*Ceratium furca*	Chlorophytes	*Desmodesmus brasiliensis*	Chlorophytes	*Crucigenia fenestrata*
Dinoflagellates	*Ceratium hirundinella*	Chlorophytes	*Kentrosphaera gibberosa*	Chlorophytes	*Scenesdesmus sp*
Dinoflagellates	*Dinophysis acuminata*	Chlorophytes	*Monoraphidium arcuatum*	Chlorophytes	*Volvox tertius*

Table A.1 (continued)

Class	**Taxa**	**Class**	**Taxa**	**Class**	**Taxa**
Dinoflagellates	*Gyrosigma acuminatum*	Chlorophytes	*Monoraphidium species*	Chrysophytes	*Dictyosphaerium nageli*
Dinoflagellates	*Karenia brevis*	Chlorophytes	Other green algae	Chrysophytes	*Synura sp.*
Dinoflagellates	*Noticula sp.*	Chlorophytes	*Pandorina sp*	Euglena	*Euglena sp.*
Dinoflagellates	*other Dinofalgellates*	Chlorophytes	*Pediastrum duplex*	Unidentified	Detritus and Unidentified
Dinoflagellates	*Prorocentrum minimum*	Chlorophytes	*Pediastrum simplex*		
Dinoflagellates	*Prorocentrum micans*				
Dinoflagellates	*Ceratium fusus*				
Dinoflagellates	*Craticula hirudinella*				
Chlorophytes	*Chlamydomonas*				

Table A.2 List of identified species found in East Mississippi Sound (EMS)

Chlorophytes	**Diatoms**	**Dinoflagellates**	**Cyanobacteria**	**Diatoms**
Dictyosphaerium nageli	*Cyclotella sp.*	*Prorocentrum micans*	*Nostoc sp.*	*Niztchia sp.*
Scenesdesmus quadricauda	*Tabellaria sp.*	*Karenia brevis*	*Microcystis wesenbergii*	*Gomphonema sp.*
Cosmarium botrys	*Synedra sp.*	*Prorocentrum micans*	*Microcystis flos aquae*	*Navicula sp.*
Synura sp.	*Tabellaria flocculosa*	*Prorocentrum minimum*	*Microcystis aeruginosa*	*Diatoma vulgaris*
Closterium sp.	*Synedra ulna*	*Dinophysis acuminatum*	*Eutonia formica*	*Cymatopleura solea*
Tetrastrum staurogeniaforme	*Symbella sp.*	*Ceratium furca*	*Coleosphaerium sp.*	*Cylindrotheca closterium*
Chlamydomonas sp.	*Stephanodiscus agassizensis*	*Alexandrium fundyense*	*Cocconies pediculus*	*Cyclotella sp.*
Botrycoccus sp.	*Pleurosigma elongatum*		*Chrococcus sp.*	*Craticula ambigua*
	Pleurosigma acuminatum			*Aulacoseria granulata*
	Pinularia sp.			*Melosira sp.*
	Pennate diatoms			*Melorisa varians*
				Gyrosigma acuminatum

Table A.3 List of identified species found in Lower Pearl River Estuary(LPRE)

Chlorophytes	**Cyanobacteria**	**Diatoms**	**Dinoflagellates**	**Euglenophytes**
Dictyosphaerium nageli	*Raphidosis curvata*	*Amphipleura pellicuda*	*Prorocentrum micans*	*Euglena sp.*
Ankistrodesmus sp.	*Anabaena circinalis*	*Aulacoseria granulata*	*Alexandrium fundyense*	*Euglena proxima*
Chlamydomonas sp.	*Anabaena flos aquae*	*Craticula ambigua*	*Ceratium fusus*	
Coelastrum sp.	*Anabaena laxa*	*Craticula sp.*	*Craticula hiudinella*	
Cosmarium botrys	*Anabaena torulosa*	*Diatoma vulgaris*	*Cyclotella sp.*	
Cosmarium botrys	*Anabaenopsis circularis*	*Gomphonema sp.*	*Gyrodinium sp.*	
Cosmarium botrys	*Aphanizomenon flos aquae*	*Gyrosigma acuminatum*	*Karenia brevis*	
Crucigenia fenestrata	*Chrococcus sp.*	*Melosira ap.*	*Other dinoflgellates*	
Crucigenia lauterbornii	*Coeloaphaerium sp.*	*Melosira varians*	*Peridinium sp.*	
Crucigenia quadracaudata	*Coelosphaerium sp.*	*Navicula sp.*	*Prorocentrum micans*	
Crucigenia quadrata	*Cylindrospermopsis raciborski*	*Niztchia sp.*	*Prorocentrum minimum*	
Crucigenia tetrapedia	*Eutonia formica*	*Othe diatoms*		
Dictyosphaerium nageli	*Johannesbaptisia primaria*	*Pennate diatoms*		
Monoraphidium sp.	*Merismopedia sp.*	*Stephanodiscus agassizensis*		
Other green algae	*Miccrocystis wesenbergii*	*Synedra sp.*		

Table A.3 (continued)

Chlorophytes	**Cyanobacteria**	**Diatoms**
Pandorina sp.	*Microcystis aeruginosa*	*Synedra ulna*
Pediastrum simplex	*Microcystis cf. firma*	*Tabellaria sp.*
Scenesdesmus quadrata	*Microcystis flos aquae*	
Scenesdesmus quadricauda	*Microcystis flos aquae*	
Senesdesmus quadratra	*Microcystis wesenbergii*	
Staurastrum planctonicum	Nostoc sp.	
Staurastrum sp.	Oocysts sp.	

Table A.4 List of identified species found in Ross Barnett Reservoir(RB)

Chlorophytes	***Cyanobacteria***	***Diatoms***	***Dinofalgellates***	***Euglenophytes***
Dictyosphaerium nageli	*Microcystis wesenbergii*	*Symbella sp.*	*Dinophysis acuminata*	*Euglena sp.*
Ankistrodesmus sp.	*Anabaena circinalis*	*Amphipleura pellicuda*	*Other dinoflagellates*	
Botrycoccus sp.	*Anabaena flos aquae*	*Aulacoseria granulata*	*Noticula sp.*	
Chlamydomonas sp.	*Anabaena laxa*	*Diatoma vulgaris*	*Craticula hirudinella*	
Closterium sp.	*Anabaena spherica*	*Gomphonema sp.*	*Ceratium fuscus*	
Cosmarium botrys	*Anabaenopsis circularis*	*Gyrosigma acuminatum*	*Alexandrium fundyense*	
Crucigenia lauterbornii	*Anabena spiriods*	*Melosira varians*	*Other dinofalgellates*	
Crucigenia quadracauda	*Aphanizomenon flos aquae*	*Melosiratoma varians*	*Noticula sp.*	
Crucigenia quadrata	*Microcystis cf. firma*	*Navicula sp.*	*Alexandrium fundyense*	
Crucigenia tetrapedia	*Microcystis wesenbergii*	*Nizchia sp.*	*Karenia brevis*	
Desmodesmus brasiliensis	*Nostoc sp.*	*Pennate diatoms*	*Alexandrium fundyense*	
Dictyosphaerium nageli	*Oocysts sp.*	*Stephanodiscus agassizensis*		
Monoraphidium arcuatum	*Oscillatoria sp.*			
Monoraphidium sp.	Other anabaena			
Other green algae	Other microcystis			

Table A.5 List of identified species found in Lake Sardis (LS)

Chlorophytes	**Cyanobacteria**	**Diatoms**	**Dinoflagellates**	**Euglenophytes**
Staurstrum tetracerum	*Raphidosis curvata*	*Synedra sp.*	*Alexandrium fundyense*	*Euglena sp.*
Chlamydomonas sp.	*Anabaena circinalis*	*Amphipleura pellicuda*	*Other dinoflagellates*	
Cosmarium botrys	*Anabaena flos aquae*	*Aulacoseria granulata*	*Noticula sp.*	
Crucigenia fenestrata	*Anabaena laxa*	*Diatoma vulgaris*	*Karenia brevis*	
Crucigenia quadrata	*Anabaena spherica*	*Gomphonema sp.*	*Dinophysis acuminata*	
Dictyosphaerium nageli	*Anabaenopsis circularis*	*Melosira sp.*		
Monoraphidium sp.	*Anabena circinalis*	*Niztchia sp.*		
Other green algae	*Aphanizomenon flos aquae*	*Pennate diatoms*		
Pedisastrum simplex	*Arthrospira stizenberger ex goment*	*Stephanodiscus agassizensis*		
Scenesdesmus acuminatus	*Coelosphaerium sp.*			
Scenesdesmus quadricaudata	*Cylindrospermosis raciborskii*			
	Merismopedia sp.			
	Microcystis aeruginosa			
	Microcystis cf. firma			
	Microcystis flos aquae			
	Microcystis wesenbergii			
	Nostoc sp.			
	Oscillatoria sp.			

Table A.6 List of identified species found in Lake Enid (LE)

Chlorophytes	**Cyanobacteria**	**Diatoms**	**Dinoflagellates**	**Euglenophytes**
Scenesdesmus quadricauda	*Abanaena planctonica*	*Stepanodiscus agassizensis*	*Cyclotella sp.*	*Euglena sp.*
Ankistrodesmus sp.	*Anabaena circinalis*	*Pleurosigma acuminatum*	*Ceratium hirudinella*	
Botrycoccus sp.	*Anabaena crassa*	*Pennate diatoms*	*Noticula sp.*	
Chlamydomonas sp.	*Anabaena laxa*	*Diatoma vulgaris*		
Crucigenia quadrata	*Anabaena planctonica*	*Aulacoseria granulata*		
Dictyosphaerium nageli	*Anabaena spiriods*	*Synedra sp.*		
Kentrosphaera gibberosa	*Anabaena torulosa*	*Stephanodiscus sgassizensis*		
Other green algae	*Anabanea laxa*	*Pennate diatoms*		
Pediastrum duplex	*Anthrospira Stizenberger ex gomont*	*Navicula sp.*		
Pediastrum simplex	*Aphanizomenon flos aquae*	*Cymbella sp.*		
Scenesdesmus quadricauda	*Chrococcus sp.*	*Aulacoseria granulata*		
Scenesdesmus sp.	*Cylindrospermopsis raciborskii*	*Amphipleura Pellicuda*		
	Gleocapsa sp.			
	Johannesbaptisia primaria			
	Merismopedia sp.			
	Microcystis aeruginosa			
	Microcystis cf. firma			
	Nostoc sp.			
	Nostoc sp.			
	Osscillatoria sp.			
	Other anabaena			
	Other microcystis			
	Planktothrix rubescens			
	Raphidosis curvata			
	Raphidosis curvispora			

Table A.7 List of identified species found in Lake Grenada (LG)

Chlorophytes	**Cyanobacteria**	**Diatoms**	**Dinoflagellates**	**Euglenophytes**
Other green algae	*Nostoc sp.*	*Diatoma vulgaris*	Other dinoflagellates	*Euglena sp.*
Ankistrodesmus sp.	*Anabaena circinalis*	*Aulacseria granulata*	*Noticula sp.*	
Chlamydomonas sp.	*Anabaena laxa*	*Amphopleura pellicuda*		
Crucigenia fenestrta	*Anabaena spherica*	*Aulacoseria granulata*		
Dictyosphaerium nageli	*Anabaena torulosa*	*Amphipleura pellicuda*		
Monoraphidium sp.	*Anabaenopsis circularis*			
Other green lagae	*Anabena torulosa*			
Pediastrum duplex	*Aphanizomenon fos aquae*			
Pediastrum simplex	*Cylindrospermopsis raciborskii*			
Scenesdesmus acuminatus	*Merismopedia specis*			
Scenesdesmus quadricauda	*Microcystis aeruginosa*			
	Microcystis cf. firma			
	Microcystis wesenbergii			
	Oscillatoria sp.			
	Other anabaena			
	Plaktothrix rubescens			
	Raphidosis curvata			

Table A.8 Average Rrs of OLCI bands in lakes

Lakes OLCI Bands	band center nm	OWT1average Rrs	OWT2 Average Rrs	OWT3 Average Rrs
Band1	400	3.35E-03	5.41E-03	0.01062
Band2	412.5	3.27E-03	5.51E-03	0.01167
Band3	442.5	3.37E-03	6.46E-03	0.01413
Band 4	490	4.10E-03	8.28E-03	0.01677
Band5	510	4.74E-03	9.60E-03	0.02139
Band6	560	7.14E-03	0.01392	0.02448
Band 7	620	5.87E-03	0.01347	0.02298
Band 8	665	5.25E-03	0.01219	0.02150
Band 9	673.75	4.85E-03	0.01162	0.02112
Band 10	681.2	4.93E-03	0.01166	0.02072
Band 11	708.75	5.67E-03	0.01165	0.01511
Band 12	753.75	2.11E-03	4.98E-03	9.93E-03

Table A.9 Average Rrs of Landsat bands in lakes

Lakes LANDSAT Bands	band center nm	OWT1 Average Rrs	OWT2 Average Rrs	OWT3 Average Rrs
Blue	482.04	4.05E-03	8.97E-03	0.015337
Green	561.41	6.93E-03	0.015103	0.024641
PAN	589.5	5.34E-03	0.013238	0.021957
Red	654.59	5.65E-03	0.014124	0.023288

Table A.10 Average Rrs of Micasense bands in lakes

Lakes MicaSense Bands	Band center nm	OWT1 Average Rrs	OWT2 Average Rrs	OWT3 Average Rrs
Blue	482	4.17E-03	9.37E-03	0.015917
Green	557	6.06E-03	0.013246	0.021718
Red	667	4.97E-03	0.012211	0.020311
Red Edge	717	4.63E-03	0.01092	0.017651
NIR	831	2.28E-03	5.87E-03	0.010458

Table A.11 Average Rrs of MicaSense bands in lakes

LPRE OLCI Bands	Band center nm	Cluster 1 Average Rrs	Cluster 2 Average Rrs	Cluster 3 Average Rrs
Band-1	400	5.32E-03	8.28E-03	2.65E-03
Band -2	412.5	5.56E-03	8.51E-03	2.75E-03
Band-3	442.5	6.93E-03	0.0101	3.42E-03
Band 4	490	9.31E-03	0.01287	4.74E-03
Band 5	510	0.010691	0.014453	5.54E-03
Band 6	560	0.01464	0.018861	7.84E-03
Band 7	620	0.016206	0.021076	7.82E-03
Band 8	665	0.016216	0.021467	7.08E-03
Band 9	673.75	0.016036	0.021329	6.78E-03
Band 10	681.2	0.016202	0.021538	6.91E-03
Band 11	708.75	0.015334	0.020485	6.88E-03
Band 12	753.75	7.13E-03	0.010991	2.74E-03

Table A.12 Average Rrs of Landsat bands in LPRE

LPRE LANDSAT Bands	Band center nm	OWT1 Average Rrs	OWT2 Average Rrs	OWT3 Average Rrs
Blue	482.04	8.78E-03	0.012996	4.55E-03
Green	561.41	0.014325	0.019313	7.76E-03
PAN	589.5	0.015438	0.021275	7.04E-03
Red	654.59	0.016162	0.0221	7.55E-03
NIR	864.67	5.54E-03	0.010029	2.26E-03

Table A.13 Average Rrs of MicaSense bands in LPRE

.LPRE Micasense Bands	Band center nm	OWT1 Average Rrs	OWT2 Average Rrs	OWT3 Average Rrs
blue	482	9.58E-03	0.013241	4.75E-03
Green	557	0.013078	0.017223	6.69E-03
Red	667	0.014485	0.019354	6.46E-03
Red Edge	717	0.012782	0.017516	5.71E-03
NIR	831	7.29E-03	0.011286	3.07E-03

Table A.14 Chlorophyll a algorithm and validation results in Lakes in OWT1 satellite sensors

Satellite sensors	Band ratio	Bands	Conc range	N	R^2	RMSE	%RMSE	%MAE	N	P-value
OLCI	Green/NIR	B6/B11	10.-57.	42	0.335	5.9	23.5	17.84	12	<0.05
Landsat	Pan/NIR	Pan/NIR	10.-57	42	0.49	5.6	22.2	20.48	12	<0.05
MODIS	Green/Red	B12/B13	10-57	42	0.07	Not statistically significant relationship	>0.05			

Table A.15 Chlorophyll a algorithm and validation results in Lakes in OWT2 satellite sensors

Satellite sensors	Band ratio	Bands	Conc range	N	R^2	RMSE	%RMSE	%MAE	N	P-value
OLCI	Green/NIR	B5/B11	1.8-40	38	0.44	13.78	64.8	50.8	12	<0.05
Landsat	Pan/NIR	Pan/NIR	1.8-40	38	0.28	9.24	45.6	38.8	12	<0.05
MODIS	Green/Red	B12/B14	1.8-40	38	0.106	14.25	70.4	57.9	12	<0.05

Table A.16 Chlorophyll a algorithm and validation results in Lakes in OWT3 satellite

Satellite sensors	Band ratio	Bands	Conc range	N	R^2	RMSE	%RMSE	%MAE	N	P-value
OLCI	Green/NIR	Band6/Band11	2.9-15	26	0.73	1.659	13.1	10.09	7	<0.05
Landsat	Green/pan	Green/pan	2.9-15	26	0.76	3.24	25.8	19.03	7	<0.05
Landsat	Green/Red	Green/Red	2.9-15	26	0.68	3.225	25.6	20.67	7	<0.05
MODIS	Green/Red	Band12/Band14	2.9-15	26	0.77	3.188	32.4	21.44	7	<0.05

Table A.17 Chlorophyll a algorithm and validation results in LPRE in OWT1 satellite sensors

Satellite sensors	Band ratio	Band ratio	Chl a	N	R^2	RMSE	%RMSE	%MAE	N	P-value
OLCI	Green/Red	Band6/Band9	1.7-21.	37	0.49	4.09	74.47	57.83	13	<0.05
MODIS	Green/Red	Band11/Band14	1.7-21.	37	0.48	3.96	72.02	55.31	13	<0.05
LANDSAT	Green/PAN	Green/PAN	1.7-21.	37	0.5	4.15	75.63	59.17	13	<0.05

Table A.18 Chlorophyll a algorithm and validation results in LPRE in OWT2 satellite sensors

Satellite sensors	Band ratio	Band ratio	Chl a	N	R^2	RMSE	%RMSE	%MAE	N	P-value
OLCI	Green/Red	Band6/Band10	1.3-10.3	19	0.25	1.396	56.699	45.99	11	<0.05
MODIS	Green/Red	Band12/Band14	1.3-10.3	19	0.16	1.481	60.181	49.06	11	<0.05
LANDSAT	Green/PAN	Green/PAN	1.3-10.3	19	0.15	2.272	64.29	42.66	11	<0.05

Table A.19 Chlorophyll a algorithm and validation results in LPRE in OWT3 satellite sensors

Satellite sensors	Band ratio	Band ratio	Chl a	N	R^2	RMSE	%RMSE	%MAE	N	P-value
OLCI	Green/Red	Band6/Band10	1.6-8.76	42	0.32	2.098	33.207	26.23	19	<0.05
MODIS	Green/Red	Band11/Band14	1.6-8.76	42	0.325	2.127	33.662	27.67	19	<0.05
LANDSAT	Green/PAN	Green/PAN	1.6-8.76	42	0.31	2.178	34.479	29.85	19	<0.05

Table A.20 Chlorophyll-a algorithm and validation in lakes in OWT1 UAS sensors

UAS Sensors	Band ratio	Band ratio	Chl a	N	R^2	RMSE	%RMSE	%MAE	N	P-value
MicaSense	Blue/NIR	Blue/NIR	10.02-57.10	42	0.42	5.08	19.9	12.85	12	<0.05
CIR	Blue/Green	Blue/Green	10.02-57.10	42	0.34	6.89	27.05	23.45	12	<0.05

Table A.21 Chlorophyll a algorithm and validation results in Lakes in OWT2 UAS sensors

UAS Sensors	Band ratio	Band ratio	Chl a	N	R^2	RMSE	%RMSE	%MAE	N	P-value
MicaSense	Green/Rededge	Green/Rededge	1.8-40	38	0.2498	11.06	54.70	46.59	12	<0.05
CIR	Blue/Green	Blue/Green	1.8-40	38	0.12	9.36	46.32	42.09	12	<0.05

Table A.22 Chlorophyll a algorithm and validation results in lakes in OWT3 UAS sensors

UAS Sensors	Band ratio	Band ratio	Chl a	N	R^2	RMSE	%RMSE	%MAE	N	P-value
MicaSense	Green/Red	Green/Red	2.9-15.7	26	0.75	3.549	28.222	21.42	7	<0.05
MicaSense	Blue/Rededge	Blue/Rededge	2.9-15.7	26	0.73	3.016	23.987	20	7	<0.05
CIR	Green/Red	Green/Red	2.9-15.7	26	0.71	3.162	25.15	19.73	7	<0.05

Table A.23 Chlorophyll a algorithm and validation results in LPE in OWT1 UAS sensors

UAS Sensors	Band ratio	Band ratio	Chl a	N	R^2	RMSE	%RMSE	%MAE	N	P-value
MicaSense	Green/Red	Green/Red	1.77-21.3	37	0.43	4.08	74.35	57.18	13	<0.05
CIR	Green/Red	Green/Red	1.77-21.3	37	0.12	4.22	76.80	42.61	13	<0.05

Table A.24 Chlorophyll a algorithm and validation results in LPRE in OWT2 UAS sensors

UAS Sensors	Band ratio	Band ratio	Chl a	N	R^2	RMSE	%RMSE	%MAE	N	P-value
MicaSense	Green/Red	Green/Red	1.3-10.3 µg/L	19	0.21	2.141	60.587	39.96	11	<0.05
CIR	Relationship not significant statistically									>0.05

Table A.25 Chloropyll a algorithm and validation results in LPRE in OWT3 UAS sensors

UAS Sensors	Band ratio	Band ratio	Chl a	N	R^2	RMSE	%RMSE	%MAE	N	P-value
MicaSense	Green/Red	Green/Red	1.6-8.76	42	0.3325	2.038	34.615	25.64	19	<0.05
CIR	Green/Red	Green/Red	1.6-8.76	42	0.3	2.167	34.306	28.59	19	<0.05